Spanish Journal of Palaeontology 39 (1), 33–70, 2024
https://doi.org/10.7203/sjp.28695
Sociedad Española de Paleontología ISSN 2255-0550 / eISSN 2660-9568

OPEN ACCESS RESEARCH PAPER

Famennian conodont assemblage in the Compte section (Upper Devonian, Central Pyrenees) and its comparison with Eurasian sequences

Asociación de conodontos del Fameniense en la sección Compte (Devónico Superior, Pirineos Centrales) y su comparación con sucesiones euroasiáticas

Héctor BARRERA-LAHOZ, José Ignacio VALENZUELA-RÍOS & Jau-Chyn LIAO

Abstract: A detailed study of the fossil assemblages of Famennian conodonts has been carried out in the Compte section in the Central Pyrenees. The studied section comprises the upper part of the Comabella Formation, the La Mena Fm and the lower part of the Barousse Fm. Fifty samples have been collected from a 11.73 m thick Famennian stratigraphic succession. Forty-seven lower–middle Famennian conodont taxa have been identified, belonging to four genera: *Palmatolepis*, *Polygnathus*, *Icriodus* and *Mehlina*. The identified conodont assemblages change through the studied section: in the lower part, *Palmatolepis* and *Icriodus* taxa are more frequent and in the overlaying strata, *Palmatolepis* and *Polygnathus* taxa are dominant. Several conodont taxa have been recorded for the first time in Central Pyrenees zone. The conodont sequence analysis suggests a lower to middle Famennian age (from the *termini* to *mg. marginifera* Zones) in the Compte section (Beds 98–120). On the other hand, a comparison of the Pyrenean conodont assemblages with those from other relevant regions has been carried out. The conodont associations from Compte shows certain similarities with those from western and eastern Europe; however, sequences from eastern and central Asian exhibit some differences.

Resumen: Se ha realizado un estudio detallado de las asociaciones fósiles de conodontos del Fameniense en la sección Compte en los Pirineos Centrales. La sección estudiada pertenece a la parte alta de la Formación Comabella, la Formación La Mena y la parte baja de la Formación Barousse. Se han recogido cincuenta muestras de una sucesión estratigráfica Fameniense de 11,73 m. Se han identificado 47 taxones de conodontos del Fameniense inferior–medio pertenecientes a cuatro géneros: *Palmatolepis*, *Polygnathus*, *Icriodus* y *Mehlina*. Las asociaciones de conodontos identificadas cambiaron a lo largo de la sección estudiada: en la parte baja de la sección taxones de *Palmatolepis* e *Icriodus* son más frecuentes y en los estratos superiores, los taxones de *Palmatolepis* y *Polygnathus* son más frecuentes. El análisis de la sucesión de conodontos sugiere una edad Fameniense inferior a medio (de las Zonas *termini* a *mg. marginifera*) en la sección Compte (Capas 98–120). Por otro lado, se ha realizado una comparación de las asociaciones de conodontos con otras zonas. Las asociaciones de conodontos provenientes de Europa occidental y oriental muestran ciertas similitudes con las de la sección Compte y algunas diferencias con las faunas de Asia central y oriental.

Received: 4 December 2023
Accepted: 5 May 2024
Published: 14 May 2024

Corresponding author:
Héctor Barrera-Lahoz
hectorpaleodevon@gmail.com

Keywords:
Conodonts
La Mena Fm
Palmatolepis
Polygnathus
Icriodus
Famennian

Palabras-clave:
Conodontos
Formación La Mena
Palmatolepis
Polygnathus
Icriodus
Fameniense

INTRODUCTION

The complex and varied lithological development of Devonian rocks in the Pyrenees was interpreted as belonging to different "facies-areas" (Mey, 1967a, 1967b). The southernmost one (the "southern facies-area), was further subdivided into four "sub-facies-areas". One of them, the Compte sub-facies-area, contains one of the richest Devonian conodont sequences in the world (Ziegler, 1959; Boersma, 1973a, 1973b; Valenzuela-Ríos, 1990, 1994a, 1994b, 2002; Valenzuela-Ríos & García-López, 1998; Valenzuela-Ríos & Murphy, 1997; Valenzuela-Ríos & Liao, 2012, 2024; Murphy & Valenzuela-Ríos, 1999; Sanz-López, 1995, 2002a, 2002b; Liao & Valenzuela-Ríos, 2008, 2013; Gouwy *et al.*, 2013, 2016, 2017; Martínez-Pérez *et al.*, 2011; Martínez-Pérez & Valenzuela-Ríos, 2012, 2014; Silvério *et al.*, 2021). These works have demonstrated an almost complete conodont record for all Devonian stages, which has been compiled from numerous, disperse outcrops of limited stratigraphic distribution. There is, however, a site, a few meters north of el Comte, where the stratigraphic record seems to be more complete although tectonics made the Lower

© The Author(s) 2024. This is an open-access article distributed under the terms of the Creative Commons Attribution 4.0 International License (for details please see http://creativecommons.org/licenses/by/4.0/), which permits use, copy, adaptation, distribution, and reproduction in any medium or format, as long as you give appropriate credit to the original author(s) and the source.

Devonian overthrust Middle and Upper Devonian rocks, as Schmidt (1931) have already depicted. Valenzuela-Ríos *et al.* (2017a) summarize the set of outcrops grouped in the Compte sections at Compte. Mainly, there are two large sequences: 1) the Lower Devonian one, comprising the Lochkovian, Pragian and lower Emsian; this section is labelled CP-I section and 2) the Middle, Upper Devonian and lower Carboniferous? sequence, consisting of Eifelian, Givetian, Frasnian, Famennian and, probably, lower Carboniferous rocks (compare Boersma, 1973b); this succession is named CP section. Liao and Valenzuela-Ríos (2017) presented the state-of-the-art of the CP section, which clearly shows the intervals that must be investigated in detail (mostly from middle Frasnian to the base of the Carboniferous). Subsequently, Silvério *et al.* (2021) partially filled this gap of information, documenting conodonts around the Frasnian–Famennian transition. Thus, a thorough examination of Famennian strata is still pending. Famennian strata in the CP section comprise three successive formations that from bottom up are Comabella Fm, La Mena Fm and Barousse Fm Valenzuela-Ríos and Liao (2006a, 2006b) denoted that the contact between the Comabella and La Mena fms is diachronic in the Compte Subfacies-area and, consequently, a comprehensive study of the conodont record of La Mena Fm in different sections of this subfacies-area, has to be implemented in the future. Accordingly, our main aim in this report is the identification, detailed description and characterization of the conodont record of La Mena Fm in the CP section. In addition, we bracket the local age of La Mena Fm and compare the conodont record with those records of other relevant areas as western and eastern Europe, central Asia and China.

GEOGRAPHIC AND GEOLOGIC SETTING

The Compte section is located in the Central Pyrenees zone, NE Spain (Fig. 1A), between La Pobla de Segur and Sort localities (Lérida, Spain), at the right bank of the Noguera Pallaresa river about 2km north of Gerri de la Sal (Fig. 1B–1C). The Pyrenees is an E-W mountain range as result of Alpine Orogeny, which main structure has a double vergence. Prevariscan rocks belong to the Axial Zone comprising the basement of the Pyrenees (Barnolas & Pujalte, 2004) (Fig. 1A). Due to the complex stratigraphy, the Devonian and Carboniferous

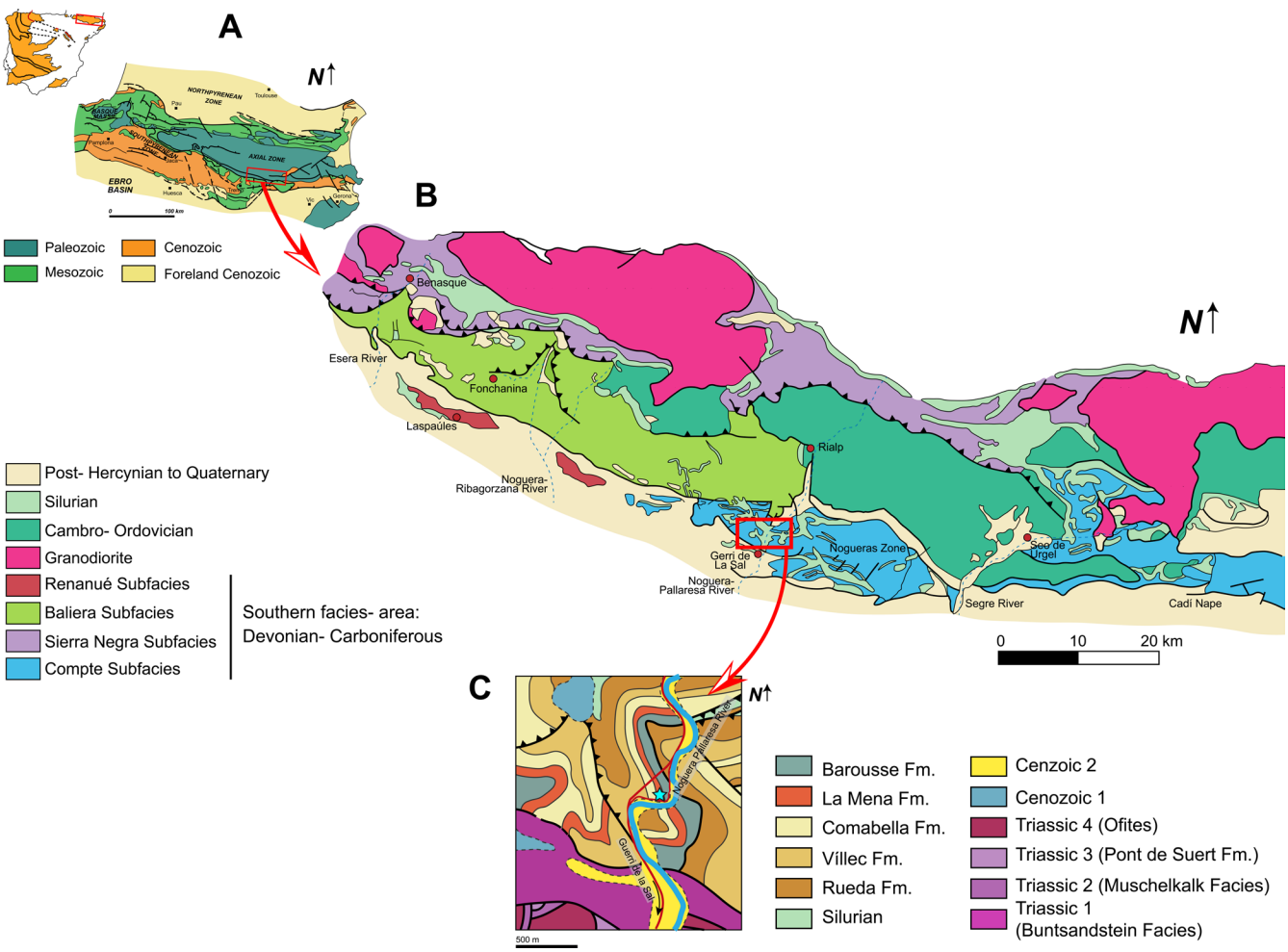

Figure 1. Geographical and geological background of the Compte section. **A,** Schematic geologic map of the Pyrenees (modified from Barnolas & Pujalte, 2004); **B,** geological map and Southern subfacies-area distribution in southern central Pyrenees zone (modified from Valenzuela-Ríos *et al.*, 2015); **C,** geological map of the Compte section (blue star) (modified from Institut Cartogràfic I Geològic de Catalunya, 2023).

of the Central Pyrenees have been subdivided into facies-area (Mey, 1967a, 1967b; Hartevelt, 1970). The main four facies-area are North Pyrenean, Northern, Central, Western and Southern (summarized in Zwart, 1979). The latter has been further subdivided in four subfacies-area: Sierra Negra, Baliera, Renanué and Compte (Mey, 1967a; Zwart, 1979; Valenzuela-Ríos & Liao, 2006); the materials analysed herein belong to the latter (Fig. 1B). The Compte subfacies comprises strata from Lower Devonian to lower Carboniferous, and it is mainly composed of limestones, shales, marls and nodular limestones in the Upper Devonian–Carboniferous part (Boersma, 1973a; Sanz-López, 1995). The palaeoenvironments during the Upper Devonian of this area consisted of pelagic marine outer platform ramp and hemipelagic condensed carbonate ramp (Liao & Valenzuela-Ríos, 2017). The CP section exhibits the Comabella, La Mena and Barousse fms (Fig. 1C), that approximately correspond to the members A, B, C of Compte Formation respectively (Boersma, 1973a; Sanz-López, 1995). The Comabella Fm (Givetian to Famennian in this area) consists of well-bedded, massive and brecciated limestones of grey, dark grey, pink and green colours (Fig. 2A). The La Mena Fm (Famennian in this area) consists in red (pseudo)nodular "griotte" limestones (Fig. 2B), red and violet bedded limestones and marly limestones that to the top, veer to red and grey nodular limestones. The Barousse Fm (Famennian to Tournaisian) consists of pink and grey nodular limestones in the lower part (Fig. 2C) that shift to light grey nodular limestones in the upper part. Generally, the thickness of the layers varies from centimetric and decametric and some of them are even metric. There are several scarce millimetric to centimetric layers of shales, among them (Fig. 3).

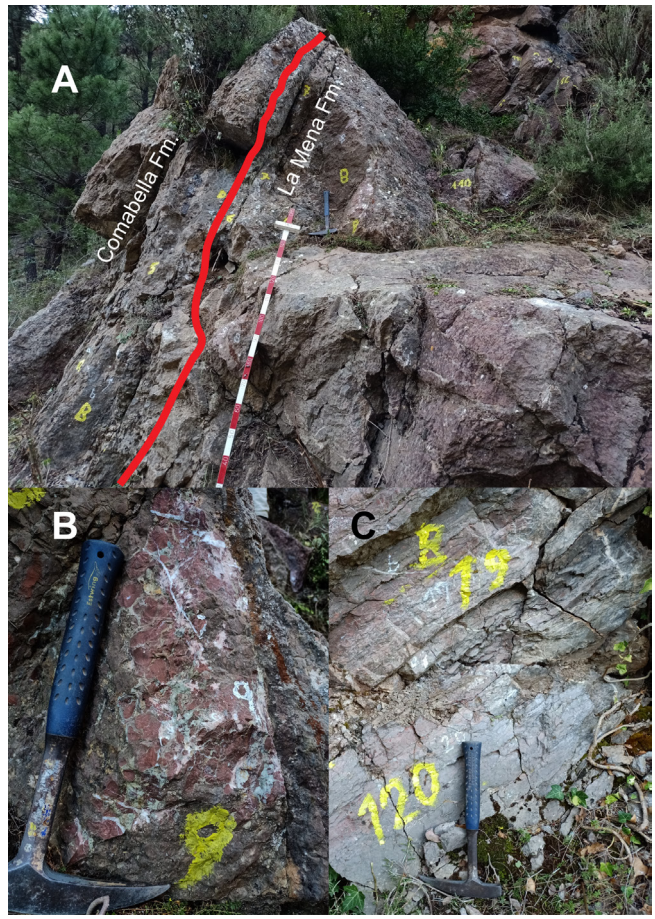

Figure 2. Field view of the studied section. **A,** Comabella and La Mena fms boundary (Beds 105–110), red line represents the boundary between Comabella–La Mena fms; **B,** detailed view of La Mena Fm: red nodular limestones (Bed 109); **C,** view of Barousse Fm: pink and grey nodular limestones (Beds 119–120).

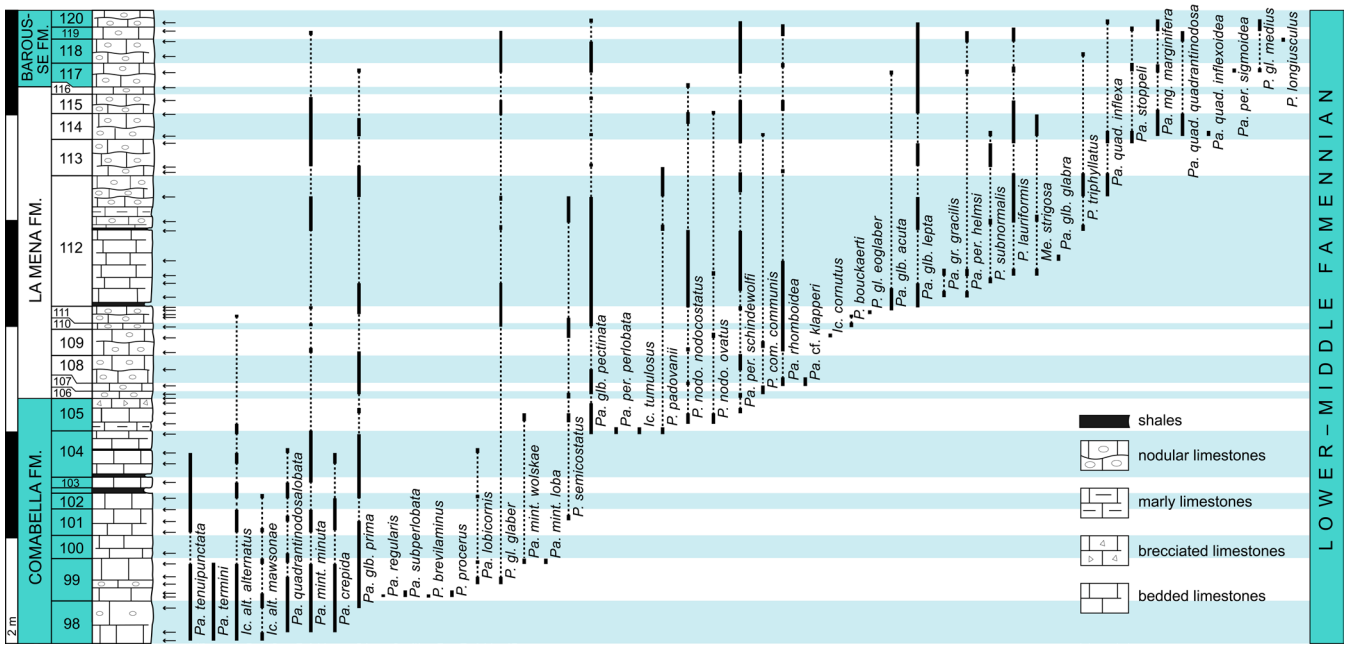

Figure 3. Stratigraphic column of the Famennian of the Compte section, with the position of the samples, indication of the layers and the stratigraphical distribution of each conodont taxa, the blue and white zones mean the beds extention.

MATERIALS AND METHODS

The studied stratigraphic succession is 11.73 m thick and comprises three formations (Fig. 3): the uppermost 4.53 m of the Comabella Fm (Beds 98 to 105), 5.75 m of the La Mena Fm (beds 106 to 116) and the lowermost 1.45 m of the Barousse Fm (beds 117 to 120). 50 samples have been taken between Beds 98–120, with weights between 0.4 to 3 kg, usually 0.5–0.6 kg (Tabs. 1–3). Each bed has been sampled, and sometimes, several consecutive samples were taken within particular beds (Fig. 3). The samples have been processed using formic and acetic acid (~7–8%) in 5–10 L solutions. The residue obtained was separated through decantation and dried in a drying stove at a temperature about 60ºC. Afterwards, the residue was picked out using a Leica WILD M3B microscope. The selected specimens were photographed by the Scanning Electron Microscope (model Hitachi S4800) at the University of Valencia.

SYSTEMATIC PALEONTOLOGY

Class CONODONTA Pander, 1856
Suborder OZARKODININA Dzik, 1976
Family SPATHOGNATHODONTIDAE Hass, 1959

Genus *Palmatolepis* Ulrich & Bassler, 1926

Type species. *Palmatolepis perlobata* Ulrich & Bassler, 1926, Famennian. Europe, North America.

Palmatolepis crepida Sannemann, 1955a

Figure 4I–4J

1955a *Palmatolepis crepida* n. sp.; Sannemann, p.134, pl. 6, fig. 21.
1993 *Palmatolepis crepida*; Ji & Ziegler, p. 59, pl. 22, figs. 1–7, text-fig. 13, fig. 4.
1995 *Palmatolepis crepida*; Rodríguez-Cañero, p. 9, pl. IV, figs. 6–8.
1995 *Palmatolepis crepida*; Sanz-López, p. 538, pl. 40, figs. 11–12.
2011 *Palmatolepis crepida*; Hartenfels, p. 243, pl. 41, fig. 3.
2015 *Palmatolepis crepida*; Mossoni, p. 89, pl. 1, fig. 8.
2021 *Palmatolepis crepida*; Silvério *et al.*, p. 212, fig. 4K.

Material. 98 specimens from samples CP/98b (4), CP/98c (4), CP/99a (4), CP/99b (4), CP/99c (6), CP/99d-1 (4), CP/99d-2 (19), CP/101a (8), CP/101b (2), CP/102a (3), CP/102b (5), CP/104a (3), CP/104b (32).

Description. Platform with oval outline or drop-shape form, generally wide. The lobe is absent or poorly developed with rounded or semicircular form, directed laterally and aligned with the azygous node or slightly anterior. Arched anterior carina, composed of numerous coarse, fused denticles; it joints the anterior end of the inner margin. Azygous node pronounced. Short posterior carina with few and tiny, poorly developed, denticles, which does not reach the posterior end. The outer anterior margin starts posteriorly than the inner margin. The outer slightly elevated developing a

Table 1. Stratigraphical distribution of the samples and conodont specimens from Beds 98–104 identified in CP section in addition of the sample names, formations and sample weight. ***Pa.***, *Palmatolepis*; ***Ic.***, *Icriodus*; ***P.***, *Polygnathus*. The sample code consists in: *i.e.,* CP/98a, means that the sample was taken in Bed 98 in the first interval of the bed.

Formation	Comabella															
Sample name	CP/98a	CP/98b	CP/98c	CP/99a	CP/99b	CP/99c	CP/99d-1	CP/99d-2	CP/100	CP/101a	CP/101b	CP/102a	CP/102b	CP/103	CP/104a	CP/104b
Sample weight (kg)	0.41	0.65	0.73	0.455	0.53	0.75	0.4	1.275	0.56	0.75	0.59	0.455	0.58	0.47	0.595	0.585
Palmatolepis tenuipunctata	1	2	17	12	5	7	2	9		8	2	2	3	2	4	7
Pa. cf. *tenuipunctata*			3		2	2			1	1		1			2	
Pa. cf. *quadrantinodosalobata*	3				1			2			3				1	4
Pa. quadrantinodosalobata		5	10	5	2	1		4	1		3		2	2		8
Pa. minuta minuta		4	2	2	1	4	1	4		5	2	2		1	3	4
Pa. crepida		4	4	4	4	6	4	19		8	2	3	5		3	32
Pa. termini	1	5	8	9	4	9	1	10								
Pa. glabra prima			25	15	4	20	7	18	3	10	2		3	5	8	34
Pa. glabra cf. *prima*			1			1	1	4		1		1				
Pa. regularis				2												
Pa. subperlobata				2	1											
Pa. cf. *subperlobata*				1												
Pa. lobicornis						2		1					1			1
Pa. cf. *lobicornis*								1								
Pa. minuta wolskae		1						1								
Pa. minuta loba								1								
Palmatolepis sp. indet.	13	8	72	26	11	29	13	32	3	26	20	13	12	12	21	57
Icriodus alternatus alternatus	1	4	1	1	14	2	1	3		1	11		2		2	
Ic. cf. *(alternatus) alternatus*					4	1				1	1		3		2	
Ic. alternatus mawsonae	1		1	3	4			5			2		2			
Icriodus sp. indet.	2	3	1		2	1	1	5			5	2	10	5	2	1
Polygnathus brevilaminus				1												
P. procerus				4	2											
P. semicostatus											1					
P. glaber glaber						2										
Polygnathus sp. indet.	1		4	12	2	2		1	1	2	4	1	5	2		2

Table 2. Stratigraphical distribution of the samples and conodont specimens from Beds 104–112 identified in CP section in addition of the sample names, formations and sample weight. ***Pa.***, *Palmatolepis*; ***Ic.***, *Icriodus*; ***P.***, *Polygnathus*; ***Me.***, *Mehlina*. The sample code consists in: *i.e.,* CP/111a-1, means that the sample was taken in Bed 111 in the first interval of the bed and, additionally, in the lower part.

Formation	Comabella					La Mena																
Sample name	CP/104c	CP/105a	CP/105b	CP/105c	CP/105d	CP/106	CP/107	CP/108	CP/109a	CP/109b	CP/110	CP/111a-1	CP/111a-2	CP/111b	CP/111c	CP/112a	CP/112b	CP/112c	CP/112d	CP/112e	CP/112f	CP/112g
Sample weight (kg)	0.645	1.255	0.735	0.52	0.61	0.53	0.49	0.57	0.52	0.485	0.565	0.59	0.025	0.56	0.715	1.13	0.665	0.95	0.56	0.69	0.465	0.72
Pa. minuta minuta	1								1		3				2					4	3	1
Pa. glabra prima	4		1			3	2	3	1				1	3	1	1	3					2
Pa. glabra cf. *prima*	1						2															
Pa. minuta wolskae		1	1																			
Pa. perlobata perlobata	1																					
Pa. glabra pectinata	2	1	6	2		5	3	3			2	2	1	6	4	3	5	2	1	5	1	3
Pa. perlobata schindewolfi			1		1	1		1	6					1		2	2	2	1	2		5
Pa. perlobata cf. *perlobata*				1																		
Pa. rhomboidea							1		2	2	13	5	8	3	4	12	15	15	3			
Pa. cf. *klapperi*							1															
Pa. glabra acuta														1	1	2	3					
Pa. glabra lepta															1	1	3			1	1	1
Pa. gracilis gracilis																1		1				
Pa. perlobata helmsi																1		1				
Pa. glabra glabra																			1			
Pa. quadrantinodosa inflexa																						2
Palmatolepis sp. indet.	8	2	8	2	1	7	9	5	4	1	4	6	4	16	18	13	6	12	5	12	5	7
Ic. alternatus alternatus	5											1										
Ic. cf. *(alternatus) alternatus*												1										
Ic. tumulosus	3																					
Ic. cornutus										1												
Icriodus sp. indet.	16	2								3												
P. semicostatus		7	4		1	5				1	4	3									1	1
P. padovanii	1																			2		2
P. nodo. nodocostatus		1	1				1		2						1	1	1	3	1	1		
P. nodo. cf. *nodocostatus*								1	1						1					1		
P. nodo. ovatus		4	1						1									1				
P. communis communis						1	1		1													
P. glaber glaber											2	2	1	1	2	5	4			2		2
P. bouckaerti											1	1										
P. glaber eoglaber													1	1								
P. subnormalis																	1				1	
P. triphyllatus																				3		1
P. lauriformis																		1			2	5
Polygnathus sp. indet.	8	13	2	11	2	23		5	9	1	9	4	3	15	5	5	3	5	2	6	5	7
Mehlina strigosa																		1			1	

parapet-like, more marked anteriorly. Posterior platform slightly or strongly elevated. Platform ornamented by random fine or coarse nodes.

Discussion. *Palmatolepis crepida* is characterized by oval to drop-shape form, small lobe and nodes ornamentation. It is similar to *Pa. perlobata perlobata* by node ornamentation but differs in the minor development of the lobe and less elevation of the outer platform. *Pa. crepida* differs from *Pa. tenuipunctata* by the less developed lobe and wider platform.

Age and geographical range. From Famennian *crepida* to *rhomboidea* Zones (Spalletta *et al.*, 2017). *Pa. crepida* has cosmopolitan distribution.

Palmatolepis glabra acuta Helms, 1963

Figure 7A–7B

1963 *Palmatolepis serrata acuta* n. sp.; Helms, p. 468, pl. 3, figs. 1–4, 6.
1990 *Palmatolepis glabra acuta*; Perri & Spalletta, p. 60, pl. 1, figs. 4a–4b.
1993 *Palmatolepis glabra acuta*; Ji & Ziegler, pl. 16, fig. 11, text-fig. 17, fig. 5.
2001 *Palmatolepis acuta*; Johnston & Chatterton; p. 24, pl. 7, figs. 1–2.
2015 *Palmatolepis glabra acuta*; Mossoni, p.89–90, pl. 5, fig. 2.
2017 *Palmatolepis glabra acuta*; Lüddecke *et al*., fig. 4f.
2017 *Palmatolepis glabra acuta*; Ovnatanova *et al*., p. 1075, pl. 47, figs. 5–6, pl. 50, figs., 1–6, 8.

Material. Eight specimens from samples CP/111b (1), CP/111c (1), CP/112a (2), CP/112b (3) and CP/117 (1).

Description. Narrow platform with sigmoidal outline. It has a pronounced subtriangular parapet, which is oblique to the carina; and the projection of its margin forms an acute angle with the azygous node and the carina. Generally, the parapet is smooth. The outer margin is straight and forms a 90 degree with the anterior outer margin. Inner margin runs from anterior to posterior ends with an outline parallel to the carina. Sigmoidal carina with the posterior part straight or

Table 3. Stratigraphical distribution of the samples and conodont specimens from Beds 113–120 identified in CP section in addition of the sample names, formations and sample weight. ***Pa.***, *Palmatolepis*; ***P.***, *Polygnathus*; ***Me.***, *Mehlina*. The sample code consists in: *i.e.,* CP/113b, means that the sample was taken in Bed 113 in the second interval of the bed.

Formation	La Mena							Barousse				
Sample name	CP/113a	CP/113b	CP/113c	CP/114a	CP/114b	CP/115	CP/116	CP/117	CP/118a	CP/118b	CP/119	CP/120
Sample weight (kg)	0.465	0.525	0.565	0.725	1.01	0.74	0.415	2.875	1	0.64	0.7	0.5
Pa. minuta minuta		1	4	28	3	1					1	
Pa. glabra prima	1	2		3	3			4				
Pa. glabra pectinata		1		7		2		17	1	1		2
Pa. perlobata schindewolfi	1		2	5	1	1		3	1	1	1	1
Pa. rhomboidea	1				4	12		10		7	10	2
Pa. glabra acuta								1				
Pa. glabra lepta		3	1		38	8	1	4	9	13	6	3
Pa. perlobata helmsi								3			3	
Pa. quadrantinodosa inflexa	1		1	1								1
Pa. stoppeli			1	4				2		2	1	
Pa. quadrantinodosa inflexoidea				1								
Pa. quadrantinodosa quadrantinodosa				2	3					1	1	
Pa. marginifera marginifera				1	1	3		6			3	2
Pa. perlobata sigmoidea								1				
Palmatolepis sp. indet.	8	6		14	47	26	6	71	24	35	14	20
P. padovanii	2	2										
P. nodo. nodocostatus					1		1					
P. nodo. cf. *nodocostatus*			1					3	1		1	
P. nodo. ovatus					1							
P. communis communis				1								
P. glaber glaber					1	1		6	1	1	2	
P. subnormalis		1	2									
P. triphyllatus	2			1					1			
P. lauriformis	4		4	12	5	3		1		3	1	
P. lauriformis cf.				2								
P. glaber medius								3			4	1
P. longiusculus										1		
Polygnathus sp. indet.	6	4	1	15	5	2	1	18	1	3	5	4
Me. strigosa				2	1							

slightly curved reaching the posterior end. The posterior margin is pointed and upwards bent. The platform surface is smooth or shagreen.

Discussion. This species is similar to the rest of the *Pa. glabra*-stock in the outline and the development of its parapet. It differs from *Pa. glabra pectinata* by the orientation of the parapet, which is oblique to the carina while it is parallel in *Pa. glabra pectinata*. It differs from *Pa. glabra distorta* by the absent of the characteristically bulge in the inner platform of the latter species. Finally, the rounded outline of the outer (inner) margin separates *Pa. glabra prima* from *Pa. glabra acuta*.

Age and geographical distribution. From Famennian *gl. pectinata* to *mg. utahensis* Zones (Spalletta *et al.*, 2017). *Pa. gl. acuta* is recorded in Italy, Germany, Russia, China and Canada.

Palmatolepis glabra glabra Ulrich & Bassler, 1926

Figure 7H

1926 *Palmatolepis glabra* n. sp.; Ulrich & Bassler, p. 51, pl. 9, fig. 20.
1993 *Palmatolepis glabra glabra*; Ji & Ziegler, p. 60–61, pl. 17, figs. 13–15, text-fig. 17, fig. 4.
1995 *Palmatolepis glabra glabra*; Rodríguez-Cañero, p. 10, pl. IV, fig. 13.
2003 *Palmatolepis glabra glabra*; Corradini, p. 79, pl. 4, figs. 1–2.
2015 *Palmatolepis glabra glabra*; Mossoni, p. 90–91, pl. 1, fig. 15.
2017 *Palmatolepis glabra glabra*; Ovnatanova *et al.*, p. 1075, pl. 47, fig. 4.

Material. One specimen from the sample CP/112c.

Description. Sigmoidal and slender platform. The outer anterior margin joints perpendicular the anterior margin, developing an elevated parapet with the anterior margin merging oblique with the carina and developing a short crest. The inner margin outline is parallel to the carina. Pointed posterior platform; its posterior end bends upwards. Sigmoidal carina reaching both ends. Smooth platform surface.

Discussion. *Pa. glabra glabra* is similar to *Pa. glabra pectinata* and *Pa. glabra prima*. From the former separates by a less pronounced, short and wide parapet. The platform of *Pa. glabra prima* is generally wider and the outer margin is straight or change direction at the azygous node, but its outline does not follow the trace of the carina.

Age and geographical distribution. From Famennian *rhomboidea* Zone to *mg. marginifera* Zone. (Spalletta, 2017). *Pa. gl. glabra* is recorded in Germany, Italy, Spain, Russia and China.

Palmatolepis glabra lepta Ziegler & Huddle, 1969

Figure 7C–7G

1969 *Palmatolepis glabra lepta* n. sp.; Ziegler & Huddle, p. 380–381.
1973 *Palmatolepis glabra lepta* early form; Sandberg & Ziegler: p. 101–102, pl. 2, fig. 16.
1973 *Palmatolepis glabra lepta* late (typical) form; Sandberg & Ziegler: p. 101–102, pl. 2, fig. 3.
1993 *Palmatolepis glabra lepta*; Ji & Ziegler, p. 61, pl. 19, figs. 11–15, text-fig. 17, fig. 3.
1995 *Palmatolepis glabra lepta*; Rodríguez-Cañero, p. 12, pl. V, figs. 5–7.
2011 *Palmatolepis glabra lepta* early morphotype; Hartenfels, p. 246, pl. 42, figs. 1–2.
2011 *Palmatolepis glabra lepta* late morphotype; Hartenfels, p. 245–246, pl. 42, figs. 3–6.
2015 *Palmatolepis glabra lepta*; Mossoni, p. 91–92, pl. 4, fig. 16.
2017 *Palmatolepis glabra lepta*; Ovnatanova, p. 1075–1076, pl. 53, fig. 10.
2017 *Palmatolepis glabra lepta*; Lüddecke *et al*., fig. 4i.
2023 *Palmatolepis glabra lepta* early morphotype; Huang *et al.*, fig. 4D

Material. 94 specimens from samples CP/111c (1), CP/112a (1), CP/112b (3), CP/112e (1), CP/112f (1), CP/112g (1), CP/113b (3), CP/113c (1), CP/114b (38), CP/115 (8), CP/116 (1), CP/117 (4), CP/118a (9), CP/118b (13), CP/119 (6) and CP/120 (3). Early morphotype is recorded between samples CP/111c and CP/114b and late morphotype is recorded between samples CP/114b and CP/120.

Description. Slender and narrow platform with a rough sigmoidal outline. The parapet has (sub) triangular to rounded outline, turned upwards and sometimes reduced to a bulge. Subtriangular posterior platform moderately to strongly bend upwards. Azygous node. Located in the posterior third of the platform, posterior to the end of the parapet. The carina is slightly to strongly sigmoidal. Nodes on the roughly arched anterior carina are high; posterior nodes are small and much lower, reaching the pointed posterior end. Smooth platform surface.

Discussion. Sandberg and Ziegler (1973) and Hartenfels (2011) described two different morphotypes. The early form (Fig. 7C–7D) is distinguished by a narrow and slightly slender and sigmoidal platform and an elevated parapet with ridge-like form and subtriangular outline. The late (typical) form (Fig. 7E–7G) has mostly slender and narrow platform and the characteristic triangular parapet. *Pa. glabra lepta* differs from others subspecies of *Pa. glabra* by the extremely narrow platform and the (sub)triangular parapet.

Age and geographical distribution. From Famennian *gl. prima* to *granulosus* Zones (Spalletta *et al.*, 2017). According to Ziegler and Sandberg (1973) and Hartenfels (2011) the late form extends from the base of the *mg. marginifera* Zone to the *granulosus* Zone. The early form extends from the *gl. prima* Zone to the top of the *gr. gracilis* Zone (Ziegler & Sandberg, 1973; Hartenfels, 2011), but in South China extends to *mg. marginifera* Zone (Huang *et al.*, 2023). *Pa. gl. lepta* is recorded in Germany, Italy, Belgium, Spain, Russia, Poland, Canada, USA, China.

Palmatolepis glabra pectinata Ziegler, 1962a.

Figure 6A–6C

1962a *Palmatolepis glabra pectinata* n. ssp; Ziegler, p. 398–399, pl. 2, figs. 3–5.
1973 *Palmatolepis glabra pectinata* morphotype 1; Sandberg & Ziegler, p. 104, pl. 2, figs. 4, 12–15, pl. 5, fig. 14.
1993 *Palmatolepis glabra pectinata*; Ji & Ziegler, p. 61, pl. 16, figs. 5–10, pl. 17, figs. 1–12, figs. 1–12; text-fig. 17, figs. 7–8.
1995 *Palmatolepis glabra pectinata*; Rodríguez-Cañero, p. 12, pl. V, figs. 1–2.
1995 *Palmatolepis glabra pectinata*; Sanz-López, p. 537, pl. 40, figs. 16–17.
2011 *Palmatolepis glabra pectinata* (typical); Hartenfels, p. 246–247, pl. 42, figs. 12–13.
2015 *Palmatolepis glabra pectinata*; Mossoni, p. 92, pl. 1, fig. 19, pl. 4, fig. 1.
2017 *Palmatolepis glabra pectinata*; Ovnatanova *et al.*, p. 1076, pl. 50, figs. 7, 9.
2017 *Palmatolepis glabra pectinata*; Lüddecke *et al.*, fig. 4j.

Material. 88 specimens from samples CP/104c (2), CP/105a (1), CP/105b (6), CP/105c (2), CP/106 (5), CP/107 (3), CP/108 (3), CP/110 (2), CP/111a-1 (2), CP/111a-2 (1), CP/111b (6), CP/111c (4), CP/112a (3), CP/112b (5), CP/112c (2), CP/112d (1), CP/112e (5), CP/112f (1), CP/112g (3), CP/113b (1), CP/114a (7), CP/115 (2), CP/117 (17), CP/118a (1), CP/118b (1) and CP/120 (2).

Description. Narrow and slightly sigmoidal platform with straight inner margin. Well-developed high parapet, parallel to the carina ending anteriorly to the azygous node. Inner and anterior margin meets at an obtuse angle. Outer margin straight, curving in the posterior third. Pointed posterior end upwards bent. Subtle sigmoidal carina with arched anterior part and mostly straight posterior of the azygous node. Smooth or finely shagreen platform.

Discussion. *Palmatolepis glabra pectinata* and *Pa. gl. acuta* have similar parapet, but in the former is parallel to the carina. *Pa. gl. pectinata* differs from *Pa. gl. distorta* by the absence of a bulge in the anterior inner platform.

Age and geographical distribution. From Famennian *gl. pectinata* Zone to the *mg. utahensis* Zone (Spalletta *et al.*, 2017). *Pa. gl. pectinata* has cosmopolitan distribution.

Palmatolepis glabra prima Ziegler & Huddle, 1969

Figure 4K–4N

1962a *Palmatolepis glabra glabra*; Ziegler, p. 397, pl. 1, fig. 11–12.

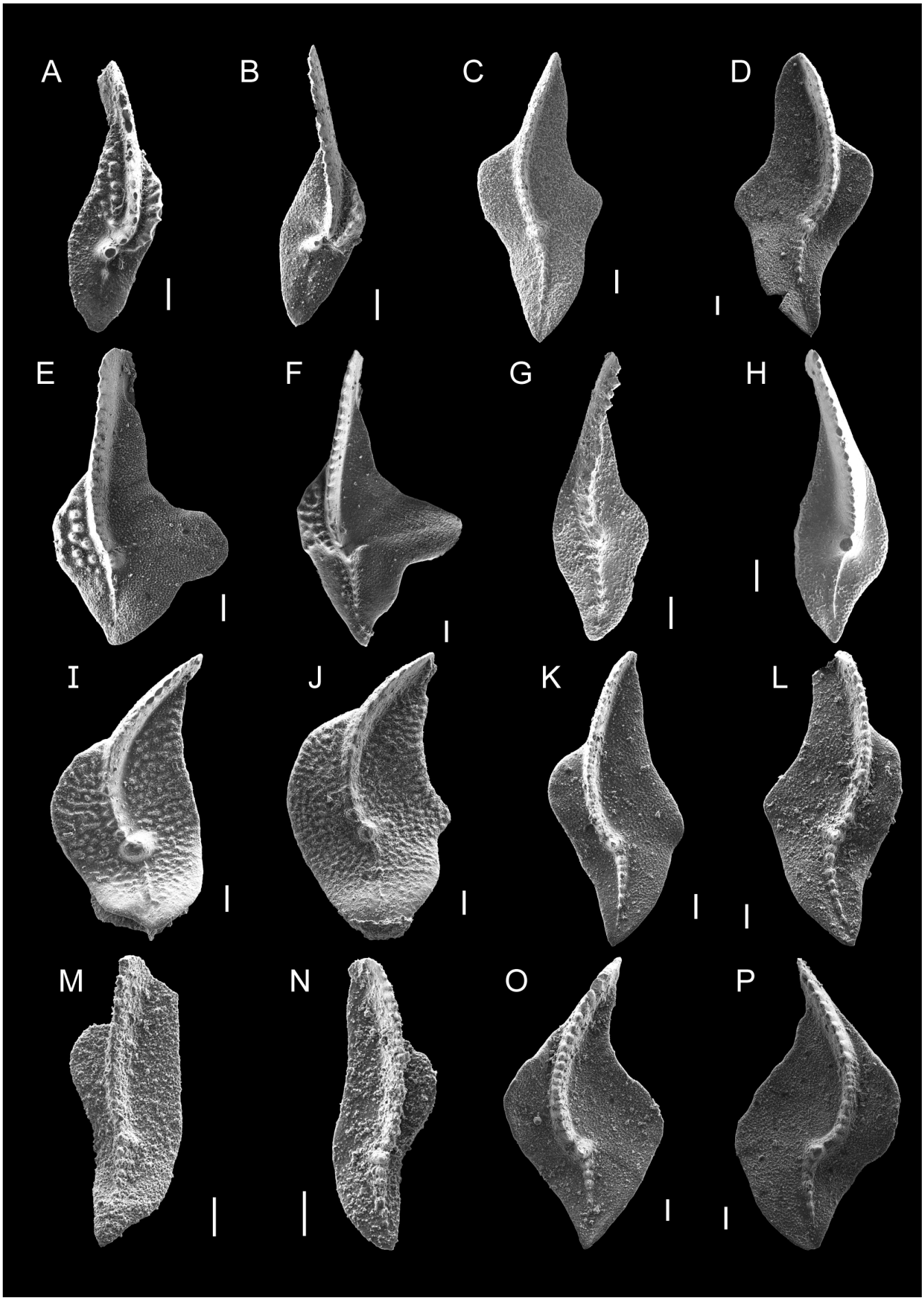
A
B
C
D
E
F
G
H
I
J
K
L
M
N
O
P

1962b *Palmatolepis glabra glabra*; Ziegler, p. 58, pl. 4, figs. 14–15.
1969 *Palmatolepis glabra prima* n. ssp. Ziegler & Huddle, p. 379–380.
1973 *Palmatolepis glabra prima* morphotype 1; Sandberg & Ziegler, p. 103, pl. 2, figs. 2, 8–10.
1973 *Palmatolepis glabra prima*; Sandberg & Ziegler, pl. 2, figs. 1, 7.
1993 *Palmatolepis glabra prima*; Ji & Ziegler, p. 61, pl. 16, figs. 14–17, text-fig. 17, figs. 2, 9, 17.
1993 *Palmatolepis glabra prima* morphotype 1; Ji & Ziegler, p. 62, pl. 16, figs. 12–13, text-fig. 19, fig. 7.
1995 *Palmatolepis glabra prima*; Rodríguez-Cañero, p.12, pl. IV, figs. 14–16.
1995 *Palmatolepis glabra prima*; Sanz-López, p. 537–538, pl. 40, fig. 15.
1999 *Palmatolepis glabra unca*; Schülke, p. 37–38, pl. 4, figs. 1–3.
2003 *Palmatolepis glabra prima*; Corradini, p. 79, pl. 4, figs. 3–6.
2011 *Palmatolepis glabra prima* morphotype 3 (typical); Hartenfels, p. 247–248, pl. 43, figs. 1–3.
2011 *Palmatolepis glabra prima* morphotype 1; Hartenfels, p. 248, pl. 42, figs. 7–11.
2015 *Palmatolepis glabra prima*; Mossoni, p. 92–93, pl. 1, fig. 16.
2017 *Palmatolepis glabra prima*; Ovnatanova *et al.*, p. 1079, pl. 50, fig. 10.
2017 *Palmatolepis glabra prima*; Lüddecke *et al.*, fig. 4k.
2019 *Palmatolepis prima*; Zhang, p. 245, pl. 29, figs. 9–12.
2019 *Palmatolepis prima* morphotype 1; Zhang, p. 245–246, pl. 29, figs. 1–8.
2020 *Palmatolepis glabra prima* morphotype 1; Suttner *et al.*, figs. 6.11a–11b.
2020 *Palmatolepis glabra prima* morphotype 3; Suttner *et al.*, figs. 6.16a–16b.

Material. 192 specimens from samples CP/98c (25), CP/99a (15), CP/99b (4), CP/99c (20), CP/99d-1 (7), CP/99d-2 (18), CP/100 (3), CP/101a (10), CP/101b (2), CP/102b (3), CP/103 (5), CP/104a (8), CP/104b (34), CP/104c (4), CP/105b (1), CP/106 (3), CP/107 (2), CP/108 (3), CP/109a (1), CP/111a-2 (1), CP/111b (3), CP/111c (1), CP/112a (1), CP/112b (3), CP/112g (2), CP/113a (1), CP/113b (2), CP/114a (3), CP/114b (3) and CP/117 (4). The morphotype 1 is recorded between samples CP/98c and CP/104c and the morphotype 3 is recorded among samples CP/104b and CP/117.

Description. Sandberg and Ziegler (1973) described three morphotypes of *Pa. glabra prima*, in the Compte section the morphotypes 1 and 3 have been identified. The morphotype 1 (Fig. 4K–4L) is characterized by a wide and elongated platform with slightly subrhombic outline. The outer platform might have a lobe-like margin but not a developed lobe. The inner platform is elevated with a feeble rounded parapet in the anterior part; pointed posterior end, downwards turned. Sigmoidal carina with nodes reaching both ends. Smooth platform surface. The morphotype 3 (Fig. 4M–4N) is characterized by a slender and slightly sigmoidal platform with a straight outer margin. Rounded and elevated but not pronounced parapet that ends anteriorly to the azygous node in the inner platform. Pointed posterior end upwards turned.

Discussion. According to Sandberg and Ziegler (1973) there are three morphotypes. The first morphotype (M1) is characterized by a wider platform and it is related to *Pa. klapperi*. It is similar to *Pa. tenuipunctata* but can be distinguished by the absence of a lobe and greater width. Also, it differs from *Pa. klapperi* by the absence of a ramp in the outer platform. The third morphotype (M3, more typical) is narrower and can be separated from other subspecies of *Pa. glabra* by the rounded and slightly elevated parapet in the inner platform.

Age and geographical distribution. From Famennian the *gl. prima* Zone to *mg. utahensis* Zone (Spalletta *et al.*, 2017). *Pa. gl. prima* has cosmopolitan distribution.

Palmatolepis gracilis gracilis Branson & Mehl, 1934
Figure 7I1–7I2.

1934 *Palmatolepis gracilis* n. sp.; Branson & Mehl, p. 238, pl. 18, fig. 8.
1993 *Palmatolepis gracilis gracilis*; Ji & Ziegler, p. 63, pl. 6, figs. 4–7, text-fig. 14, fig. 2.
1995 *Palmatolepis gracilis gracilis*; Rodríguez-Cañero p. 12, 14, pl. V, figs. 11–13.
1995 *Palmatolepis gracilis gracilis*; Sanz-López, p. 544, pl. 43, figs. 12–13.
2011 *Palmatolepis gracilis gracilis*; Hartenfels, p. 249–250, pl. 44, figs. 1–3.
2015 *Palmatolepis gracilis gracilis*; Mossoni, p. 94, pl. 2, figs. 15–16.
2017 *Palmatolepis gracilis gracilis*; Ovnatanova *et al.*, p. 1079–1080, pl. 48, fig. 8, pl. 53, figs. 7–8.
2017 *Palmatolepis gracilis gracilis*; Lüddecke *et al.*, fig. 4l.

Material. Two specimens from samples CP/112a (1) and CP/112c (1).

Description. Small, narrow and slender platform with slightly asymmetrical fusiform outline. It has a reduced lobe and raised margin rim. Straight, oblique anterior carina that curves strongly near the azygous node;

Figure on previous page

Figure 4. A, *Palmatolepis termini*, sample CP/98c; **B,** *Palmatolepis termini*, sample CP/99d-2; **C,** *Palmatolepis tenuipunctata*, sample CP/99a; **D,** *Palmatolepis tenuipunctata*, sample CP/99a; **E,** *Palmatolepis quadrantinodosalobata*, sample CP/99d-2; **F,** *Palmatolepis quadrantinodosalobata*, sample CP/98c; **G,** *Palmatolepis minuta minuta*, sample CP/112g; **H,** *Palmatolepis minuta minuta*, sample CP/112e; **I,** *Palmatolepis crepida*, sample CP/101a; **J,** *Palmatolepis crepida*, sample CP/99a; **K,** *Palmatolepis glabra prima* M1, sample CP/98c; **L,** *Palmatolepis glabra prima* M1, sample CP/99c; **M,** *Palmatolepis glabra prima* M3, sample CP/111b; **N,** *Palmatolepis glabra prima* M3, sample CP/112b; **O,** *Palmatolepis regularis*, sample CP/99a; **P,** *Palmatolepis regularis*, sample CP/99a; scale bar = 100 µm.

straight to slightly arched posterior carina reaching the posterior end. Pointed posterior margin. Long free blade, as large as the platform length or longer. The keel is constricted or twisted at the middle of the platform. Smooth or finely shagreen platform surface.

Discussion. *Pa. gracilis gracilis* is similar to *Pa. minuta minuta* in the platform outline and size of juvenile specimens of *Pa. minuta minuta*, they can be distinguished by the twisted keel and the length of the free blade, additionaly, the basal cavity of *Pa. min. minuta* is more reduced than *Pa. gr. gracilis*.

Age and geographical distribution. From Famennian *gr. gracilis* to *ultimus* Zones (Spalletta *et al.*, 2017). *Pa. gr. gracilis* has cosmopolitan distribution.

Palmatolepis cf. *klapperi* Sandberg & Ziegler, 1973

Figure 6E

1973 *Palmatolepis klapperi* n. sp.; Sandberg & Ziegler, p. 104, pl. 2, figs. 6, 17–28, pl. 5, fig. 12.
1993 *Palmatolepis klapperi*; Ji & Ziegler, p. 67, pl. 18, figs. 1–8, text-fig. 17, fig. 18.
2011 *Palmatolepis klapperi*; Hartenfels, p. 258, pl. 43, figs. 8–11.
2013 *Palmatolepis klapperi*; Strelchenko & Kruchek, p. 161, pl. 1, fig. 26.
2019 *Palmatolepis klapperi*; Zhang, p. 229, pl. 31, figs. 9–12.

Material. One specimen from sample CP/107.

Description. Biconvex, oval platform with oval outline that turns downwards at the posterior end. Arched inner platform without developing a lobe. Slightly elevated outer platform that develops an elongated bulge-like called ramp. The outer margin meets the carina at an obtuse angle. Strongly arched anterior carina; short posterior carina with few, minute denticles that does not reach the posterior end. Elongated, narrow and pointed posterior margin. The free blade is absent and the platform surface is shagreening.

Discussion. *Pa. klapperi* separates from *Pa. glabra prima* morphotypes 1 and 2 by the characteristic curvature of the inner platform, the ramp in the outer platform and the intersection of the anterior outer margin with the free blade. The specimen from Compte section (Fig. 6E) has a not well-preserved ramp and the characteristic curvature is slighter pronounced.

Age and geographical distribution. From Famennian *gl. prima* to *mg marginifera* Zones (Spalletta *et al.*, 2017). *Pa. klapperi* is recorded in Germany, Morocco, Belarus, China, Iran and USA.

Palmatolepis lobicornis Schülke, 1995

Figure 5B

1995 *Palmatolepis lobicornis* n. sp.; Schülke, p. 40–41, pl. 4, figs. 1–17.
1999 *Palmatolepis lobicornis*; Schülke, p. 40–41, pl. 2, fig. 10.
2004 *Palmatolepis lobicornis*; Klapper *et al.*, p. 379, fig. 7.30.
2013 *Palmatolepis lobicornis*; Strelchenko & Kruchek, pl. 1, fig. 29.
2016 *Palmatolepis lobicornis*; Huang & Gong, figs. 6.2, 6.11.
2019 *Palmatolepis lobicornis*; Zhang, p. 242, pl. 20, figs. 5–16.
2021 *Palmatolepis lobicornis*; Silvério *et al.*, p. 213, fig. 4L.

Material. Five specimens from samples CP/99c (2), CP/99d-2 (1), CP/102b (1) and CP/104b (1).

Description. Platform relative wide and with subtriangular outline. Convex anterior inner margin; convex outer platform that starts posteriorly than the inner. Well-developed lobe, with rounded outline and projected laterally, with a small bulge in the anterior side. The platform develops weak sinuses around the lobe. Arched anterior carina; straight posterior carina that reaches close to the posterior end. Posterior platform turned upwards. Posterior end slightly pointed or rounded and turned downwards. Short free blade. Smooth platform surface; which have small nodes in the outer platform.

Discussion. *Pa. lobicornis* is similar to *Pa. subperlobata* in the platform outline and the smooth surface. Nevertheless, it differs by the presence of a small bulge in the lobe, rounded posterior end and more developed sinuses. Besides, the outer platform of *Pa. superlobata* exhibits two files of nodes.

Age and geographical distribution. From Famennian *min. minuta* to *rhomboidea* Zones (Spalletta *et al.*, 2017). *Pa. lobicornis* is recorded in Germany, France, Spain, Belarus, Turkey, China, Canada and USA.

Palmatolepis marginifera marginifera Helms, 1959

Figure 8F–8G

1959 *Palmatolepis quadrantinodosa marginifera*; Helms, p. 649, pl. 5, figs. 22–23.
1973 *Palmatolepis marginifera marginifera*; Sandberg & Ziegler, p. 104, pl. 3, figs. 13–14.
1993 *Palmatolepis marginifera marginifera*; Ji & Ziegler, p. 64, pl.13, figs. 7–10, pl.14, figs.1–6, text-fig.17, fig.14.
1995 *Palmatolepis marginifera marginifera*; Sanz-López, p. 523–524, pl. 41, figs. 6–7, 11.
2003 *Palmatolepis marginifera marginifera*; Corradini, p. 80, pl. 5, figs. 1–3.
2011 *Palmatolepis marginifera marginifera*; Hartenfels, p. 260–261, pl. 41, figs. 6–8.
2013 *Palmatolepis marginifera marginifera*; Mossoni *et al.*, p. 24, fig. 6.18.
2013 *Palmatolepis marginifera marginifera*, Savage, p. 19, figs. 12.21–23, 13.14–16.
2015 *Palmatolepis marginifera marginifera*; Mossoni, p. 96, pl. 2, fig. 18, pl. 3, fig. 2.
2017 *Palmatolepis marginifera marginifera*; Ovnatanova et al., p. 1091–1092, pl. 47, figs. 1–2, 9, pl. 51, figs. 6–7, 9–10.
2017 *Palmatolepis marginifera marginifera*; Lüddecke *et al.*, figs. 4m–4n.
2019 *Palmatolepis marginifera marginifera*; Zhang, p. 234, pl. 27, figs. 9–12.

Material. 16 specimens from samples CP/114a (1), CP/114b (1), CP/115 (3), CP/117 (6), CP/119 (3) and CP/120 (2).

Description. Elongated (Fig. 8G) or wide (Fig. 8F) platform with oval outline. Straight inner margin, or slightly concave in the anterior and convex in the posterior. The outer platform has a well-developed parapet, which is smooth with a crest (Fig. 8G) or denticulate with coarse nodes parallel to the carina (Fig. 8F); the parapet ends near the azygous node (Fig. 8F) or extend beyond it (Fig. 8G). Arched anterior carina; straight posterior carina reaching the posterior end. The posterior margin is pointed to subtriangular and is turned upwards. No free blade and smooth surface.

Discussion. *Pa. mg. marginifera* is similar to some taxa from the *quadrantinodosa*-stock, *e.g. Pa. quadrantinodosa quadrantinodosa* and *Pa. quad. inflexa* and also, *Pa. stoppeli*, but it differs from all of them by the well-developed parapet in the outer platform. Also, it separates from *Pa. mg. utahensis* by the absence of nodes in the inner platform. It differs from *Pa. mg. duplicata* by having one parapet. Ji and Ziegler (1993) described *Pa. mg. sinensis* using as diagnostic character the extension of the parapet, which reaches the posterior end of the platform. However, Corradini (2003) did not accept this taxon and assumed that this character is part of the specific variability.

Age and geographical distribution. From Famennian *mg. marginifera* to *rg. trachytera* Zones (Spalletta *et al.*, 2017). *Pa. mg. marginifera* has cosmopolitan distribution.

Palmatolepis minuta loba Helms, 1963

Figure 5C

1963 *Palmatolepis minuta loba* n. ssp.; Helms, p. 470, pl. 2, figs. 13–14, pl. 3 fig. 12.
1993 *Palmatolepis minuta loba* Ji & Ziegler, p. 64–65, pl.10, figs. 1–16, text-fig.13, figs.11–12.
1995 *Palmatolepis minuta loba*; Rodríguez-Cañero, p. 16, pl. III, fig. 17.
2003 *Palmatolepis minuta loba*; Corradini, p. 80, pl. 6, fig. 9.
2011 *Palmatolepis minuta loba*; Hartenfels, p. 262, pl. 46, figs. 7–8.
2013 *Palmatolepis minuta loba*; Mossoni *et al.*, p. 24, fig. 5.11.
2015 *Palmatolepis minuta loba*; Mossoni, p. 98, pl. 1, fig. 11.
2019 *Palmatolepis loba loba*; Zhang, p. 252–253, pl. 32, figs. 5–8.

Material. One specimen from sample CP/99d-2.

Description. Small platform with lanceolate outline and developed lobe. Roughly convex anterior inner margin with straight margins anterior and posterior to the lobe; small sinuses are present. Elongated, rounded subtriangular lobe, laterally oriented, anterior to the well-developed azygous node. Straight anterior carina, slightly arched. Thin posterior carina that does not reach the posterior end. Posterior end pointed and turned upwards bent. Free blade about 1/3 to 1/5 of the platform length. Smooth platform surface.

Discussion. *Pa. minuta loba* is similar to *Pa. min. minuta*, but differs by the well-developed lobe. It separates from *Pa. min. wolskae*, by the presence of the posterior carina.

Age and geographical distribution. From Famennian *crepida* to *rhomboidea* Zones (Spalletta *et al.*, 2017). *Pa. min. loba* is recorded in Italy, Germany, Spain, Turkey, Poland, Russia, Iran and China.

Palmatolepis minuta minuta Branson & Mehl, 1934

Figure 4G–4H

1934 *Palmatolepis minuta*; Branson & Mehl, p. 236, pl. 18, figs.1, 6–7.
1962b *Palmatolepis minuta minuta*; Ziegler, pl. 3, figs. 1–10,
1993 *Palmatolepis minuta minuta*; Ji & Ziegler, p. 65, pl. 7, figs. 1–19; pl. 9, figs. 8–18, text-fig. 13, figs. 9, 15–16.
2011 *Palmatolepis minuta minuta*; Hartenfels, p. 261–262, pl. 46, figs. 1–6.
2013 *Palmatolepis minuta minuta*; Mossoni *et al.*, p. 24, fig. 6.17.
2015 *Palmatolepis minuta minuta*; Mossoni, p. 97–98, pl. 2, fig. 7.
2017 *Palmatolepis minuta minuta*; Ovatanova *et al.*, p. 1092, 1095, pl. 46, figs. 3, 8, pl. 47, fig. 10, pl. 48, figs. 12, 14, pl. 52, fig. 1.
2017 *Palmatolepis minuta minuta*; Lüddecke *et al.*, figs. 4o–4r.

Material. 88 specimens from samples CP/98b (4), CP/98c (2), CP/99a (2), CP/99b (1), CP/99c (4), CP/99d-1 (1), CP/99d-2 (4), CP/101a (5), CP/101b (2), CP/102a (2), CP/103 (1), CP/104a (3), CP/104b (4), CP/104c (1), CP/109a (1), CP/110 (3), CP/111c (2), CP/112e (4), CP/112f (3), CP/112g (1), CP/113b (1), CP/113c (4), CP/114a (28), CP/114b (3), CP/115 (1) and CP/119 (1).

Description. Flat platform with biconvex, lanceolate outline, with a small lobe, which in some specimens is absent. Convex anterior and inner margins; outer posterior margin is slightly concave. Rounded small lobe, at the same level than the azygous node. Straight to slightly arched anterior carina; denticulate posterior carina; with discrete denticles or fused in a thin crest, that almost reaches the posterior end. Pointed and slightly turning upwards posterior margin. The carinas are arranged in a sigmoid pathway. Short free blade, about 1/4 or 1/5 of the platform length. Arched or straight keel. Platform surface smooth or finely shagreen.

Discussion. This taxon is similar to other *minuta* taxa; the difference with *Pa. min. loba* is explained there. It separates from *Pa. min. wolskae* by the presence of the posterior carina. Juvenile specimens can be confused with small platforms of *Pa. gr. gracilis* but besides the differences explained there, they can also be discriminated by wider platform of *Pa. min. minuta*.

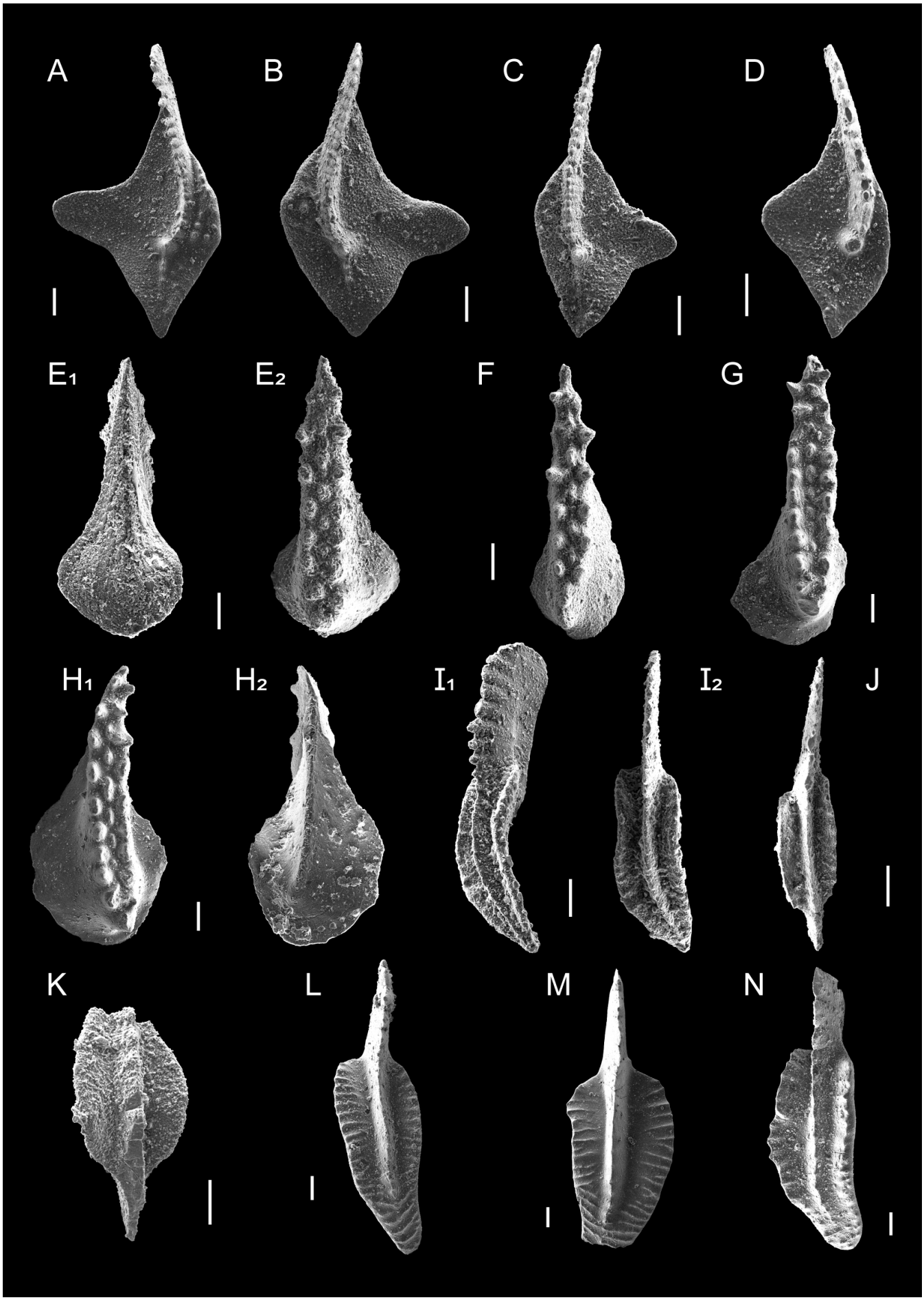
A
B
C
D
E1
E2
F
G
H1
H2
I1
I2
J
K
L
M
N

Age and geographical distribution. From Famennian *min. minuta* to *granulosus* Zones (Spalletta *et al.*, 2017). *Pa. min. minuta* has cosmopolitan distribution.

Palmatolepis minuta wolskae Szulczewski, 1971

Figure 5D

1971 *Palmatolepis minuta wolskae* n. ssp.; Szulczewski, p. 36, pl. 15, figs. 2, 12–14.
1993 *Palmatolepis minuta wolskae*; Ji & Ziegler, p. 85 pl. 11, figs. 1–11, text-fig. 13, figs. 7–8.
1995 *Palmatolepis minuta wolskae*; Rodríguez-Cañero, p. 16, pl. III, fig. 18.
2003 *Palmatolepis minuta wolskae*; Corradini, p. 80, pl. 6, figs. 7–8.
2015 *Palmatolepis minuta wolskae*; Mossoni, p. 99–100, pl. 5, fig. 4.
2019 *Palmatolepis loba wolskae*; Zhang, p. 253, pl. 32, figs. 9–12.

Material. Four specimens from samples CP/98b (1), CP/99d-2 (1), CP/105a (1) and CP/105b (1).

Description. Flat platform with lanceolate to subtriangular outline. Concave or straight inner anterior margin. Poor developed lobe; some specimens develop a posterior sinus. Slightly arched anterior carina; well-developed azygous node and absent posterior carina. Pointed posterior end turned upwards. Smooth platform surface.

Discussion. Main difference with other *minuta* taxa lies on the absent of posterior carina.

Age and geographical distribution. From Famennian *termini* to *rhomboidea* Zones (Spalletta *et al.*, 2017). *Pa. min. wolskae* is recorded in Italy, Spain, Poland, France and China

Palmatolepis perlobata helmsi Ziegler, 1962b

Figure 7J

1962b *Palmatolepis helmsi* n. sp.; Ziegler, p. 184, pl. 8, figs. 16–17.
1977 *Palmatolepis perlobata helmsi*; Ziegler (catalogue), p. 355–356, pl. 5 (*Palmatolepis*), figs. 1–2.
1979 *Palmatolepis perlobata helmsi*; Sandberg & Ziegler, p. 179, pl. 1, figs. 20–21.
1993 *Palmatolepis perlobata helmsi*; Ji & Ziegler, p. 66, pl. 18, figs. 7–10, text-fig. 15, fig. 9.
1995 *Palmatolepis perlobata helmsi*; Sanz-López, p. 521, pl. 42, fig. 2.
2011 *Palmatolepis perlobata helmsi*; Hartenfels, p. 479, pl. 47, figs. 4–5.
2015 *Palmatolepis perlobata helmsi*; Mossoni, p. 101, pl. 5, fig. 7.
2017 *Palmatolepis perlobata helmsi*; Ovnatanova *et al.*, p. 1099–1100, pl. 52, fig. 2.
2017 *Palmatolepis perlobata helmsi*; Lüddecke *et al.*, figs. 5a–5b.
2019 *Palmatolepis helmsi*; Zhang, p. 207, pl. 37, figs. 1–4.

Material. Eight specimens from samples CP/112a (1), CP/112c (1), CP/117 (3) and CP/119 (3).

Description. Subtriangular platform with the widest zone in the anterior half. Subtriangular, barely developed to almost absent lobe. Convex outer margin, slightly elevated with straight anterior and posterior parts meeting at an acute angle. Strongly arched anterior; straight to slightly arched posterior carina that does not reach the posterior end; the carinas pathway draws a subtle sigmoidal layout. The posterior margin is turned upwards. Free blade absent. Platform surface smooth or shagreen.

Discussion. *Pa. perlobata helmsi* differs from other members of the *perlobata* group by the less developed lobe. *Pa. per. perlobata* has also a weak-developed lobe, but this taxon has a platform ornamented by nodes. Besides the posterior carina of *Pa. per. perlobata* reaches the posterior end.

Age and geographical distribution. From Famennian *rhomboidea* to *ac. aculeatus* (Spalletta *et al.*, 2017). *Pa. per. helmsi* is recorded in Germany, Belgium, Spain, Italy, Poland, Russia, Morocco, China and Australia.

Palmatolepis perlobata perlobata Ulrich & Bassler, 1926

Figure 6D

1926 *Palmatolepis perlobata perlobata* n. sp.; Ulrich & Bassler, p. 49–50, pl. 7, figs. 19, 21–22.
1977 *Palmatolepis perlobata perlobata*; Ziegler (catalogue), p. 349–351, pl. 10 (*Palmatolepis*), figs. 5–7.
1995 *Palmatolepis perlobata perlobata*; Rodríguez-Cañero, p. 16, pl. IV, figs. 1–2.
1995 *Palmatolepis perlobata perlobata*; Sanz-López, p. 520, pl. 41, fig. 13.
2003 *Palmatolepis perlobata perlobata*; Corradini, p. 81, pl. 7, fig. 10.
2011 *Palmatolepis perlobata perlobata*; Hartenfels, p. 263, pl. 47, fig. 6.
2013 *Palmatolepis perlobata perlobata*; Strelchenko & Kruchek, pl. 1, fig. 6.
2017 *Palmatolepis perlobata perlobata*; Ovnatanova *et al.*, p. 1099, pl. 48, fig. 10.

Figure on previous page

Figure 5. A, *Palmatolepis subperlobata*, sample CP/99b; **B,** *Palmatolepis lobicornis*, sample CP/99d-2; **C,** *Palmatolepis minuta loba*, sample CP/99d-2; **D,** *Palmatolepis minuta wolskae*, sample CP/99d-2; **E1,** *Icriodus alternatus alternatus*, lower view, sample CP/99b; **E2,** *Icriodus alternatus alternatus*, upper view, sample CP/99b; **F,** *Icriodus alternatus alternatus*, sample CP/102b; **G,** *Icriodus alternatus mawsonae*, sample CP/99d-2; **H1,** *Icriodus alternatus mawsonae*, upper view, sample CP/99d-2; **H2,** *Icriodus alternatus mawsonae*, lower view, sample CP/99d-2; **I1,** *Polygnathus procerus*, lateral view, sample CP/99a; **I2,** *Polygnathus procerus*, upper view, sample CP/99a; **J,** *Polygnathus brevilaminus*, sample CP/99a; **K,** *Polygnathus glaber eoglaber*, CP/111a-2; **L,** *Polygnathus semicostatus*, sample CP/106; **M,** *Polygnathus semicostatus*, sample CP/105b; **N,** *Polygnathus semicostatus*, sample CP/105a; scale bar = 100 µm.

Material. One specimen from sample CP/104c.

Description. Wide platform with slightly sigmoidal outline. Convex and elevated outer platform. Weakly developed lobe with rounded subtriangular outline. Sinuses are present. Sigmoidal arched anterior carina; straight to slightly curved posterior carina that reaches the posterior end; the carinas pathway draws a sigmoidal layout. Subtriangular and markedly turned upwards margin. Free blade absent. The platform surface is covered by nodes.

Discussion. This taxon is similar to *Pa. per. schindewolfi* in the platform outline, but the posterior carina of the latter doesn't reach the posterior margin and has a feeble ornamented platform.

Age and geographical distribution. From Famennian *min. minuta* Zone to the upper part of *gl. pectinata* Zone. (Spalletta *et al.*, 2017). *Pa. per. perlobata* is recorded in Germany, Italy, Russia, Spain, Morocco, Iran, China and USA.

Palmatolepis perlobata schindewolfi Müller, 1956

Figure 7K–7L

1956 *Palmatolepis schindewolfi* n. sp.; Müller, p. 27, pl. 8, figs. 22–31, pl. 9, fig. 33.
1979 *Palmatolepis perlobata schindewolfi*; Sandberg & Ziegler, p. 180, pl. 1, figs. 22–24, pl. 2, fig. 13.
1993 *Palmatolepis perlobata schindewolfi*; Ji & Ziegler, p. 67, pl. 18, figs. 9–15, text-fig.15, fig. 3.
1995 *Palmatolepis perlobata schindewolfi*; Rodríguez-Cañero, p. 18, pl. IV, figs. 4–5.
1995 *Palmatolepis perlobata schindewolfi*; Sanz-López, p. 521–522, pl. 41, figs. 14–17, pl. 42, fig. 1, pl. 54, fig. 6.
2003 *Palmatolepis perlobata schindewolfi*; Corradini, p. 82, pl. 7, figs. 1–5.
2011 *Palmatolepis perlobata schindewolfi*; Hartenfels, p. 268–269, pl. 47, figs. 1–3.
2013 *Palmatolepis schindewolfi*; Savage, p. 23, figs. 13.3–13.4, 14.7–14.8, 15.25–15.27, 17.27–17.29, 18.1–18.5, 20.1–20.7.
2015 *Palmatolepis perlobata schindewolfi*; Mossoni, p. 102–103, pl. 2, fig. 20, pl. 5, fig. 1a–1b.
2017 *Palmatolepis perlobata schindewolfi*; Lüddecke *et al.*, fig. 5d.
2017 *Palmatolepis perlobata schindewolfi*; Ovnatanova *et al.*, p. 1100, pl. 52, figs. 3–5.
2019 *Palmatolepis perlobata schindewolfi*; Zhang, p. 209–210, pl. 36, figs. 1–4.

Material. 42 specimens from samples CP/105b (1), CP/105d (1), CP/106 (1), CP/108 (1), CP/109a (6), CP/111b (1), CP/112a (2), CP/112b (2), CP/112C (2), CP/112d (1), CP/112e (2), CP/112g (5), CP/113a (1), CP/113c (2), CP/114a (5), CP/114b (1), CP/115 (1), CP/117 (3), CP/118a (1), CP/118b (1), CP/119 (1) and CP/120 (1).

Description. Elongated, narrow platform with straight inner margin and subtriangular outer margin, which is convex and elevated. Small, well pronounced, subtriangular and pointed lobe located clearly anteriorly of the azygous, which is positioned in the posterior third. Arched anterior carina; short, poorly developed and straight posterior carina that does not reach the posterior margin, which is turned upwards. The carinas pathway draws a subtle sigmoidal layout. Absent free blade. Platform surface smooth, shagreen or with thin nodes.

Discussion. *Pa. per. schindewolfi* is similar to other *perlobata* subspecies. The differences with *Pa. per. perlobata* are discussed there. It differs from *Pa. per. sigmoidea* by a narrower platform, less sigmoidal outline and lack of ribs on the margins. Finally, *Pa. per. schindewolfi* is similar to *Pa. tenuipunctata* in the platform outline and small lobe, however, the lobe in *Pa. tenuipunctata* is less developed and more anteriorly located. The azygous node is also located in a more anterior position and the posterior carina starts with nodes than continue in a thin crest that reaches the posterior end.

Age and geographical distribution. From the Famennian lower part of the *gl. prima* Zone to *ultimus* Zone (Spalletta *et al.*, 2017). *Pa. per. schindewolfi* has cosmopolitan distribution.

Palmatolepis perlobata sigmoidea Ziegler, 1962b

Figure 8H

1962b *Palmatolepis perlobata sigmoidea* n. ssp.; Ziegler, p. 71, pl. 8, figs. 7, 9–11.
1977 *Palmatolepis perlobata sigmoidea*; Ziegler (catalogue), p. 365–366, pl. 11 (*Palmatolepis*), figs. 8–11.
1995 *Palmatolepis perlobata sigmoidea*; Sanz-López, p. 522, pl. 42, figs. 3–4.
2009 *Palmatolepis perlobata sigmoidea*; Over *et al.*, figs. 5.5, 5.7, 6.9–6.10, 6.12, 7.2.
2011 *Palmatolepis perlobata sigmoidea*; Hartenfels, p. 269–270, pl. 48, fig. 1.
2017 *Palmatolepis perlobata sigmoidea*; Ovnatanova *et al.*, p. 1100, pl. 52, figs. 6–8.
2019 *Palmatolepis sigmoidea*; Zhang, p. 213, pl. 38, figs. 9–12.

Material. One specimen from sample CP/117.

Description. Relatively wide platform with strongly arched outer margin. Platform markedly constricted close to azygous node. High outer margin, almost developing a parapet and ornamented by straight ribs, some of which are aligned fused nodes. Triangular, pointed lobe located approximately in the half-length of the platform and clearly anteriorly to the azygous node, which settles clearly in the posterior third. Strongly arched anterior carina; straight posterior carina that almost reaches the posterior end. The carinas pathway draws a sigmoidal layout. Posterior margin pointed and strongly turned upwards. Absent free blade. Inner and outer margins ornamented with irregular nodes and ribs.

Discussion. The differences between *Pa. per. sigmoidea* and *Pa. per. schindewolfi* are discussed there. Besides, the former has a strong platform constriction in the posterior third.

Age and geographical distribution. From near to the base of the Famennian *mg. marginifera* Zone to *gr. manca* Zone (Spalletta *et al.*, 2017). *Pa. per. sigmoidea* is recorded in Germany, Spain, Russia, China and USA.

Palmatolepis quadrantinodosa inflexa Müller, 1956

Figure 8A–8B

1956 *Palmatolepis quadrantinodosa inflexa* n. ssp.; Müller, p. 67, pl. 10, figs. 5, 8, 11.
1973 *Palmatolepis quadrantinodosa inflexa*; Sandberg & Ziegler, p. 105, pl. 4, figs. 7–13.
1974 *Palmatolepis inflexa*; Dreesen & Dusar, p. 54, pl. 6, fig. 11.
1977 *Palmatolepis inflexa inflexa*; *Dreesen*, p. 518–519, pl. 1, figs. 52–53.
1993 *Palmatolepis quadrantinodosa inflexa*; Ji & Ziegler p. 68, pl. 15, figs. 4–12, text-fig.17, fig. 10.
2003 *Palmatolepis quadrantinodosa inflexa*; Corradini, p. 82, pl. 5, fig. 13.
2017 *Palmatolepis quadrantinodosa inflexa*; Lüddecke *et al.*, fig. 5f.
2017 *Palmatolepis inflexa*; Ovnatanova *et al.*, p. 1083, pl. 47, fig. 3, pl. 48, fig. 11, pl. 51, figs. 4–5.
2019 *Palmatolepis inflexa inflexa*; Zhang, p. 233, pl. 26, figs. 13–16.

Material. Six specimens from samples CP/112g (2), CP/113a (1), CP/113c (1), CP/114a (1) and CP/120 (1).

Description. Narrow platform with suboval outline. Outer platform elevated forming a smooth bulge or parapet-like. Straight anterior inner margin, slightly concave that changes to slightly arched and convex posteriorly. Curved anterior carina; subtle posterior carina composed of few and small denticles or a thin crest that does not reach the posterior margin, which is subtriangular and slightly turned up. Absent free blade. Platform surface shagreen.

Discussion. *Pa. quadrantinodosa inflexa* has high morphological variably. Sandberg and Ziegler (1973) describe three morphotypes and Sandberg and Ziegler (1973) and Dreesen (1977) report intermediate forms between this taxon and *Pa. quad. inflexoidea*. The platform outline is similar with the *quadrantinodosa*-stock and *Pa. marg. marginifera*. It differs with *Pa. quad. inflexoidea* by the wider platform, the more anterior position of the azygous node and the presence of a posterior carina. It differs with *Pa. mg. marginifera* by the absence of a true parapet. It differs from *Pa. stoppeli* by a marked narrower platform.

Age and geographical distribution. From the Famennian lower part of the *gr. gracilis* Zone to the begging of the *mg. utahensis* Zone (Spalletta *et al.*, 2017). *Pa. quad. inflexa* has a broad geographical distribution.

Palmatolepis quadrantinodosa inflexoidea Ziegler, 1962b

Figure 8D

1962b *Palmatolepis quadrantinodosa inflexoidea* n. ssp.; Ziegler, p. 176, pl. 5, figs. 14–18.
1973 *Palmatolepis quadrantinodosa inflexoidea*; Sandberg & Ziegler, pl. 4, figs. 1–3.
1977 *Palmatolepis inflexa inflexoidea*; Dreesen, p. 517–518, pl. 1, figs. 45–49.
1993 *Palmatolepis quadrantinodosa inflexoidea*; Ji & Ziegler, p. 68, pl. 15, figs. 1–3, text-fig.17, fig. 11.
1995 *Palmatolepis inflexa inflexoidea*; Sanz-López, p. 525, pl. 41, figs. 8–9, 12.
2017 *Palmatolepis quadrantinodosa inflexoidea*; Lüddecke *et al.*, fig. 5h.
2017 *Palmatolepis inflexoidea*; Ovnatanova *et al.*, p. 1083–1084, pl. 51, figs. 1–2.

Material. One specimen from sample CP/114a.

Description. Slender and elongated platform with suboval outline. High outer platform developing a bulge-like. The outer and inner margin are subparallel and the inner margin is slightly straight. Curved anterior carina; posterior carina absent. Azygous node located in the posterior third of the platform. Subtriangular posterior margin, slightly turned downwards. Absent free blade. Platform surface smooth.

Discussion. Similarities and differences with *Pa. quad. inflexa* have already been discussed.

Age and geographical distribution. From Famennian *mg. marginifera* Zone to the lower part of *mg. utahensis* Zone (Spalletta *et al.*, 2017). *Pa. quad. inflexoidea* is recorded in Germany, Belgium, Poland, Spain, Russia, Australia, China, USA.

Palmatolepis quadrantinodosa quadrantinodosa Branson & Mehl, 1934

Figure 8E

1934 *Palmatolepis quadrantinodosa* n. sp.; Branson & Mehl, p. 235, pl. 18, figs. 3, 17, 20.
1973 *Palmatolepis quadrantinodosa quadrantinodosa*; Sandberg & Ziegler, pl. 3, figs. 29–30.
1974 *Palmatolepis quadrantinodosa*; Dreesen & Dusar, p. 27, pl. 5, figs. 9–14.
1977 *Palmatolepis quadrantinodosa*; Dreesen, p. 523, pl. 1, figs. 2–9.
1993 *Palmatolepis quadrantinodosa quadrantinodosa*; Ji & Ziegler, p. 69, text-fig. 17, fig. 13.
1993 *Palmatolepis quadrantinodosa quadrantinodosa*; Matyja, pl. 27, figs. 12–13.
2001 *Palmatolepis quadrantinodosa*; Johnston & Chatterton, p. 33, pl. 15, fig. 17.
2007 *Palmatolepis quadrantinodosa quadrantinodosa*; Over, figs. 14.16, 14.19–14.20.
2019 *Palmatolepis* cf. *quadrantinodosa*; Zhang, p. 232, pl. 27, figs. 1–4.

Material. Seven specimens from samples CP/114a (2), CP/114b (3), CP/118b (1), CP/119 (1).

Description. Broad platform with suboval outline. Slightly straight inner anterior margin that turns convex in the posterior half. High outer platform developing a bulge and ornamented by coarse nodes, some of them can be fused into a broad ridge; they connect the outer margin with the posterior half of the anterior

carina meeting in an acute angle. Curved anterior carina; short posterior carina, composed of two to three nodules, that does not reach the posterior end. Broad subtriangular posterior margin moderately turned up.

Discussion. The distinctive character of *Pa. quad. quadrantinodosa* is the presence of nodes in the outer platform. Sandberg and Ziegler (1973) described two morphotypes based in the orientation of the nodes: the first by rows and the second irregularly.

Age and geographical distribution. This taxon is exclusively recorded in the Famennian *mg. marginifera* Zone (Spalletta *et al.*, 2017). *Pa. quad. quadrantinodosa* is recorded in Belgium, Poland, China, Canada and USA.

Palmatolepis quadrantinodosalobata Sannemann, 1955b

Figure 4E–4F

1955b *Palmatolepis quadrantinodosalobata* n. sp.; Sannemann, p. 328, pl. 24, fig. 6.
1973 *Palmatolepis quadrantinodosalobata*; Sandberg & Ziegler, p. 105, pl. 4, figs. 33–41.
1973 *Palmatolepis quadrantinodosalobata* morphotype 1; Sandberg & Ziegler, p. 105–106, pl. 4, figs. 27–32.
1993 *Palmatolepis quadrantinodosalobata*; Ji & Ziegler, p. 69, pl. 23, figs. 5–7, fig.12, figs. 3,7–8.
1995 *Palmatolepis quadrantinodosalobata*; Rodríguez-Cañero, p. 18, 20, pl. III, figs. 10–11.
1995 *Palmatolepis quadrantinodosalobata*; Sanz-López, p. 534, pl. 40, figs. 2–4.
2003 *Palmatolepis quadrantinodosalobata*; Corradini, p. 83, pl. 5, figs. 7–9.
2011 *Palmatolepis quadrantinodosalobata*; Hartenfels, p. 270, pl. 40, figs. 1–3.
2013 *Palmatolepis quadrantinodosalobata*; Mossoni *et al.*, p. 25–27, fig. 5.14.
2015 *Palmatolepis quadrantinodosalobata*; Mossoni, p. 103, pl. 1, fig. 14.
2017b *Palmatolepis quadrantinodosalobata*; Valenzuela-Ríos *et al.*, fig. 4.7.
2017 *Palmatolepis quadrantinodosalobata*; Ovnatanova *et al.*, p. 1104, 1107, pl. 45, figs. 3, 5.
2019 *Palmatolepis quadrantinodosalobata* morphotype 1; Zhang, p. 217, pl. 21, figs. 5–8.

Material. 43 specimens form samples CP/98b (5), CP/98c (10), CP/99a (5), CP/99b (2), CP/99c (1), CP/99d-2 (4), CP/100 (1), CP/101b (3), CP/102b (2), CP/103 (2) and CP/104b (8).

Description. Subtriangular platform with well-developed lobe, approximately aligned with the azygous node. Roughly biconvex margins. Convex posterior inner margin and convex anterior inner margin, appears anterior to the outer margin. The lobe is well developed and elongated and positioned at the same level of the azygous node. Subtriangular to semicircular lobe outline directed laterally or slightly anteriorly; some specimens develop a thin ridge obliquely connecting the azygous node with the tip of the lobe (Fig. 4F). Slightly arched to straight anterior carina; straight posterior carina that almost reaches the posterior end. Posterior platform pointed and turned up. Free blade short. Outer platform ornamented by coarse discrete or fused nodes forming ridges perpendicular to the anterior carina; this ornamentation is restricted to the part anterior to the azygous node.

Discussion. *Pa. quadrantinodosalobata* is similar to *Pa. subperlobata* and *Pa. lobicornis* in the platform outline and well-developed lobe, however it differs from both by the coarse node ornamentation in the outer platform. Sandberg and Ziegler (1973) described the morphotype 1 based in the presence of nodes in the inner platform, which differs from *Pa. poolei* by the size of the lobe. Later, Ji and Ziegler (1993) described another two morphotypes. The morphotype 2 is most typical, characterized by a wider platform, well developed lobe and nodes in the outer platform. The morphotype 3, is characterized by a narrower platform, slightly arched to straight carina, pointed lobe and nodes in the outer platform. On the other hand, *Pa. quadrantinodosalobata* differs with *Pa. sandbergi*, which has nodes along entire outer platform.

Age and geographical distribution. From Famennian *crepida* to *rhomboidea* Zones (Spalletta *et al.*, 2017). The morphotype 1 appears from *gl. pectinata* to *rhomboidea* Zones (Sandberg & Ziegler, 1973). *Pa. quadrantinodosalobata* has cosmopolitan distribution.

Palmatolepis regularis Cooper 1931

Figure 4O–4P

1931 *Palmatolepis regularis* n. sp.; Cooper, p. 242, pl. 28, fig. 36.
1973 *Palmatolepis* cf. *regularis*; Sandberg & Ziegler, p. 106, pl. 4, figs. 14–26.
1993 *Palmatolepis* cf. *regularis*; Ji & Ziegler, pl. 20, figs. 1–2, text-fig. 16 figs. 7, 9.
1995 *Palmatolepis* cf. *regularis*; Rodríguez-Cañero, p. 20, pl. IV, figs. 11–12.
1995 *Palmatolepis* cf. *regularis*; Sanz-López, p. 534, pl. 39, figs. 9–10.
1999 *Palmatolepis* cf. *Pal. regularis*; Schülke, p. 45–46, pl. 10, fig. 8.
2004 *Palmatolepis regularis*; Klapper *et al.*, p. 381, figs. 7.28, 7.31.
2007 *Palmatolepis regularis*; Over, p. 1213, figs. 14.21–14.23.
2011 *Palmatolepis regularis*; Hartenfels, p. 270–271, pl. 41, fig. 5.
2015 *Palmatolepis regularis*; Mossoni, p. 104, pl. 1, fig. 12.
2019 *Palmatolepis regularis*; Zhang, p. 239, pl. 18, figs. 5–8.

Material. Two specimens from sample CP/99a.

Description. Sigmoidal platform with parallelogram outline without lobe. Anterior inner margin meets the carina anteriorly than the outer margin. Outer platform slightly elevated and bent. Strongly arched anterior carina; posterior carina, composed of several aligned nodules, straight or slightly oblique, almost reaching the posterior end, which is pointed and upwards turned.

The carinas pathway draws a sigmoidal layout. Short free blade. Smooth platform surface.

Discussion. Cooper (1931) described the holotype from a specimen imbedded in a shale matrix. Later, Ziegler (1962b) pointed that the described holotype belongs to the lower view and questioned its description. The next descriptions (see synonymy), based on platform outline similarities, have the cf. attribution. Klapper *et al.* (2004) provided upper views of the paratypes and a coincident description and platform outline with the holotype and finally, rejected the cf. attribution. Ji and Ziegler (1993) described two morphotypes of *Pa. regularis*, based on the platform width. The first morphotype has a narrow platform, however, the description is still questionable because of the similarity of this platform with *Pa. arta*. On the other hand, the anterior margins of *Pa. arta* appear at the same level, instead the inner anterior margin of *Pa. regularis* starts anteriorly to the outer margin. *Pa. regularis* differs with *Pa. subperlobata*, *Pa. linguiloba* and *Pa. lobicornis* by the absence of lobe.

Age and geographical distribution. From Famennian *min. minuta* Zone to lower half of *rhomboidea* Zone (Spalletta *et al.*, 2017). *Pa. regularis* is recorded in Spain, Italy, Germany, Belarus, Poland, Turkey, Uzbekistan, Mongolia, China, Canada and USA.

Palmatolepis rhomboidea Sannemann, 1955b

Figure 6F–6G

1955b *Palmatolepis rhomboidea* n. sp.; Sannemann, p. 329, pl. 24, fig. 14.
1993 *Palmatolepis rhomboidea*; Ji & Ziegler, p. 70, pl. 21, figs. 1–5, text-fig. 13, fig. 18.
1995 *Palmatolepis rhomboidea*; Sanz-López, p. 526, pl. 41, fig. 4, pl. 46, fig. 1.
1999 *Palmatolepis rhomboidea*; García-López *et al.*, pl. I, fig. 8.
2003 *Palmatolepis rhomboidea*; Corradini, p. 83, pl. 3, figs. 19–21.
2004 *Palmatolepis rhomboidea*; Klapper *et al.*, fig. 7.14.
2011 *Palmatolepis rhomboidea*; Narkiewicz & Bultynck, pl. XI, fig. 12.
2013 *Palmatolepis rhomboidea*; Mossoni *et al.*, p. 27–28, fig. 5.9.
2013 *Palmatolepis rhomboidea*; Savage, figs. 12.27–12.29.
2015 *Palmatolepis rhomboidea*; Mossoni, p. 104–105, pl. 1, fig. 9.
2019 *Palmatolepis rhomboidea rhomboidea*; Zhang, p. 230, pl. 26, figs. 1–4.
2020 *Palmatolepis rhomboidea*; Suttner *et al.*, fig. 6.13a–6.13b.
2020 *Palmatolepis rhomboidea*; Izokh *et al.*, fig. 3r–3s.

Material. 129 specimens from samples CP/107 (1), CP/109a (2), CP/109b (2), CP/110 (13), CP/111a-1 (5), CP/111a-2 (8), CP/111b (3), CP/111c (4), CP/112a (12) CP/112b (15), CP/112c (15), CP/112d (3), CP/113a (1), CP/114b (4), CP/115 (12), CP/117 (10), CP/118b (7), CP/119 (10) and CP/120 (2).

Description. Platform with rhomboidal outline and without marked lobe. The anterior inner margin meets the carina markedly anteriorly to the outer margin. The outer platform has an elongated parapet-like bulge. Straight to moderate arched anterior carina; posterior carina composed of a poor-developed thin ridge that does not reach the posterior end. Pointed posterior margin, slightly turned up. Short free blade. Platform surfaces smooth or shagreen.

Discussion. *Pa. rhomboidea* could resemble *Pa. min. minuta* in the platform outline; however, the latter has a narrower fusiform platform with a well-developed posterior carina and clear sigmoidal carina layout; besides *Pa. rhomboidea* develops a bulge in the outer platform.

Age and geographical distribution. From Famennian *rhomboidea* to *mg. utahensis* Zones (Spalletta *et al.*, 2017). *Pa. rhomboidea* has cosmopolitan distribution.

Palmatolepis stoppeli Sandberg & Ziegler, 1973

Figure 8C

1973 *Palmatolepis stoppeli* n. sp.; Sandberg & Ziegler, p. 107, pl. 3, figs. 1–11, pl. 5, fig. 13.
1993 *Palmatolepis stoppeli*; Ji & Ziegler, p. 71, pl. 14, figs. 7–12, text-fig. 17, fig. 12.
1995 *Palmatolepis stoppeli*; Sanz-López, p. 526.
2004 *Palmatolepis stoppeli*; Klapper *et al.*, fig. 7.15.
2011 *Palmatolepis stoppeli*; Narkiewicz & Bultynck, pl. 11, fig. 13.
2013 *Palmatolepis stoppeli*; Mossoni *et al.*, p. 28, fig. 6.19.
2015 *Palmatolepis stoppeli*; Mossoni, p. 108, pl. 2, fig. 19.
2017 *Palmatolepis stoppeli*; Ovnatanova *et al.*, p. 1108, 1111, pl. 49, figs. 1–3, pl. 51, fig. 8.
2019 *Palmatolepis stoppeli stoppeli*; Zhang, p. 231–232, pl. 26, figs. 7–8.

Material. 10 specimens from samples CP/113c (1), CP/114a (4), CP/117 (2), CP/118b (2) and CP/119 (1).

Description. Broad platform with suboval outline. The margin of the outer platform has an elevated ramp-like. Curved anterior carina; very short or absent posterior carina. The posterior margin is slightly pointed and can be somewhat turned up. Shagreen platform surface.

Discussion. The differences between *Pa. stoppeli* and *Pa. quad. inflexa* have been discussed above. Besides, the wider platform, *Pa. stoppeli* develops a ramp-like elevation on the outer margin. On the other hand, it differs from *Pa. mg. marginifera* by the lack of a true parapet in the outer platform.

Age and geographical distribution. From the Famennian upper part of *gr. gracilis* Zone to the lower half of *mg. marginifera* Zone (Spalletta *et al.*, 2017). *Pa. stoppeli* is recorded in Belgium, Italy, Spain, Germany, Poland, Russia, China, USA and Canada.

Palmatolepis subperlobata Branson & Mehl, 1934

Figure 5A

1934 *Palmatolepis subperlobata*; Branson & Mehl, p. 235, pl. 18, figs. 11, 21.

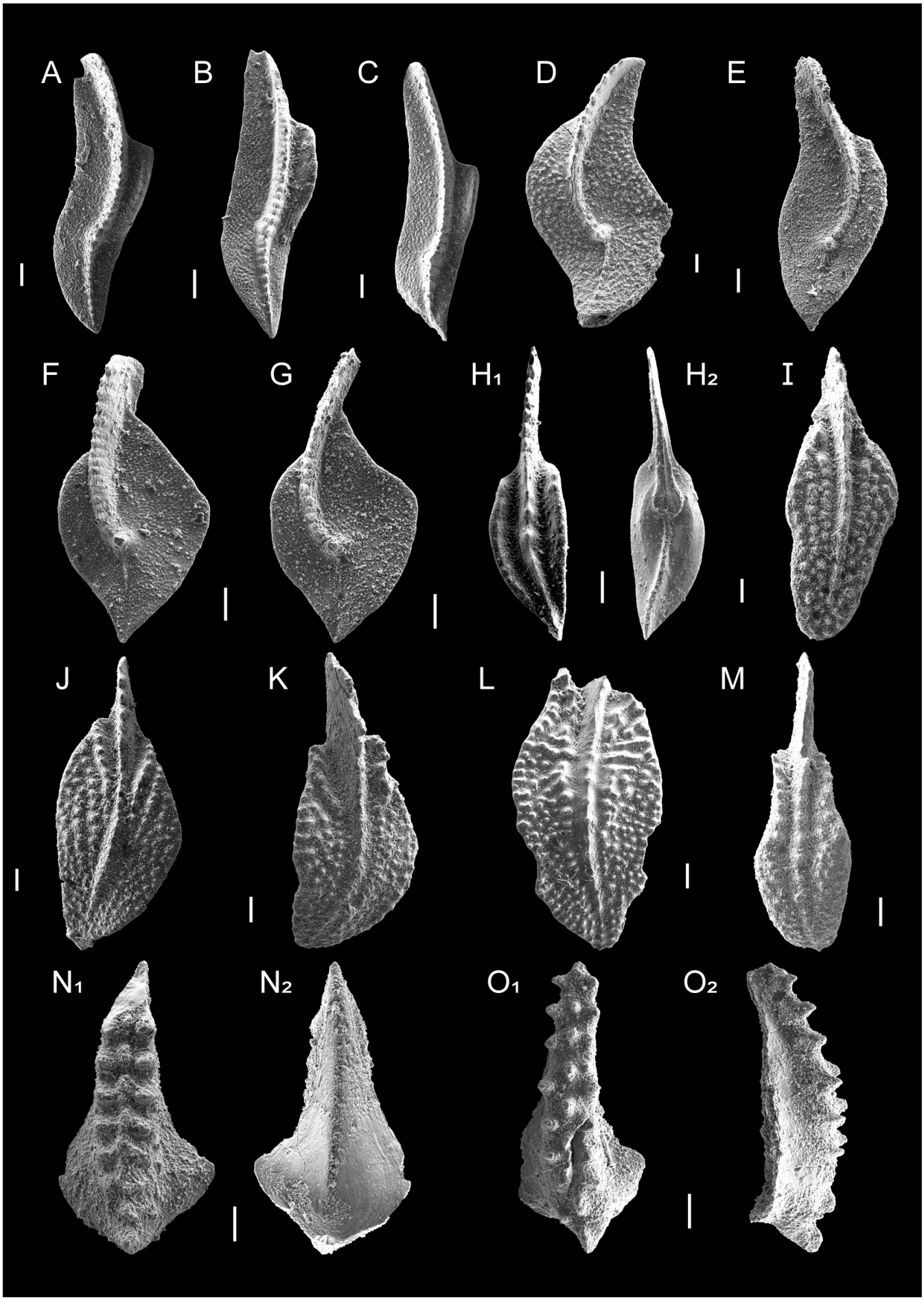
A
B
C
D
E
F
G
H1
H2
I
J
K
L
M
N1
N2
O1
O2

1993 *Palmatolepis subperlobata*; Ji & Ziegler, p. 72, pl. 20, figs. 3–9, pl. 21, figs. 11–12, text-fig. 16, figs. 5–6, 8.
1995 *Palmatolepis subperlobata*; Sanz-López, p. 535, pl. 39, figs. 14–15, pl. 40, fig. 1.
1997 *Palmatolepis subperlobata*; Over, p. 170, 172, figs. 10.2–10.3, 10.6–10.7, 10.9.
1999 *Palmatolepis subperlobata*; Schülke, p. 50–51, pl. 7, figs. 15–25.
2003 *Palmatolepis subperlobata*; Corradini, p. 84, pl. 3, figs. 1–4.
2004 *Palmatolepis subperlobata*; Klapper *et al.*, p. 380, figs. 7.35–7.36.
2007 *Palmatolepis subperlobata*; Klapper, pl. 2, figs. 1, 9.
2008 *Palmatolepis subperlobata*; Sánchez de Posada *et al.*, pl. 2, fig. 4.
2015 *Palmatolepis subperlobata*; Mossoni, p. 108–109, pl. 1, fig. 7.
2016 *Palmatolepis subperlobata*; Huang & Gong, fig. 5.3–5.4.
2019 *Palmatolepis subperlobata*; Zhang *et al.*, fig. 6.15.
2019 *Palmatolepis subperlobata*; Zhang, p. 243, pl. 22, figs. 1–16.
2021 *Palmatolepis* cf. *subperlobata*; Silvério *et al.*, p. 212, fig. 4M.

Material. Three specimens from samples CP/99a (2) and CP/99b (1).

Description. Platform slightly elongated, with subtriangular outline and well-developed lobe with sinuses. The inner margin meets the carina at a more anterior position than the outer and is slightly concave. The outer margin is moderately elevated and slightly convex in the anterior part and concave in the posterior one. Elongated lobe with subtriangular to rounded outline and laterally or anteriorly oriented in a position anterior to the azygous node. Arched to sigmoidal anterior carina; straight posterior carina, composed of several tiny nodules, ending close to the posterior end. Pointed to subtriangular posterior margin and slightly turned upwards. Short free blade. Platform surface shagreen or smooth that can be ornamented by fine nodes in the outer platform.

Discussion. *Pa. subperlobata* is similar to *Pa. triangularis* and *Pa. ultima* in the platform outline and the well-developed lobe, but it differs by having a less coarse, or lacking, platform ornamentation. Also, it shows some similarities with the *perlobata*-stock, but it separates from this group by a less elongated platform, less elevated outer platform and by the lobe outline. Finally, it can also be similar to *Pa. tenuipunctata*, but it can be discriminated by a less elongated platform and more developed lobe.

Age and geographical distribution. From Famennian *subperlobata* to *mg. marginifera* Zones (Spalletta *et al.*, 2017). *Pa. subperlobata* has cosmopolitan distribution.

Palmatolepis tenuipunctata Sannemann, 1955a

Figure 4C–4D

1955a *Palmatolepis tenuipunctata* n. sp.; Sannemann, p. 136, pl. 6, fig. 22.
1993 *Palmatolepis tenuipunctata*; Ji & Ziegler, p. 72, pl. 19, figs.1–6, text-fig.16, fig. 2.
1995 *Palmatolepis tenuipunctata*; Rodríguez-Cañero, p. 21, pl. IV, figs. 9–10.
1999 *Palmatolepis tenuipunctata*; García-López *et al.*, pl. I, fig. 4.
1999 *Palmatolepis glabra tenuipunctata*; Schülke, p. 35–36, pl. 3, figs. 14–27.
2001 *Palmatolepis tenuipunctata*; Johnston & Chatterton; p. 27, pl. 10, figs. 6–9, 11, 13–14.
2003 *Palmatolepis tenuipunctata*; Corradini, p. 84, pl. 3, figs. 11–13.
2011 *Palmatolepis tenuipunctata*; Hartenfels, p. 276–277, pl. 41, fig. 2.
2013 *Palmatolepis tenuipunctata*; Strelchenko & Kruchek, pl. 1, fig. 7.
2015 *Palmatolepis tenuipunctata*; Mossoni, p. 109, pl. 1, fig. 13.
2017b *Palmatolepis tenuipunctata*; Valenzuela-Ríos *et al.*, fig. 4.6.
2019 *Palmatolepis tenuipunctata*; Zhang, p. 246–247, pl. 23, figs. 9–12.
2020 *Palmatolepis tenuipunctata*; Bahrami *et al.*, fig. 9.41.

Material. 83 specimens from samples CP/98a (1), CP/98b (2), CP/98c (17), CP/99a (12), CP/99b (5), CP/99c (7), CP/99d-1 (2), CP/99d-2 (9), CP/101a (8), CP/101b (2), CP/102a (2), CP/102b (3), CP/103 (2), CP/104a (4) and CP/104b (7).

Description. Elongated platform with slightly sigmoidal outline and a small lobe. The anterior inner margin is moderately convex or straight and meets the carina with a convex pathway (Fig. 4D). Outer margin meets the carina posteriorly to the inner margin, convex and elevated in the anterior half. Small lobe with rounded outline, laterally or posteriorly oriented and located anteriorly to the azygous node. Anterior carina moderate curved; straight to slightly curved posterior carina that almost reaches the posterior end. The carinas pathway

Figure on previous page

Figure 6. A, *Palmatolepis glabra pectinata*, sample CP/111b; **B,** *Palmatolepis glabra pectinata*, sample CP/112e; **C,** *Palmatolepis glabra pectinata*, sample CP/105b; **D,** *Palmatolepis perlobata perlobata*, sample CP104c; **E,** *Palmatolepis* cf. *klapperi*, sample CP/107; **F,** *Palmatolepis rhomboidea*, sample CP/110; **G,** *Palmatolepis rhomboidea*, sample CP/112c; **H1,** *Polygnathus communis communis*, upper view, sample CP/107; **H2,** *Polygnathus communis communis*, lower view, sample CP/107; **I,** *Polygnathus nodocostatus nodocostatus*, sample CP/114b; **J,** *Polygnathus nodocostatus nodocostatus*, sample CP/112a; **K,** *Polygnathus nodocostatus nodocostatus*, sample CP/109a; **L,** *Polygnathus nodocostatus ovatus*, sample CP/105a; **M,** *Polygnathus nodocostatus ovatus*, sample CP/105a; **N1,** *Icriodus tumulosus*, upper view, sample CP/104c; **N2,** *Icriodus tumulosus*, lower view, sample CP/104c; **O1,** *Icriodus cornutus*, upper view, sample CP/109b; **O2,** *Icriodus cornutus*, lateral view, sample CP/109b; scale bar = 100 µm.

draws a sigmoidal layout. Subtriangular, pointed and turned upwards posterior margin. Smooth platform surface.

Discussion. In the Compte section, specimens from *Pa. tenuipunctata* are similar to those of *Pa. gl. prima* M1 in the platform outline. Nevertheless, they can be separated by the presence of a true lobe and the narrower platform of the former. The differences with *Pa. per. schindewolfi* have been described above.

Age and geographical distribution. From Famennian *min. minuta* to *gl. pectinata* Zones (Spalletta *et al.*, 2017). *Pa. tenuipunctata* has cosmopolitan distribution.

Palmatolepis termini Sannemann, 1955a

Figure 4A–4B

1955a *Palmatolepis termini* n. sp.; Sannemann, p. 149, pl. 1, figs. 1–3.
1993 *Palmatolepis termini*; Ji & Ziegler, p. 72, pl. 12, figs. 6–10, text-fig.13, fig. 5.
1995 *Palmatolepis termini*; Rodríguez-Cañero, p. 21, pl. IV, figs. 9–10.
1999 *Palmatolepis termini*; García-López *et al.*, pl. I, fig. 6.
1999 *Palmatolepis termini*; Schülke, p. 51–52, pl. 10, figs. 13–17.
2003 *Palmatolepis termini*; Corradini, p. 84, pl. 3, figs. 9–10.
2006 *Klapperilepis termini*; Dzik, p. 122, figs. 86M–86V, 133.
2013 *Palmatolepis termini*; Strelchenko & Kruchek, pl. I, fig. 25.
2019 *Palmatolepis termini*; Zhang *et al.*, fig. 6.21.

Material. 47 specimens from samples CP/98a (1), CP/98b (5), CP/98c (8), CP/99a (9), CP/99b (4), CP/99C (9), CP/99d-1 (1), CP/99d-2 (10).

Description. Elongated platform with lanceolate outline and without lobe. From the azygous node, one (Fig. 4B) or two (Fig. 4A) rows of nodes appear and extends along the anterior platform to the anterior margins. Inner margin meets the carina anteriorly. Straight anterior carina that strongly curved next to the azygous node; poorly developed or absent posterior carina that does not reach the posterior end. Pointed posterior margin. Flat or strongly turned upwards posterior platform. Smooth platform surface.

Discussion. The lanceolate platform outline is similar to *Pa. min. minuta* in but the presence of a row(s) of nodes in the anterior platform clearly distinguished both taxa.

Age and geographical distribution. From Famennian *termini* to *gl. prima* Zones (Spalletta *et al.*, 2017). *Pa. tenuipunctata* has cosmopolitan distribution.

Genus *Polygnathus* Hinde, 1879

Type species. *Polygnathus dubius* Hinde, 1879, Givetian–Frasnian, Europe, North America, Asia, North Africa.

Polygnathus bouckaerti Dreesen & Dusar, 1974

Figure 7N–7O

1974 *Polygnathus bouckaerti* n. sp.; Dreesen & Dusar, p. 11–12, pl. 1, figs. 1–7, pl. 2, figs. 1–12.
1993 *Polygnathus bouckaerti*; Matyja, pl. 30, fig. 9, pl. 31, fig. 1.
1995 *Polygnathus bouckaerti*; Sanz-López, p. 485.
1995 *Polygnathus bouckaerti*; Matyja & Narkiewicz, pl. IV, fig. 5.

Material. Two uncomplete specimens from samples CP/110 (1) and CP/111a-1 (1).

Description. Free blade is not preserved. Asymmetric and arched platform with oval outline; arched short carina, composed of 8 to 12 denticles that ends in the second third of the platform just before the subtriangular tongue with transverse ridges. Deep and narrow adcarinal throughs running parallel to the carina; lateral transversal short ridges or nodes are present in the anterior two thirds of the platform margins.

Discussion. Besides very different platform outline, *P. bouckaerti* can be distinguished from the *nodocostatus*-stock by the development of a tongue, which limits the extension of the carina to the anterior two thirds of the platform. It also differs from *Polylophodonta* taxa by the absence of the characteristic patterns of the platform ornamentation.

Age and geographical distribution. From Famennian *rhomboidea* to *mg. marginifera* Zones (Dreesen & Dusar, 1974). *P. bouckaerti* is recorded in Belgium, Spain and Poland.

Polygnathus brevilaminus Branson & Mehl, 1934

Figure 5J

1934 *Polygnathus brevilaminus* n. sp.; p. 146, pl. 21, figs. 3–6.
1993 "*Polygnathus brevilaminus*"; Ji & Ziegler, p. 75, pl. 35, figs. 1–3.
1995 *Polygnathus brevilaminus*; Sanz-López, p. 485–486, pl. 34, figs. 16–19.
1997 *Polygnathus brevilaminus*; Çapkınoğlu, p. 176, pl. 4, fig. 8.
1999 *Polygnathus brevilaminus*; García-López *et al.*, pl. II, figs. 2–3.
2003 *Polygnathus*? *brevilaminus*; Corradini, p. 87, pl. 8, figs. 1–2.
2006 *Ctenopolygnathus brevilamina*; Dzik, p. 84–85, figs. 55–56, 129.
2011 *Ctenopolygnathus brevilaminus*; Hartenfels, p. 236–237, pl. 61, fig. 5.
2013 *Polygnathus brevilaminus*; Bahrami *et al.*, fig. 8FF–8GG, 8PP–8QQ.
2018 *Polygnathus brevilaminus*; Bahrami *et al.*, fig. 6.36–6.37.
2019 *Polygnathus brevilaminus*; Zhang, p. 283, pl. 41, figs. 12–14.
2023 *Polygnathus brevilaminus*; Yuan & Sun, fig. 10C–10E.

Material. One specimen from sample CP/99a.

Description. Short and narrow rectangular platform with parallel margins; it does not reach the end of the element. Long and high free blade with denticles of different size and high, meets the straight carina obliquely. Carina extends beyond the platform at the

posterior end. Deep adcarinal grooves; platform lateral margins ornamented by fine nodes. Inner anterior platform margin joints at an obtuse angle the free blade and in an anterior position with respect to the outer margin; the latter joins perpendicularly the free blade.

Discussion. This taxon is distinguished by the short and narrow platform, which doesn't reach the end of the element and by its ornamentation, as well. The genus status of *P. brevilaminus* has been questioned and even some authors consider that a new genus should be erected (Ji & Ziegler, 1993; Corradini, 2003). Müller and Müller (1957) established the new genus *Ctenopolygnathus*, to accommodate this taxon (Dzik, 2002, 2006; Hartenfels, 2011).

Age and geographical distribution. From Frasnian *linguiformis* (FZ13b) Zone to Famennian *granulosus* Zone (Spalletta *et al.*, 2017). *P. brevilaminus* has a broad geographical distribution.

Polygnathus communis communis Branson & Mehl, 1934

Figure 6H1–6H2

1934 *Polygnathus communis* n. sp.; Branson & Mehl, p. 293, pl. 24, figs. 1–4.
1993 *Polygnathus communis communis*; Ji & Ziegler, p. 76, pl. 35, figs. 4–6, text-fig. 21, figs. 2, 5.
1995 *Polygnathus communis communis*; Sanz-López, p. 486–487, pl. 51, figs. 5–8.
1999 *Polygnathus communis communis*; García-López *et al.*, pl. II, fig. 5.
2000 *Polygnathus communis communis*; Çapkınoğlu & Gedík, pl. 5, figs. 25–26.
2006 *Neopolygnathus communis*; Dzik, p. 102, figs. 70A–70S, 130.
2011 *Neopolygnathus communis*; Hartenfels, p. 241–242, pl. 61, figs. 1–4.
2013 *Polygnathus communis communis*; Bahrami *et al.*, fig. 8H–8K, 8P.
2013 *Polygnathus communis communis*; Savage, figs. 11.23–11.25, 13.17–13.18.
2015 *Polygnathus communis communis*; Mossoni, p. 121, pl. 4, fig. 11.
2016 *Neopolygnathus communis communis*; Weiner & Kalvoda, fig. 5k.
2017 *Neopolygnathus communis communis*; Lüddecke *et al.*, fig. 4e.
2019 *Polygnathus communis communis*; Zhang, p. 273, pl. 43, figs. 9–10, pl. 52, figs. 17–18.
2020 *Polygnathus communis communis*; Bahrami *et al.*, fig. 8.19, 8.22.

Material. Four specimens from samples CP/106 (1), CP/107 (1), CP/109a (1) and CP/114a (1).

Description. Narrow and slightly arched, almost straight and symmetrical platform with lanceolate to ovate outline. Deep and narrow adcarinal grooves, high platform margins are elevated bearing nodes which are limited to the margins. Long, straight free blade, about half of element length, with 8 high denticles. The carina bens at its midlength, separating a denticulated anterior segment from a thin crest with few, if any, poorly developed and isolated denticles; it reaches the posterior end. Pointed posterior margin. Bulb-like basal cavity located in the anterior part of the platform; it follows posteriorly in a sulcate keel and anteriorly continues in an open and deep groove that narrows progressively to became appressed at the anterior end.

Discussion. The platform outline of *P. com. communis* can superficially resemble the *P. glaber*-stock; however, the platform of the latter is clearly bowed, wider, with sallow, or absent, adcarinal grooves and without ornamentation on the lateral margins. Basal cavity is very narrow, restricted to a pit, that continues to both ends in narrow, appressed sulci that close to both ends.

Age and geographical distribution. From Famennian *crepida* Zone to Tournaisian *anchoralis* Zone (Spalletta *et al.*, 2017). *P. com. communis* has a broad geographical distribution.

Polygnathus glaber eoglaber Ji & Ziegler, 1993

Figure 5K

1993 *Polygnathus eoglaber* n. sp.; Ji & Ziegler, p. 78, pl. 36, figs. 10–15, text-fig. 21, fig. 10.
2003 *Polygnathus glaber eoglaber*; Corradini, p. 82, pl. 8, fig. 2.
2015 *Polygnathus glaber eoglaber*; Mossoni, p. 124, pl. 5, fig. 14.

Material. Two specimens from samples CP/111a-2 (1) and CP/111b (1).

Description. Small and symmetrical platform with lanceolate outline and bowed margins. Straight carina that extends beyond the posterior part of the platform, forming a posterior free blade. Deep and narrow (restricted to an area adjacent to the carina) adcarianl grooves. Smooth platform surface.

Discussion. The free blade of the figurated specimen is broken (Fig. 5K), but the bowed, wide platform with restricted adcarinal grooves and smooth platform surface and posterior carina are distinctive characters in the *glaber*-stock.

Age and geographical distribution. From Famennian *min. minuta* to *gr. gracilis* Zones (Spalletta *et al.*, 2017). *P. gb. eoglaber* is recorded in France, Italy and China.

Polygnathus glaber glaber Ulrich & Bassler, 1926

Figure 8M–8N

1926 *Polygnathus glaber* n. sp.; Ulrich & Bassler, p. 46, pl. 7, fig.13.
1995 *Polygnathus glaber glaber*; Sanz-López, p. 495, pl. 47, fig. 13.
1993 *Polygnathus glaber glaber*; Ji & Ziegler, p. 79, pl. 36, figs. 1–6, text-fig. 21, fig. 11.
2003 *Polygnathus glaber glaber*; Corradini, p. 87–88, pl. 8, figs. 3–5.
2006 *Lagovignathus glaber*; Dzik, p. 104, figs. 71 A–L, 131.
2011 *Polygnathus glaber glaber*; Hartenfels, p. 284, pl. 51 figs. 1–3.

2013 *Polygnathus glaber glaber*; Savage, p. 31, figs. 11.20–11.22, 12.30–12.32, 13.11–13.13.
2015 *Polygnathus glaber glaber*; Mossoni, p. 125, pl. 2, fig. 13.
2017 *Polygnathus glaber glaber*; Lüddecke *et al.*, fig. 5i.
2017 *Polygnathus glaber glaber*; Ovnatanova *et al.*, pl. 49, figs. 5, 7.
2019 *Polygnathus glaber glaber*; Zhang, p. 274, pl. 43, figs. 1–4.
2020 *Polygnathus glaber glaber*; Bahrami *et al.*, fig. 8. 24.

Material. 35 specimens from samples CP/99c (2), CP/110 (2), CP/111a-1 (2), CP/111a-2 (1), CP/111b (1), CP/111c (2), CP/112a (5), CP/112b (4), CP/112e (2), CP/112g (2), CP/114b (1), CP/115 (1), CP/117 (6), CP/118a (1), CP/118b (1) and CP/119 (2).

Description. Bowed platform almost symmetrical with ovate to lanceolate outline. Moderately deep adcarinal grooves running through the platform close to the carina. Straight carina or slightly arched with fused denticles. Short free blade. Inner anterior margin joins the free blade in a more anterior position than the outer margin. Platform surface smooth or shagreen. Basal cavity located in the anterior third and reduced to a pit, which continues in narrow appressed sulci that taper to both ends.

Discussion. *P. gb. glaber* is similar to *P. gb. medius* in the platform outline, but it differs by deeper adcarinal grooves and because the platform anterior margins of *P. gl. medius* join the free blade at the same point conferring the platform a more symmetrical aspect. On the other hand, it differs from *P. gb. bilobatus* by the lack of a lobe in *P. gb. glaber*. The carina of *P. gb. eoglaber* extends beyond the platform posteriorly with the differences with *P. com. communis* are described above.

Age and geographical distribution. From Famennian *termini* to *rg. trachytera* Zones (Spalletta *et al.*, 2017). *P. gb. glaber* has cosmopolitan distribution.

Polygnathus glaber medius Helms & Wolska, 1967

Figure 8O–8P

1967 *Polygnathus glaber medius* n. ssp.; Helms & Wolska p. 233, pl. 15, figs. 2–3.
1990 *Polygnathus glaber medius*; Perri & Spalletta, pl. 5, fig. 3a–3b.
1993 *Polygnathus glaber medius*; Ji & Ziegler, p. 79, pl. 36, figs. 1–6, text-fig. 21, fig. 13.
1995 *Polygnathus glaber medius*; Sanz-López, p. 496.
1997 *Polygnathus glaber medius*; Çapkınoğlu, p. 178–179, pl. 5, figs. 5–9.
2009 *Polygnathus glaber medius*; Navas-Parejo *et al.*, fig. 4.10.
2017 *Polygnathus glaber medius*; Lüddecke *et al.*, fig. 5j.
2020 *Polygnathus glaber medius*; Izokh *et al.*, fig. 4m–4o.

Material. Eight specimens from samples CP/117 (3), CP/119 (4), CP/120 (1).

Description. Bowed platform with ovate or lanceolate outline; the anterior half is wider. Deep and narrow adcarinal grooves restricted to the anterior half. The margins might develop ridges in the anterior half (Fig. 8P). Anterior margins join the long free blade at the same point. Straight to slightly arched carina formed by moderately isolated denticles. High free blade bearing denticles, which are higher than those of the carina, and decreasing in high from the anterior end to the platform. Pointed posterior platform end. Except for the marginal nodes, the platform is smooth. Fine keel and reduced to a pit basal cavity.

Discussion. The differences with *P. gb. glaber* are discussed there.

Age and geographical distribution. From Famennian *mg. marginifera* to *mg. utahensis* Zones (Spalletta *et al.*, 2017). *P. gb. medius* is recorded in Germany, Spain, Italy, Turkey, Uzbekistan and China.

Polygnathus lauriformis Dreesen & Dusar, 1974

Figure 8I–8K

1974 *Polygnathus lauriformis* n. sp.; Dreesen & Dusar, p. 16, pl. 1, figs. 8–11, pl. 3, figs. 1–12.
1990 *Polygnathus lauriformis*; Perri & Spalletta, p. 65, pl. 5, figs. 6a–6b.
1993 *Polygnathus lauriformis*; Matyja, pl. 29, fig. 4.
1995 *Polygnathus lauriformis*; Sanz López, p. 500, pl. 47, figs. 7–10.
1998 *Polygnathus lauriformis*; Perri & Spalletta, pl. 1.3.1, fig. 11a–11b.
1999 *Polygnathus lauriformis*; García-López *et al.*, pl. II, fig. 8.
2006 *Polygnathus lauriformis*; Woroncowa-Marcinowska, fig. 15I.
2006 *Polygnathus lauriformis*; Dzik, p. 81, figs. 51N, 51O, 52A–52L.

Material. 41 specimens from samples CP/112c (1), CP/112f (2), CP/112g (5), CP/113a (4), CP/113c (4), CP/114a (12), CP/114b (5), CP/115 (3), CP/117 (1), CP/118b (3) and CP/119 (1).

Description. Moderately narrow and almost symmetrical platform with lanceolate outline. High and short free blade with 5–6 high denticles. Straight or slightly curved carina formed by denticles descending in high to the posterior end; in some specimens denticles are fused (Fig. 8I1). Narrow and deep adcarinal grooves. The platform is ornamented by, more or less, evenly spaced transverse ridges running from the platform margins to the adcarinal grooves. Rounded posterior margin. High keel excels the posterior end. Broad basal cavity located in the anterior third.

Discussion. *P. lauriformis* resembles *P. fallax* in the lanceolate platform outline; however, the latter has a narrower platform ornamented by nodes.

Age and geographical distribution. From Famennian *termini* to *vel. velifer* Zones (Spalletta *et al.*, 2017). *P. lauriformis* is recorded in Belgium, Italy, Spain and Poland.

Polygnathus longiusculus Çapkınoğlu, 1997

Figure 8Q

1997 *Polygnathus longiusculus* n. sp.; Çapkınoğlu, p. 180, pl. 5, figs. 19–25.
1999 *Polygnathus longiusculus*; Sanz-López *et al.*, pl. 2, fig. 16.
2015 *Polygnathus longiusculus*?; Mohamed, fig. 20a.

Material. One specimen from sample CP/118b.

Description. Narrow, elongated and symmetrical platform with ovate outline. Long, straight free blade, about half of the element, which continues in the straight carina depicting a straight medium line-like. Carina composed of nine denticles, which are closer (even fused) anteriorly and discrete posteriorly. Platform margins ornamented by nodes and ridges. Shallow and narrow adcarinal grooves. Pointed posterior margin.

Discussion. Platform outline and marginal nodes are similar to *P. fallax*, but the disposition of denticles on the carina distinguished both taxa.

Age and geographical distribution. *P. longiusculus* is exclusively recorded in the Famennian *mg. marginifera* Zone (Çapkınoğlu, 1997). *P. longiusculus* is recorded in Spain and Turkey.

Polygnathus nodocostatus nodocostatus Branson & Mehl, 1934

Figure 6I–6K

1934 *Polygnathus nodocostata*; Branson & Mehl, p. 246, pl. 20, figs. 9–13, pl. 21, fig. 15.
1993 *Polygnathus nodocostatus*; Ji & Ziegler, pl. 34, figs. 13–15, text-fig. 20, fig. 1.
1995 *Polygnathus nodocostatus nodocostatus*; Sanz López, p. 505, pl. 47, figs. 1–2.
1997 *Polygnathus nodocostatus nodocostatus*; Çapkınoğlu, p. 180, pl. 5, figs. 12–13.
2003 *Polygnathus nodocostatus nodocostatus*; Corradini, p. 89, pl. 9, figs. 1–2.
2011 *Polygnathus nodocostatus nodocostatus*; Hartenfels, p. 289, pl. 53, figs. 5–7.
2013 *Polynodosus nodocostatus nodocostatus*; Strelchenko & Kruchek, pl. I, fig. 43.
2015 *Polygnathus nodocostatus nodocostatus*; Mossoni, p. 128, pl. 2, figs. 3, 14.
2017 *Polygnathus nodocostatus nodocostatus*; Lüddecke *et al.*, fig. 5l.
2019 *Polygnathus nodocostatus*; Zhang, p. 278–279, pl. 42, figs. 1–5.
2020 *Polygnathus nodocostatus nodocostatus*; Bahrami *et al.*, fig. 9.2–9.3.
2020 *Polygnathus nodocostatus nodocostatus*; Suttner *et al.*, fig. 6.20a–6.20b.
2021 *Polygnathus nodocostatus*; Sattari *et al.*, fig. 6.23.

Material. 15 specimens from samples CP/105a (1), CP/105b (1), CP/107 (1), CP/109a (2), CP/111c (1), CP112a (1), CP/112b (1), CP/112c (3), CP/112d (1), CP/112e (1), CP/114b (1) and CP/116 (1).

Description. Slightly asymmetrical platform with diverse outlines, mainly ovate to rhombic. Platform width ranges from broad (more frequent) to narrow (Fig. 6l). Short free blade with few, high denticles. Straight to arched carina that does not reach de posterior end. The inner margin is straight or moderately convex, while the outer margin is convex. The platform is ornamented by rows of nodes, subparallel to the carina; nodes in broad-platform specimens are aligned in “V” forming ridges join the carina in an acute angle. Deep and short adcarinal grooves are restricted to the anterior part of the platform. The keel is fine and on the anterior third, a reduced basal cavity appears in the anterior third; it continues in thin keels.

Discussion. *P. nod. nodocostatus* is similar to others *nodocostatus*-stock taxa. *P. nod. ovatus* has a comparable platform outline, but the latter has a symmetrical platform with a marked constriction in the posterior third and an irregular arrangement of the nodes. *P. nodoundatus* shows a concave margin in the anterior outer platform, a strongly asymmetrical platform and irregular arrangement of the nodes. The absence of a collar separates *P. nod. nodocostatus* from *P. perplexus*. The platform of *P. granulosus* has a heart-like outline (broader in the anterior side and narrower in the posterior side), straight margins, irregular arrangement of nodes and absence of V-like ridges in the anterior side. *P. margaritatus* is similar to the narrow forms of *P. nod. nodocostatus*, but the distinctive collar and nearly fused rows of nodes parallel to the carina in the former, separates both taxa. The strongly asymmetrical and nearly sigmoidal outline of the platform distinguished *P. pennatuloideus* inform *P. nod. nodocostatus*. The carina of *P. diversus* is clearly offset.

Age and geographical distribution. From Famennian *crepida* to *gr. expansa* Zones (Spalletta *et al.*, 2017). *P, nod. nodocostatus* has a broad geographical distribution.

Polygnathus nodocostatus ovatus Helms, 1961

Figure 6L–6M

1961 *Polygnathus nodocostatus ovata* n. ssp.; Helms, p. 688–690, pl. 1, figs. 25–26, pl. 2, figs. 24, 27–28.
1995 *Polygnathus nodocostatus ovatus*; Sanz-López, p. 505.
1997 *Polygnathus nodocostatus ovatus*; Çapkınoğlu, p. 181, pl. 5, fig. 11.
2011 *Polygnathus nodocostatus ovatus*; Hartenfels, p. 290–291, pl. 53, figs. 8–9.
2013 *Polygnathus nodocostatus ovatus*; Rytina *et al.*, pl. 2, fig. 9.
2017 *Polygnathus nodocostatus ovatus*; Lüddecke *et al.*, fig. 5m.
2023 *Polygnathus nodocostatus ovatus*; Huang *et al.*, fig. 11B.

Material. Eight specimens from samples CP/105a (4), CP/105b (1), CP/109a (1), CP/112C (1) and CP/114b (1).

Description. Platform varies from broad to narrow, nearly symmetrical with ovate to lanceolate outline.

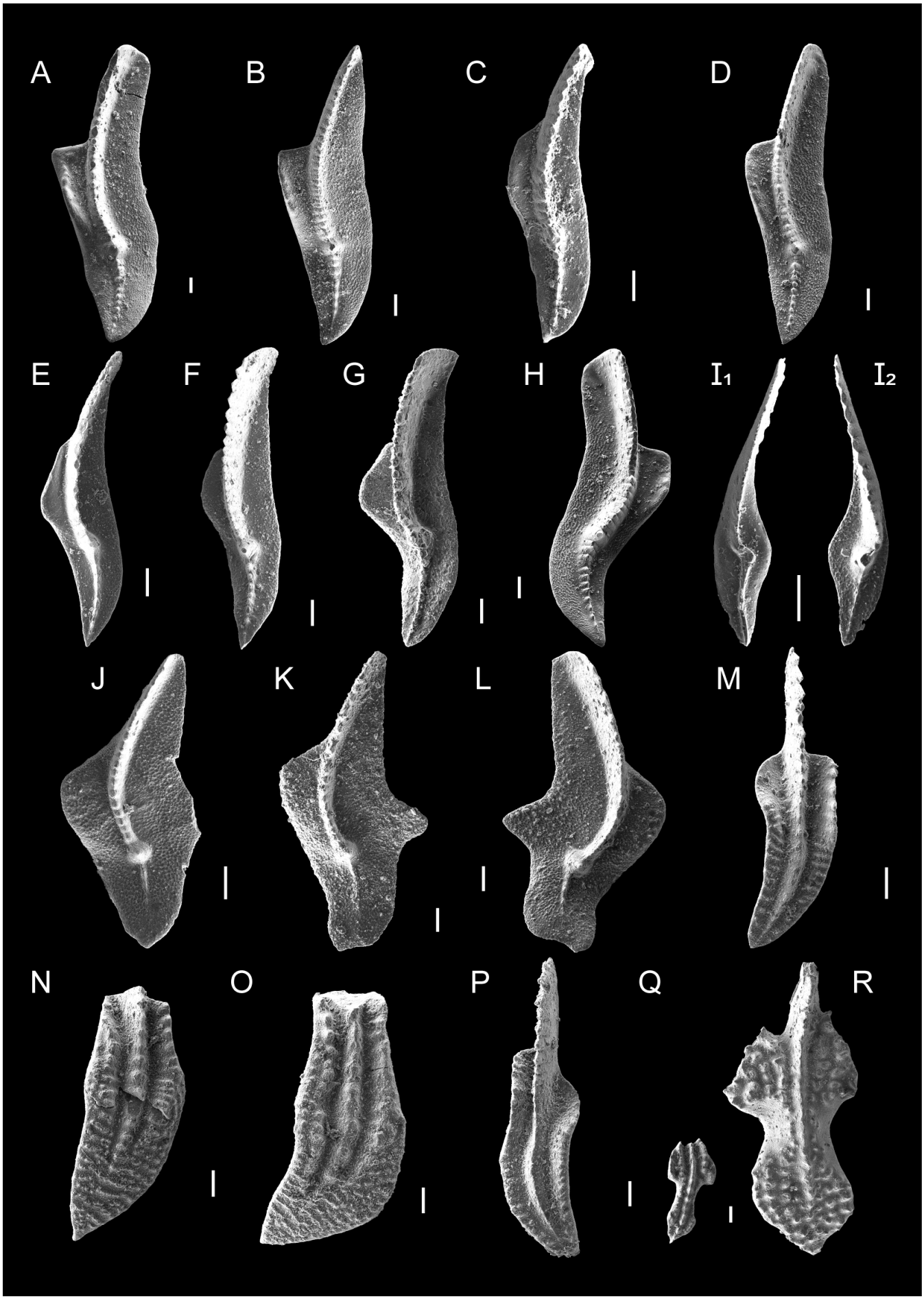
A
B
C
D
E
F
G
H
I1
I2
J
K
L
M
N
O
P
Q
R

Short free blade with fused denticles. Platform shows a constriction in the posterior part (broad forms) or in the anterior part (narrow forms). Slightly curved carina that ends before the posterior end. Platform ornamented by nodes, some of them fused in ridges, irregularly arranged or aligned in faint lines perpendicular or oblique to the carina (broad forms); the narrow forms have less nodes and most of them run parallel to the margins. Reduced basal cavity continues in thin keels.

Discussion. This differences with *P. nod. nodocostatus* have been described there.

Age and geographical distribution. From Famennian *gl. prima* to *styriacus* Zones (Spalletta *et al.*, 2017). *P. nod. ovatus* is recorded in Germany, Spain, Turkey and China.

Polygnathus padovanii Perri & Spalletta, 1990

Figure 7M

1990 *Polygnathus padovanii* n. sp.; Perri & Spalletta, p. 66, pl. 6, figs. 1–5, pl. 7, figs. 1–3.
1993 *Polygnathus limbatus* n. sp.; Matyja, p. 38, pl. 28, figs. 1–12.
1995 *Polygnathus padovanii*; Sanz-López, p. 507, pl. 48, fig. 1.
2003 *Polygnathus padovanii*; Corradini, p. 89–90, pl. 10, fig. 1.
2011 *Polygnathus padovanii*; Hartenfels, p. 299, pl. 51, figs. 6–10.
2017 *Polygnathus padovanii*; Ovnatanova *et al.*, p. 1132, pl. 48, fig. 9.
2017 *Polygnathus padovanii*; Lüddecke *et al.*, fig. 5n.
2020 *Polygnathus padovanii*; Bahrami *et al.*, figs. 8.23, 8.43, figs. 9.16, 9.18.
2021 *Polygnathus padovanii*; Sattari *et al.*, fig. 5.28–5.29.
2022 *Polygnathus padovanii*; Bahrami *et al.*, fig. 6.39.

Material. Nine specimens from samples CP/104c (1), CP/112e (2), CP/112g (2), CP/113a (2), and CP/113b (2).

Description. Moderately asymmetric and bowed platform with lanceolate outline. High anterior margins; the outer is straight and denticulated and the inner is bowed outwards; this differential development of the anterior part confers the platform an asymmetrical aspect, which is limited, however, to this first anterior fourth. The anterior margins join the blade at almost right angles. Straight carina that curves in the posterior half and reaches the posterior end. Platform is ornamented by thick and long transverse ridges along the platform. Wide and deep adcarinal grooves in the anterior part of the platform that change to narrow and shallow in the posterior part. Free blade about one third the length of the element, with about 6–7 denticles. The posterior end is pointed and moderately turned downwards. Reduced basal cavity continues in thin keels.

Discussion. The platform outline shows great variability and, in some cases, can be similar to *P. subnormalis* in Compte section; however, the latter is strongly asymmetrical, has more elevated anterior margins, deeper and broader adcarinal grooves, shorter ridges and the anterior margins do not join the free blade at the same point. Matyja (1993) described *P. limbatus* in the polish Pomerania region; this species shares diagnostic characters with *P. padovanii* like slender, arched and asymmetrical platform, elevated anterior margins with flange-like form and transversal ridges. Consequently, *P. limbatus* was considered as a junior synonym of *P. padovanii* (Corradini, 2003; Hartenfels, 2011).

Age and geographical distribution. According to Perri and Spalletta (1990) the range extends from Famennian *mg. utahensis* to *r. trachytera* Zones. Including the synonym list of *P. limbatus* as *P. padovanii*, the range extends to *gl. pectinata* Zone in the Lublin-basin area and *mg. marginifera* Zone in West-Pomerania (Matyja, 1993). Corradini (2003) mentioned a longer record in the Carnic Alps from the original range. Hartenfels (2011) extends its range to *granulosus* Zone in the Thuringia region. In central Iran region, the lower range is recorded from the *rhomboidea* Zone (Sattari *et al.*, 2021) and in the North Iran region, is recorded from *gl. pectinata* to *granulosus* Zones (Bahrami *et al.*, 2022). *P. padovanii* has a broad geographical distribution.

Polygnathus procerus Sannemann, 1955b

Figure 5I1–5I2

1955b *Polygnathus procerus* n. sp.; Sannemann, p. 150, pl. 1, fig. 11.
1993 *Polygnathus procerus*; Ji & Ziegler, p. 83–84, pl. 38, figs. 4–8, text-fig. 21, fig. 1.
1993 *Polygnathus procerus*; Matyja, pl. 24, fig. 10, pl. 26, fig. 1.
1999 *Polygnathus procerus*; Schülke, p. 63–64, pl. 13, figs. 1–11.
1999 *Polygnathus procerus*; García-López *et al.*, pl. II, fig. 7.

Figure on previous page

Figure 7. A, *Palmatolepis glabra acuta*, sample CP/111b; **B,** *Palmatolepis glabra acuta*, sample CP/112b; **C,** *Palmatolepis glabra lepta* early morphotype, sample CP/111c; **D,** *Palmatolepis glabra lepta* early morphotype, sample CP/112b; **E,** *Palmatolepis glabra lepta* late morphotype, sample CP/118b; **F,** *Palmatolepis glabra lepta* late morphotype, sample CP/114b; **G,** *Palmatolepis glabra lepta* late morphotype, sample CP/118a; **H,** *Palmatolepis glabra glabra*, sample CP/112d; **I1,** *Palmatolepis gracilis gracilis*, lower view, sample CP/112a; **I2,** *Palmatolepis gracilis gracilis*, upper view, sample CP/112a; **J,** *Palmatolepis perlobata helmsi*, sample CP/117; **K,** *Palmatolepis perlobata schindewolfi*, CP/112g; **L,** *Palmatolepis perlobata schindewolfi*, CP/119; **M,** *Polygnathus padovanii*, sample CP/112e; **N,** *Polygnathus bouckaerti*, sample CP/111a-1; **O,** *Polygnathus bouckaerti*, sample CP/110; **P,** *Polygnathus subnormalis*, sample CP/112b; **Q,** *Polygnathus triphyllatus* juvenile specimen, sample CP/113a; **R,** *Polygnathus triphyllatus* adult specimen, sample CP/112e; scale bar = 100 µm.

2003 *Polygnathus procerus*; Corradini, p. 90, pl. 8, fig. 14.
2007 *Polygnathus procerus*; Gholamalian, fig. 10O–10P.
2008 *Polygnathus procerus*; Sánchez de Posada *et al.*, pl. 1, figs. 18–19.
2013 *Polygnathus procerus*; Bahrami *et al.*, fig. 8OO.
2016 *Polygnathus procerus*; Huang & Gong, figs. 7.4, 7.18.
2020 *Polygnathus procerus*; Suttner *et al.*, fig. 6.21a–6.21b.
2021 *Polygnathus procerus*; Zamani *et al.*, pl. 4, fig. 10.

Material. Six specimens from samples CP/99a (4) and CP/99b (2).

Description. Small, slender, slightly asymmetrical platform with lanceolate outline. Straight, fan-shape free blade with 9 denticles; it represents about 1/3 of the platform length. Bowed platform with posterior half strongly turned downward. Outer margin with a sinuous outline with a weak constriction in the anterior half; inner margin straight. High anterior margins and slightly concave outwards, the outer more markedly. Deep and broad adcarinal grooves in the anterior half that shallows to disappear in the posterior half. Carina denticles fused in a thin arched crest to the posterior end. Weak transverse ridges irregularly spaced and more abundant in the posterior half. Reduced basal cavity continues in thin keels.

Discussion. *P. procerus* resembles *P. praecursor*; however, the narrower and slenderer platform ornamented with fine transverse ridges separate both taxa.

Age and geographical distribution. Initially, Ji and Ziegler (1993) extend the range from Frasnian *rot. rotundiloba* (FZ2b) to *gl. prima* Zones. In the Montagne Noire, Schülke (1999) limited its range to the Famennian, from the upper part of the *triangularis* Zone to *gl. prima* Zone. In Sardinia, Corradini (2003) extended the record to the *gl. pectinata* Zone. However, in Central Iran Bahrami *et al.*, (2013) extended its range downward from Frasnian *bogartensis* (FZ13a) Zone and Zamani *et al.* (2021) recorded this taxon up to the *gl. pectinata* Zone. In South China, Huang and Gong (2016) recorded this species from the *linguiformis* (FZ13) Zone. Finally, Spalletta *et al.*, (2017) restricted the range from the *min. minuta* to *gl. pectinata* Zones. *P. procerus* is recorded in France, Italy, Spain, Turkey, Iran and China.

Polygnathus semicostatus Branson & Mehl, 1934

Figure 5L–5N

1934 *Polygnathus semicostata* n. sp.; Branson & Mehl, p 247–248, pl. 21, figs. 1–2.
1974 *Polygnathus semicostatus*; Dreesen & Orchard, p. 3, pl. 1, figs. 1–8, pl. 2, figs. 1–25.
1979 *Polygnathus semicostatus*; Sandberg & Ziegler, p. 187, pl. 5, figs. 1–5.
1993 *Polygnathus semicostatus*; Ji & Ziegler, p. 84, text-fig. 19, fig. 4.
1993 *Polygnathus semicostatus*; Sanz-López, p. 513, pl. 47, figs. 4–6, 11–12.
2003 *Polygnathus semicostatus*; Corradini, p. 90, pl. 10, fig. 6.
2009 *Polygnathus semicostatus*; Over *et al.*, fig. 4.3–4.4.
2011 *Polygnathus semicostatus*; Hartenfels, p. 299–300, pl. 59, figs. 1–10, pl. 61, fig. 6.
2011 *Polygnathus semicostatus*; Narkiewicz & Bultynck, pl. XII, fig. 6.
2013 *Polygnathus semicostatus*; Rytina *et al.*, pl. 2, fig. 11.
2013 *Polygnathus semicostatus*; Bahrami *et al.*, p. 382, fig. 9LL.
2020 *Polygnathus semicostatus*; Bahrami *et al.*, fig. 8.25–8.27, 8.44.

Material. 28 specimens from samples CP/101b (1), CP/105a (7), CP/105b (4), CP/105d (1), CP/106 (5), CP/109b (1), CP/110 (4), CP/111a-1 (3), CP/112f (1) and CP/112g (1).

Description. Broad to elongated platform with tongue-shape outline. Short, straight free blade with fused denticles; it continues “in line” with the straight carina, consisting also of a crest of fused denticles that do not reach the posterior end because in the posterior third a tongue with transverse ridges develops. Straight to oblique anterior margins, slightly high, joining the free blade at the same point. Narrow and moderately shallow adcarinal grooves that end before the posterior tongue. Posterior platform turned downward. Long, transverse ridges run from the margins perpendicular to the carina up to the adcarinal grooves. Reduced basal cavity continues in thin keels.

Discussion. This species has a high morphological variety, Dreesen and Orchard (1974) described eight morphological trends, which were based on the increase of the number of transversal ridges in the posterior platform, the flexion of the platform, the deepening of the adcarinal grooves and the wide of the tongue. The two most frequent forms are: 1) the “central morphotype” with a tongue-shape outline platform, margins convex or straight and the wide tongue with transverse ridges; 2) the morphotype 3 of Dreesen and Orchard (1974), characterized by a narrower platform and a constriction of the posterior end at the last nodule level. *P. semicostatus* differs from *P. obliquicostatus* because the latter has oblique transverse ridges.

Age and geographical distribution. From Famennian *termini* to *ultimus* Zones (Spalletta *et al.*, 2017). *P. semicostatus* has a broad geographical distribution.

Polygnathus subnormalis Vorontsova & Kuzmin, 1984

Figure 7P

1984 *Polygnathus subnormalis* n. sp.; Vorontsova & Kuzmin, p. 62, pl. 1, figs. 6–10.
1990 *Polygnathus subnormalis*; Kuzmin, p. 67–68, pl. 4, figs. 7, 10.
1994 *Polygnathus subnormalis*; Metzger, p. 640, 644, fig. 19.10–19.22.
1997 *Polygnathus subnormalis*; Çapkınoğlu, p. 181, pl. 5, fig. 18.
1997 *Polygnathus subnormalis*; Mawson & Talent, p. 222, fig. 15.9–15.14.
2003 *Polygnathus subnormalis*; Corradini, p. 91, pl. 10, fig. 2.
2005a *Polygnathus subnormalis*; Çapkınoğlu, fig. 5.24.

2019 *Polygnathus subnormalis*; Zhang, p. 270, pl. 52, figs. 25–28, 37.
2020 *Polygnathus subnormalis*; Suttner *et al.*, fig. 6.17a–6.17b.
2021 *Polygnathus subnormalis*; Zhang *et al.*, fig. 4Y–4AB, 4AK.

Material. Five specimens from samples CP/112b (1), CP/112f (1), CP/113b (1) and CP/113c (2).

Description. Moderately slender, strongly asymmetrical platform with lanceolate outline. Short free blade, about 1/4 of platform length, with denticles fused in a thin crest that continues in the curved and bowed carina, which is represented by a thin crest that ends close before the posterior end. High anterior margins; the outer anterior is slightly constricted, bear a few denticles and joins the free blade at a markedly anterior position than the inner one. A denticulate inner anterior margin, outward bowed. Deep anterior adcarinal grooves that shallow posteriorly. Platform ornamented by fine transverse ridges. Posterior margin is moderately downward turned.

Discussion. The difference with *P. padovanii* has been discussed above. The platform outline of *P. buzmakovi* is similar, but the more symmetrical and wider platform, ornamented by fine ridges and nodes and straight anterior margins enables separation between the two taxa.

Age and geographical distribution. From Famennian *rhomboidea* to *granulosus* Zones (Kuzmin, 1990). *P. subnormalis* is recorded in Russia, Italy, Turkey, Spain, Australia, Mongolia, China and USA.

Polygnathus triphyllatus Helms, 1961
Figure 7Q–7R

1961 *Polygnathus triphyllata* Helms, p. 696, pl 1, figs. 2–3, pl. 3, figs. 12, 15–17.
1994 *Polygnathus* cf. *triphyllatus*; Metzger, p. 644, fig. 19.7–19.9.
1997 *Polygnathus triphyllatus*; Çapkınoğlu, p. 181, pl. 5, figs. 16–17.
2003 *Polygnathus triphyllatus*; Corradini, p. 91, pl. 91, figs. 11–13.
2006 *Polynodosus triphyllatus*; Dzik, p. 81, 82, fig. 54A–54I.
2020 *Polygnathus triphyllatus*; Bahrami *et al.*, fig. 9.1.
2022 *Polygnathus triphyllatus*; Bahrami *et al.*, figs. 5.7, 7.20.

Material. Eight specimens from samples CP/112e (3), CP/112g (1), CP/113a (2), CP/114a (1) and CP/118a (1).

Description. Symmetrical, slightly curved platform with a strong constriction about the middle part conferring an inverted violin-shape outline. Concave anterior margins joining the free blade at different positions (the inner more anteriorly). Platform ornamented by parallel rows of coarse nodes. Shallow adcarinal grooves. Short free blade. Juvenile specimens (Fig. 7Q) have a small, slender, arched and constricted platform, with moderately deep adcarinal groves and ornamented by a unique row of nodes, parallel to the carina, in both sides.

Discussion. The most distinctive feature of *P. triphyllatus* is the middle constriction of the platform. Pa elements described as *P.* cf. *diversus* in Metzger (1994) may belong to juvenile specimens of *P. triphyllatus*.

Age and geographical distribution. From the upper half of the Famennian *gr. gracilis* Zone to the lower half of the *mg. marginifera* Zone (Spalletta *et al.*, 2017). *P. triphyllatus* is recorded in Italy, Spain, Germany, Poland, Turkey, Iran and USA.

Order PRIONIODONTIDA Dzik, 1976
Family ICRIODONTIDAE Müller & Müller, 1957

Genus *Icriodus* Branson & Mehl, 1938

Type species. *Icriodus expansus* Branson & Mehl, 1938, Givetian–Frasnian, Europe, North America, North Africa.

Icriodus alternatus alternatus Branson & Mehl, 1934
Figure 5E–5F

1934 *Icriodus alternatus alternatus* n. sp.; Branson & Mehl, p. 225–226, pl. 13, figs. 4–6.
1984 *Icriodus alternatus alternatus*; Sandberg & Dreesen, pl. 2, figs. 5, 11.
1993 *Icriodus alternatus alternatus*; Ji & Ziegler, p. 55, pl. 5, figs. 5–8, text-fig. 6, fig. 2.
1995 *Icriodus alternatus alternatus*; Sanz-López, p. 428–429, pl. 35, fig. 12, pl. 36, figs. 4–11.
2003 *Icriodus alternatus alternatus*; Corradini, p. 92, pl. 2, figs. 9–12.
2013 *Icriodus alternatus alternatus* morphotype 1; Hartenfels, pl. 39, figs. 1–3.
2013 *Icriodus alternatus alternatus*; Bahrami *et al.*, p. 384, 386, fig. 9F–9K.
2015 *Icriodus alternatus alternatus*; Mossoni, p. 143–144, pl. 1, fig. 5.
2017b *Icriodus alternatus alternatus*; Valenzuela-Ríos *et al.*, fig. 4.1.
2017 *Icriodus alternatus alternatus*; Ovnatanova *et al.*, pl. 54, figs. 6–8.
2020 *Icriodus alternatus alternatus*; Suttner *et al.*, fig. 6.5a–6.5b.

Material. 49 specimens from samples CP/98a (1), CP/98b (4), CP/98c (1), CP/99a (1), CP/99b (14), CP/99c (2), CP/99d-1 (1), CP/99d-2 (3), CP/101a (1), CP/101b (11), CP/102b (2), CP/104a (2), CP/104c (5) and CP/111a-1 (1).

Description. Biconvex to very slightly concave-convex, elongated and narrow platform with parallel sides composed of 6–7 transversal rows of disconnected, rounded, laterally compressed denticles with the middle row ones located anterior to the corresponding lateral ones. The middle row continues posteriorly with two cusps aligned with this row. Rounded, semicircular expansions reaching the third or fourth lateral rows. Expanded, fully excavated drop shaped basal cavity, which is wider and deeper posteriorly.

Discussion. This taxon is similar to *Ic. alternatus helmsi*, however, the latter differs because the cusp

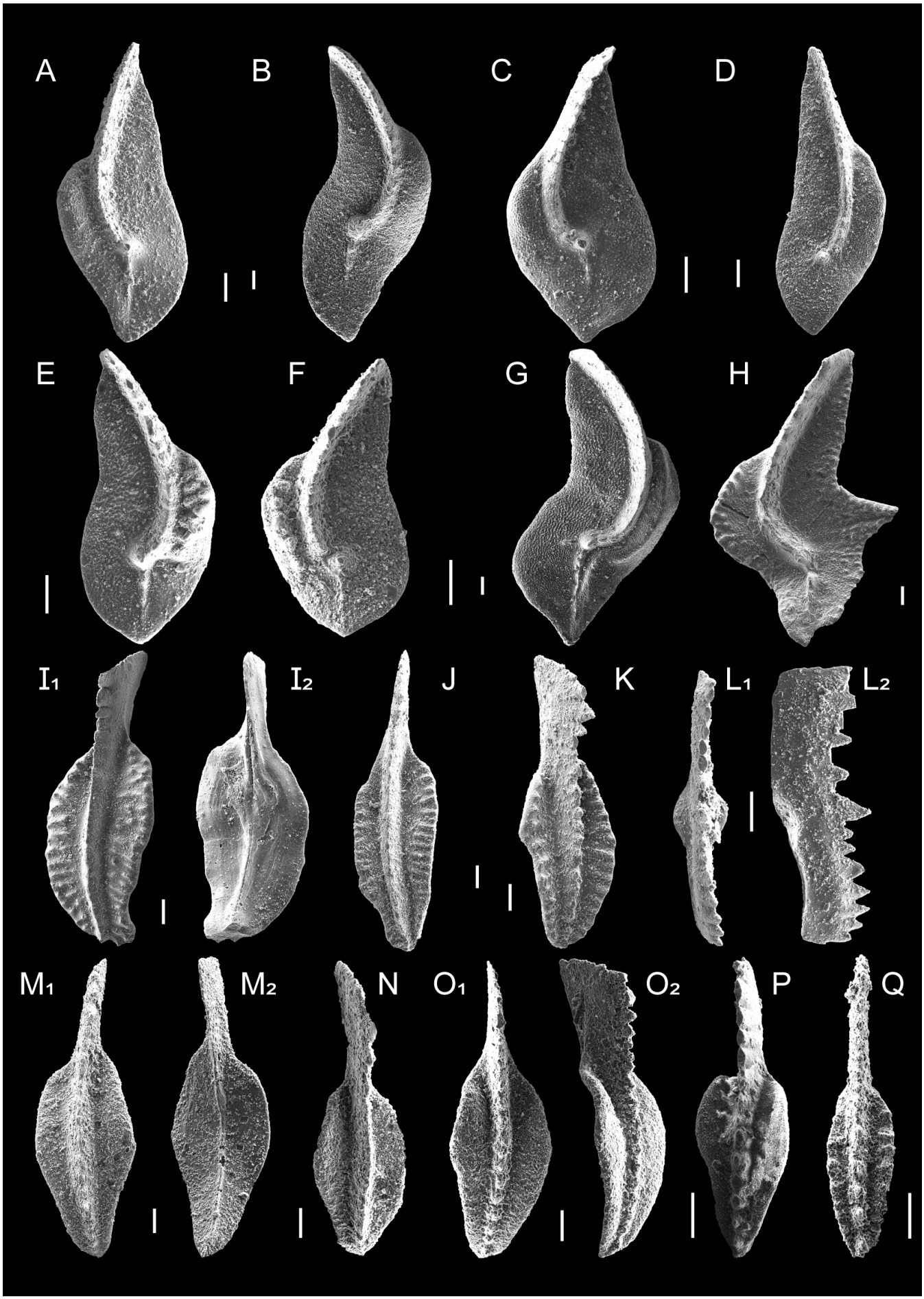
A
B
C
D
E
F
G
H
I1
I2
J
K
L1
L2
M1
M2
N
O1
O2
P
Q

is not aligned with the middle row. Sandberg and Dreesen (1984) reported two morphotypes of *Ic. alt. alternatus* according to the compression of the middle row denticles. The first morphotype is characterized by the laterally compressed and elongated middle row denticles and the second morphotype is characterized by the rounded middle row denticles.

Age and geographical distribution. From Frasnian *bogartensis* (FZ13a) Zone to Famennian *gl. pectinata* Zone (Bultynck, 2003). *Ic. alt. alternatus* has cosmopolitan distribution.

Icriodus alternatus mawsonae Yazdi, 1999

Figure 5G–5H

1991 *Icriodus alternatus* n. ssp.; Clausen *et al.*, pl. 8, fig. 4.
1999 *Icriodus alternatus mawsonae* n. ssp.; Yazdi, p. 197, pl. 1, fig. 15, pl. 2, figs. 3–4.
1999 *Icriodus alternatus mawsonae*; Talent *et al.*, pl. 5, fig. 9.
2000 *Icriodus alternatus mawsonae*; Yazdi *et al.*, p. 201, fig. 4.9–4.13.
2007 *Icriodus alternatus mawsonae*; Gholamalian, p. 465, fig. 9R.
2009 *Icriodus alternatus mawsonae*; Gholamalian *et al.*, pl. 1, fig. 5.
2020 *Icriodus alternatus mawsonae*; Becker *et al.*, fig. 19.18.

Material. 18 specimens from samples CP/98a (1), CP/98c (1), CP/99a (3), CP/99b (4), CP/99d-2 (5), CP/101b (2) and CP/102b (2).

Description. Biconvex to moderately concave-convex, elongate platform. Lateral rows composed of 8–9 denticles that can be fused. Middle row weakly developed or absent, in the posterior half of the platform. When transversal rows consist of three denticles, the middle one is advanced anteriorly. Reduced cusp of irregular shape. Drop shaped basal cavity, wider and deeper posteriorly, shallowing and narrowing anteriorly. Basal cavity expansions reach different positions; frequently the outer one roughly extends more anteriorly than the inner.

Discussion. The weak or absent middle row denticles in the posterior half distinguish this taxon from *Ic. alt. alternatus.*

Age and geographical distribution. From Frasnian *ultima* (FZ13c) Zone to the Famennian first half of the *gl. prima* Zone (Spalletta *et al.*, 2017). *Ic. alt. mawsonae* is recorded in Iran, Pakistan and Morocco.

Icriodus cornutus Sannemann, 1955b

Figure 6O1– 6O2

1955b *Icriodus cornutus* n. sp.; Sannemann, p. 130, pl. 4, figs. 19–21.
1984 *Icriodus cornutus*; Sandberg & Dreesen, p. 162, pl. 2, fig. 8, pl. 4, figs. 19–20.
1993 *Icriodus cornutus*; Matyja, pl. 24, fig. 1.
1997 *Icriodus cornutus*; Çapkınoğlu, p. 183, pl. 4, figs. 1–2.
1999 *Icriodus cornutus*; Sanz-López *et al.*, pl. 1, figs. 8–9.
1999 *Icriodus cornutus*; Schülke, p. 66–67, pl. 13, figs. 19–20.
2006 *Icriodus cornutus*; Dzik, p. 32–33, fig. 11A–11G.
2013 *Icriodus cornutus*; Bahrami *et al.*, fig. 9L–9P.
2013 *Icriodus cornutus*; Savage, fig. 10.4–10.6.
2019 *Icriodus cornutus*; Zhang, p. 168, pl. 51, figs. 10, 15–18.
2023 *Icriodus cornutus*; Yuan & Sun, fig. 9A–9B.

Material. One specimen from sample CP/109b.

Description. Narrow, slightly curved, elongated, platform. 6 transversal rows of disconnected denticles, with the middle ones advanced. Middle row continues in two reclined cusps, being the posterior one higher and projected outward. In lateral view, the unit is strongly bowed. Asymmetrical basal cavity.

Discussion. The strongly reclined cusp is the most characteristic feature of *Ic. cornutus*.

Age and geographical distribution. From Famennian *del. platys* to *granulosus* Zones (Spalletta *et al.*, 2017). *Ic. cornutus* has a broad geographical distribution.

Icriodus tumulosus Sanz-López, 1995

Figure 6N1–6N2

1955b *Icriodus nodosus*; Sannemann, pl. 4, figs. 17–18.
1970 *Icriodus symmetricus*; Olivieri, pl. 14, figs. 8–9.
1995 *Icriodus tumulosus* n. sp.; Sanz-López, p. 444–445, pl. 37, figs. 4–20.
1999 *Icriodus tumulosus*; García-López *et al.*, pl. II, fig. 20.

Material. Three specimens from sample CP/104c.

Description. Straight to slightly curved biconvex or concave-convex platform, with spindle-shape outline. Six transversal rows of close, almost touching, but isolated denticles with the middle ones clear (in the posterior part) to slightly (in the anterior part) advanced. Posterior carina with 2–3 denticles growing in high posteriorly and aligned with the middle row denticles. The anterior expansion or spur is laterally

Figure on previous page

Figure 8. A, *Palmatolepis quadrantinodosa inflexa*, sample CP/113c; **B,** *Palmatolepis quadrantinodosa inflexa*, sample CP/112g; **C,** *Palmatolepis stoppeli*, sample CP/113c; **D,** *Palmatolepis quadrantinodosa inflexoidea*, sample CP/114a; **E,** *Palmatolepis quadrantinodosa quadrantinodosa*, sample CP/114a; **F,** *Palmatolepis marginifera marginifera*, sample CP/114a; **G,** *Palmatolepis marginifera marginifera*, sample CP/115; **H,** *Palmatolepis perlobata sigmoidea*, sample CP/117; **I1,** *Polygnathus lauriformis*, upper view, CP/113a; **I2,** *Polygnathus lauriformis*, lower view, sample CP/113a; **J,** *Polygnathus lauriformis*, sample CP/113a; **K,** *Polygnathus lauriformis*, sample CP/113c; **L1,** *Mehlina strigosa*, upper view, sample CP/114a; **L2,** *Mehlina strigosa*, lateral view, sample CP/114a; **M1,** *Polygnathus glaber glaber*, upper view, sample CP/112b; **M2,** *Polygnathus glaber glaber*, lower view, sample CP/112b; **N,** *Polygnathus glaber glaber*, sample CP/112a; **O1,** *Polygnathus glaber medius*, upper view, sample CP/119; **O2,** *Polygnathus glaber medius*, lateral view, sample CP/119; **P,** *Polygnathus glaber medius*, sample CP/117; **Q,** *Polygnathus longiusculus*, sample CP/118b; scale bar = 100 µm.

or slightly anteriorly directed. Deep, broadly expanded asymmetrical basal cavity that narrows anteriorly.

Discussion. The number of denticles and the platform shape shows similarities with *Ic. alt. alternatus*, however, the presence of a spurn and the closer (almost touching) arrangement of denticles separates *Ic. tumulusus* from the former taxon. *Ic. iowaensis iowaensis* has greater develop of the transversal ridges and the posterior carina process is turned downwards.

Age and geographical distribution. In the Cadí nappe the range is recorded from Famennian *gl. pectinata* to *rhomboidea* Zones (Sanz-López, 1995). *Ic. cornutus* is recorded in Spain.

Suborder OZARKODININA Dzik, 1976
Family SPATHOGNATHODONTIDAE Hass, 1959

Genus *Mehlina* Youngquist, 1945

Type species. *Mehlina gradata* = *Mehlina irregularis* Youngquist, 1945, Frasnian–Famennian, Europe, North America.

Mehlina strigosa Branson & Mehl, 1934
Figure 8L1–8L2

1934 *Spathodus strigosus* Branson & Mehl, p. 187, pl. 17, fig. 17.
1962b *Spathognathodus strigosus*; Ziegler, p. 111, pl. 12, figs. 21–23 (cum syn.).
1984 *Mehlina strigosa*; Ziegler & Sandberg, p. 183, fig. 4.
1991 *Mehlina strigosa*; Perri & Spalletta, p. 60, pl. 3, fig. 6.
1995 *Mehlina strigosa*; Sanz-López, p. 431, pl. 49, figs. 5, 9.
1997 *Mehlina strigosa*; Çapkınoğlu, p. 183, pl. 4, figs. 3–7.
2005a *Mehlina strigosa*; Çapkınoğlu, fig. 5.28–5.29.
2011 *Mehlina strigosa*; Bahrami *et al.*, pl. 1, figs. 31–32.
2011 *Mehlina strigosa*; Hartenfels, p. 240–241, pl. 38, figs. 7–9.
2015 *Mehlina strigosa*; Mossoni, p. 119–120, pl. 5, fig. 16.
2017 *Mehlina strigosa*; Lüddecke *et al.*, fig. 4c–4d.
2020 *Mehlina strigosa*; Suttner *et al.*, fig. 6.4.

Material. Five specimens from samples CP/112c (1), CP/112f (1), CP/114a (2) and CP/114b (1).

Description. Pa elements with concave-convex upper margin and stepped lower one, with the posterior part lower. The blade has 14–15 fused and aligned denticles, with different heights. Anteriorly there are two or three slightly higher, decreasing in high to the cusp, which is conspicuous. Posterior to the cusp denticles increase in high up to the one before the last two, then they diminish in high. Slightly expanded asymmetrical semicircular platform lobes located in mid position, Reduced basal cavity beneath the lobes.

Discussion. This taxon can be similar to *Me. gradata*, but the latter has the denticles backwards inclined.

Age and geographical distribution. From Famennian *termini* Zone to Tournaisian *bransoni* Zone (Spalletta *et al.*, 2017). *Me. strigosa* has a broad geographical distribution.

DISCUSSION

Following Spalletta *et al.* (2017) the conodont assemblage in the section Compte, which is mainly composed by the *glabra*-stock, *minuta*-stock, *perlobata*-stock, *quadrantinodosa*-stock, *nodocostatus*-stock, *marginifera*-stock and *glaber*-stock, points to a lower–middle Famennian age. La Mena Fm is approximately bounded between the records of *Pa. rhomboidea* and *Pa. mg. marginifera*, revealing the presence of the *rhomboidea–mg. marginifera* conodont Zones.

The Compte section conodont assemblage is rich and diverse allowing its comparison with others assemblages worldwide. The Pyrenean Cadí Nape zone (east of Compte section) yields different Upper Devonian outcrops with conodont faunas (Sanz-López, 1995). The La Coma Oriola section comprises a lower–middle Famennian conodont sequence, similar to Compte section: both sections share the *Ic. alternatus*-stock, *P. nodocostatus*-stock, *Pa. glabra*-stock, *Pa. perlobata*-stock, *Pa. quadrantinodosa*-stock and *P. glaber*-stock. However, *Ic. alt. helmsi*, *Pa. protorhomboidea*, *P. webbi*, *Pa. min. subgracilis*, *P. planirostratus*, *Alternognathus pseudostrigosus* and *P. diversus* are taxa that are recorded in La Coma Oriola section; they are absent in the section Compte.

Conodont assemblages from Montagne Noir are similar, with abundance of *Palmatolepis* over *Polygnathus* and some peaks of *Icriodus* and the presence of *Branmehla*, *Ancyrognathus*, *Bispathodus* and *Pelekysgnathus* genera in Col des Tribes section (Girard *et al.*, 2014). Some French taxa, which are not present in the Compte section are: *P. diversus*, *Bis. stabilis*, *Pe. inclinatus*, *Ic. olivierii*, *Ag. sinelaminus*. La Serre trench yields lower Famennian conodont fauna including: *Pa. gl. glabra*, *Pa. termini*, *Pa. crepida*, *P. procerus*, *P. brevilaminus-eoglaber*, *Ic. alt. alternatus*, *Pa. minuta*-stock, *Ag. sinelaminus* and *Pe. planus* (Schülke, 1999).

The conodont faunas from Corona Mizziu I in Sardinia (Corradini, 2003) are also comparable to the Pyrenean ones, with dominance of *Palmatolepis*: the whole subspecies of the *glabra*-stock are recorded; additionally, also the morphotype M1 from *Pa. gl. pectinata* was distinguished. The *minuta*-stock is represented by the records of *Pa. min. minuta*, *Pa. min. schleizia* and *Pa. min. subgracilis*. The *quadrantinodosa*-stock, including the morphotype 1 of *Pa. quadrantinodosalobata*, is almost fully represented; though *Pa. quad. quadrantinodosa* is not recorded. A frequent recorded taxon is *Ic. olivierii*. The *Polygnathus* genera are present with *P. diversus*, *P. glaber*-stock without *P. gb. eoglaber*, *P. nod. nodocostatus*, *P. nodountatus*, *P. padovanii*, *P. subnormalis* and *P. triphyllatus*. The *perlobata*-stock is also present. The Corona Mizziu II section (Corradini, 2003) provides a slightly different conodont fauna, which includes the *alternatus*-stock, *Ic. cornutus*, *Ic. olivierii*, *Me. strigosa*, all the *glabra*-stock (without distinction of morphotypes). *Pa. per. perlobata*, *Pa. protorhomboidea*, *Pa. regularis*,

Pa. triangularis, *Pe. planus*, *P. brevilaminus*, *P. nod. nodocostatus*, *P. padovanii*, *P. procerus*, *P. semicostatus*, *P. triphyllatus*, *Pa. quad. inflexa*, *Pa. quad. inflexoidea*, *Pa. mg. marginifera*, *Pa. gracilis*-stock and all the species of the *P. glaber*-stock. The faunas of Sardinia are composed by the dominance and variety of *Palmatolepis* with several *Icriodus* taxa and a variety of *Polygnathus*, sharing similarities with Compte, however, several frequent taxa (*e.g., Ic. olivierii*, *P. diversus*, morphotypes of *Pa. gl. pectinata*) and other genera (*Pe. planus*) are not recorded in the Compte section.

The Pizzul West section in the Carnic Alps (Mossoni *et al.*, 2013) yields a similar conodont assemblage with few *Ic. alt. alternatus* and *Ic. olivierii*. The groups represented are: the *glabra*-stock, except *Pa. gl. lepta*, the *minuta*-stock, the *perlobata*-stock, except *Pa. per. sigmoidea* and *Pa. per. helmsi*, the *P. glaber*-stock, excluding *P. gb. eoglaber*. Other taxa recorded are *Pa. regularis*, *Pa. stoppeli*, *Pa. subperlobata* and *Pa. tenuipunctata*.

The German Buschteich section in the Thuringian zone (Girard *et al.*, 2017) provides a rich conodont fauna. Recorded conodont faunas are similar to those from the Compte section, especially regarding diversity and abundance of taxa of *Palmatolepis*. However, there are several taxa which are not recorded in the Compte section: *Pa. circularis*, *Ic. olivierii*, *P. diversus*, *Pa. min. subgracilis*, *Bi. stabilis*, *Me. gradata* and *Po. pennatuloideus*.

In the Rhenish Massif, Beringhauser Tunnel section (Schülke & Popp, 2005), the following taxa are recorded: *minuta*-stock, *glabra*-stock, *perlobata*-stock, *quadrantinodosa*-stock, *Pa. poolei*, *Pa. lobicornis*, *Pa. tenuipunctata*, *Pa. termini*, *Pa. rhomboidea*, *Pa. klapperi*, *Pa. quadrantinodosalobata*, *Pa. mg. marginifera*. Remarkably, the genus *Icriodus* is not recorded. The conodont faunas in Hönne Valey Reef area (Stichling *et al.*, 2022) are more variable and comprises *Pa. delicatula platys*, *Ag. sinelaminus*, *Pa. arta*, *Pa. linguiloba*, *Br. ampla* and the late morphotype of *Pa. gl. lepta*.

The conodont faunas in Łagów section in the Holy Cross Mountains (Woroncowa-Marcinowska, 2006) are composed of *Ic. cornutus*, *glabra*-stock, *minuta*-stock, *perlobata*-stock, *quadrantinodosa*-stock, *marginifera*-stock and polygnathids *P. gb. glaber*, *P. nod. nodocostatus*, *P. fallax*, *P. triphyllatus*. The Janczyce section (Woroncowa-Marcinowska, 2006) yields similar assemblage; additionally, *Pa. circularis*, *P. pomeranicus*, *P. subnormalis*, *Pa. regularis*, *Pa. termini*, *Pa. tenuipunctata*, *Pa. quadrantinodosalobata* and *Polylophodonta linguiformis* are recorded.

The Western Pomerania Region (Matyja, 2003) provides a large conodont record with relative abundance of *Palmatolepis*: *Pa. wolskajae*, *Pa. poolei*, *Pa. quadrantinodosa*, *Pa. crepida*, *Pa. tenuipunctata*, *glabra*-stock, full *quadrantinodosa*-stock, *marginifera*-stock and *perlobata*-stock. The record of polygnathids is also large with the same taxa recorded as in Compte section: *P. lauriformis*, *P. semicostatus*, *P. padovanii*, *P. bouckaerti*, *P. triphyllatus*, *P. com. communis*, *nodocostatus*-stock and *glaber*-stock; besides, the polish record contains other taxa: *P. pomeranicus*, *P. fallax*, *P. rhomboideus* and *P. szulczewskii*. Further recorded taxa are *Ic. alt. alternatus*, *Ic. helmsi*, *Ic. chojnicensis*, *Me. strigosa* and *Pe. inclinatus*.

Conodont faunas from Büyükada Island area (Çapkınoğlu, 1997) in Istanbul region (Northwestern Turkey) are similar to those of Compte with abundance of *Palmatolepis* and relative diversity of *Polygnathus*. The *glabra*-stock, *perlobata*-stock, *minuta*-stock, *marginifera*-stock, *quadrantinodosa*-stock and *gracilis*-stock are the most frequent palmatolepids. The record of polygnathids is diverse consiting of *glaber*-stock, *nodocostatus*-stock, *P. semicostatus*, *P. subnormalis*, *P. diversus*, *P. fallax*, *P. longiusculus*, *P, brevilaminus*, *P. triphyllatus*. Other conodonts are *Ic. cornutus*, *Me. strigosa* and *Me. arcuata*. Conodont faunas from Tuzla Peninsula area in Istanbul region (Çapkınoğlu, 2005b) share similarities with the previous zone; in addition, *Pe. planus*, *Pe. inclinatus*, *P. lodinensis*, *Pa. lobicornis*, *P. procerus* and *Pa. regularis* are recorded.

Other similar conodont faunas from the Petrikovskaya section (Strelchenko & Kruchek, 2013) in Pripyat Through basin, Southeastern Belarus, are composed of *glabra*-stock, *minuta*-stock, *gracilis*-stock, *nodocostatus*-stock, *Pa. per. helmsi*, *Pa. rhomboidea*, *Pa. klapperi*, *P. semicostatus*, *P. depressus*, *Pa. subperlobata*.

Conodont faunas from the Shar'yu River area in the Polar Urals region (North Russia) are characterized by the dominace of *Palmatolepis* with few *Polygnathus* taxa (Ovnatanova *et al.*, 2017). The assemablage is composed of *Pa. subperlobata*, *Pa. klapperi*, almost full *glabra*-stock without *Pa. gl. pectinata*, *perlobata*-stock without *Pa. per. sigmoidea* and *Pa. per. helmsi*, *Pa. poolei*, *P. quadrantinodosalobata*, *Pa. rhomboidea*, *Pa. stoppeli*, *quadrantinodosa*-stock, *minuta*-stock, *Pa. mg. marginifera*, *P. gb. glaber*, *P. fallax* and *P. padovanii*.

The Lali section in Guangxi Region (South China) provides an extensive conodont assemblage record with numerous endemic conodont taxa (Zhang, 2019; Zhang *et al.*, 2019). There are several recorded peaks of *Icriodus* composed by *Ic. cornutus*, *Ic. deformatus deformatus*, *Ic. def. jiqiangi*, *Ic. iow. chengyuani*, *Ic. lateralis*. Some polygnathid taxa are: *P. hassi*, *P. nod. nocostatus*, *P. perplexus*, *P. subnormalis*. The numerous palmatolepid fauna is formed by the *glabra*-stock, *minuta*-stock, *marginifera*-stock, *quadrantinodosa*-stock, *perlobata*-stock, *Pa. clarki*, *Pa. loba parva*, *Pa. schuelki*, *Pa. angulata*, *Pa. lapoensis*, *Pa. linguiloba*, *Pa. werneri*, *Pa. mystica*, *Pa. regularis*, *Pa. arta*, *Pa. sihongshanensis*, *Pa. crepida*, *Pa. tenuipunctata*, *Pa. quadrantinodosalobata*, *Pa. ningi*, *Pa. poolei*, *Pa. siyunae*, *Pa. weddigei*, *Pa. subtilis*, *Pa. angularis*, *Pa. donoghuei*, *Pa. glabra chengyuani*, *Pa. rhomboidea*,

Pa. rhomboidea jiqiangi, *Pa. pararhomboidea* and *Pa. stoppeli*.

The conodont faunas from Bulongguoer section in Junggar zone (Zhang *et al.* 2021), (Northwest China) differ from those recorded in the Compte section by having more numerous *Polygnathus* and *Icriodus* taxa, instead *Palmatolepis* taxa, with several endemic species. The icriodid and polygnathid assemblage is: *Ic. nitidus*, *Ic. ballbergensis*, *Ic. triserialis*, *Ic. prominodosus*, *Neopolygnathus huijunae*, *P. mutabilis*, *P. guttiformis*, *P. hamiformis*, *P. subnormalis*, *P. argutus*, *P. xinjiangensis*, *P. planirostratus*. Other conodont taxa, which complete the recorded association are: *Pa. gl. prima*, *Pa. gl. glabra*, *Pa. rhomboidea*, *Ag. skeletalis*, *Ag. bifurcatus*, *Pol. linguiformis* and *Alveognathus sinister*.

The Hushoot Shiveetiin gol section in the Baruunhuuri Terrane (West Mongolia) yields a similar conodont assemblage dominated by *Palmatolepis* and *Polygnathus* with some peaks of *Icriodus*, *Ancyrognathus* and *Mehlina* (Suttner *et al.*, 2020). Some taxa, which differ from the Compte section are: *Ag. symmetricus*, *Ag. minjini*, *Ag. bifurcatus* and *Pa. poolei*. The morphotypes 1 and 3 of *Pa. gl. prima* have also been distinguished.

Conodont faunas from several sections of Central Iran show some differences with the conodont assemblages from the Compte section. The Baqer-Abad section (Bahrami *et al.*, 2020) provides a *Polygnathus* and *Palmatolepis* dominance with several peaks of *Icriodus* and *Pelekysgnathus*. The recorded taxa are: *Ic. iow. iowaensis*, *Ic. alt. alternatus*, *P. procerus*, *perlobata*-stock, *glabra*-stock, *Pa. tenuipunctata*, *Pa. subperlobata*, *minuta*-stock, *Pe. serradentatus*, *P. triphyllatus*, *Pa. quad. inflexoidea*, *Pa. klapperi*. The conodont fauna from shallow water sediments in the Ghale-kalaghu section (Bahrami *et al.*, 2013) is composed by numerous polygnathid taxa: *P. brevilaminus*, *P. normalis*, *P. ratebi*, *P. com. communis*, *P. buzmakovi*, *P. semicostatus*. Other subordinated taxa are: *Ic. iow. iowaensis*, *Ic. alt. helmsi*, *Ic. alt. alternatus*, *Ic. cornutus*, *Pa. quadrantinodosalobata*, *Pa. gl. pectinata*, *Pa. per. perlobata* and *Pe. inclinatus*. Slightly similar to the Compte record are the conodont faunas from Anarak section (Sattari *et al.*, 2021), which are composed of: *Ic. alt. alternatus*, *minuta*-stock, *P. semicostatus*, *glabra*-stock, *Me. strigosa*, *Ic. cornutus*, *P. padovanii*, *P. inconcinnus*, *Pa. gr. gracilis*, *Pa. per. maxima*, *Pa. quadrantinodosalobata* and *Bi. stabilis vulgaris*.

CONCLUSIONS

The Compte section has yielded an ample record of Famennian conodonts consisting of 47 taxa, belonging to four genera. Several taxa have been recorded for the first time in the Spanish Central Pyrenees area: *Pa. gl. acuta*, *Pa. gl. lepta*, *Pa. quad. quadrantinodosa*, *P. longiusculus*, *P. subnormalis*, *Ic. alt. mawsonae*. In the upper part of the Comabella Fm (Beds 98a to 104b) the conodont assemblage is mainly composed of *Palmatolepis crepida*, *Pa. tenuipunctata*, *Pa. glabra prima* (M1) and *Icriodus alternatus* group. In the transition to the overlying La Mena Fm (Beds 104c to 106) the conodont association changes and the most frequent taxa are components of the *Pa. glabra* group, *Pa. perlobata* group and *Polygnathus nodocostatus* group and *P. semicostatus*. Through the La Mena Fm (Beds 107 to 116), *Pa. glabra* group, *Pa. perlobata* group, *Pa. rhomboidea*, *Pa. minuta minuta* and several *Polygnathus* species are the most frequent taxa. The *Pa. quadrantinodosa* group appears in the upper part of La Mena Fm (Bed 112g). The mainly assemblage in the lower part of the following Barousse Fm (Beds 117 to 120) is composed of species of the *Pa. glabra* group, *Pa. quadrantinodosa* group and *P. glaber* group. The *Pa. glabra* group shows a strong morphological variety in the Compte section allowing the identification of several morphotypes. The *Pa. gl. prima* morphotype 1 is recorded from Bed 98c to Bed 104c and the morphotype 3 from Bed 104b to Bed 117b. The early morphotype of *Pa. gl. lepta* is recorded from Bed 111c to Bed 114b and the late morphotype from Bed 114b to Bed 120. The conodont sequence suggests a lower to middle Famennian age in the upper part of Comabella Fm to the base of Barousse Fm. Comparing with other conodont assemblages, there are some similarities with the faunas from western and eastern Europe. The faunas from Montagne Noir, Sardinia, Rhenish Massif Pomerania, and Turkey shares similar taxa, however, the Compte section is characterized in this interval by the lack of any taxa of the genera *Ancyrognathus*, *Alternognathus*, *Bispathodus*, *Branmehla* and *Pelekysgnathus*. The conodont faunas from China provide numerous endemic taxa. Conodonts from shallower facies in Iran have more *Polygnathus*, *Icriodus* and *Pelekysgnathus* taxa and scarce *Palmatolepis* taxa. The recorded association contributes to enlarge the, insufficient, information for the studied interval in this Perigondwanan region and augments the global database for the Famennian.

Supplementary information. The article has no additional data.

Author's contributions. Conception of the research: H. B.-L., J. I. V.-R. and J-C. L.; sampling: H. B.-L., J. I. V.-R. and J.-C. L.; laboratory work: H. B.-L. and J. I. V.-R.; data analysis and taxonomical interpretation: H. B.-L., J-C. L. and J. I. V.-R.; first draft and critical revision of this article: H.B.-L, J. I. V.-R and J.-C. L.

Competing interests. The authors declare that they do not have any competing interests.

Funding. Héctor Barrera-Lahoz was funded by Sociedad Española de Paleontología.

Author details. **Héctor Barrera-Lahoz**[1], **José I. Valenzuela-Ríos**[2,3] & **Jau-Chyn Liao**[3]. [1]Department of Earth Sciences, University of Zaragoza, C/ Pedro Cerbuna 12, 50009 Zaragoza, Spain; hectorpaleodevon@gmail.com; [2]Department of Botany and Geology, University of Valencia, C/ Dr. Moliner 50, 46100 Burjasot, Spain; jose.i.Valenzuela@

uv.es; [3]Department of Geodynamic, Stratigraphy and Paleontology, University Complutense of Madrid, C/ José Antonio Novais 12, 28040 Madrid, Spain; jaucliao@ucm.es.

Acknowledgments. This work represents a contribution to the Project IGCP-652 of UNESCO and, in addition, it conforms a contribution of the research groups GIUV2017-395, GEO-TRANSFER E32 17R and PERIGONDWANA UCM 910231. We are thankful to the Microscopy section of the Support Research Center, University of Valencia. J. C-L is supported by Maria Zambrano Grant (MIU Next Generation EU, ZA21-005) and José Castillejo Fellowship (MICCIN-MIU, CAS22/00148). The comments by two anonymous reviewers and editorial comments are greatly appreciated; all them helped to improve the initial version. We also thank the facilities provided by the UNESCO Global Geopark Orígens to carry out our work.

REFERENCES

Bahrami, A., Corradini, C., & Yazdi, M. (2011). Conodont biostratigraphy across the Devonian–Carboniferous boundary in the Shotori Range, Tabas area, central east Iran Microplate. *Bollettino della Società Paleontologica Italiana*, *50*(1), 35–53.

Bahrami, A., Corradini, C., Over, D. J., & Yazdi, M. (2013). Conodont biostratigraphy of the upper Frasnian–lower Famennian transitional deposits in the Shotori Range, Tabas area, Central-East Iran Microplate. *Bulletin of Geosciences, 88*(2), 369–388. doi: 10.3140/bull.geosci.1353

Bahrami, A., Königshof, P., Boncheva, I., Yazdi, M., Khalaji, M. A. N., & Zarei, E. (2018). Conodont biostratigraphy of the Kesheh and Dizlu sections, and the age range of the Bahram Formation in Central Iran. *Palaeobiodiversity and Palaeoenvironments*, *98*, 315–329. doi: 10.1007/s12549-017-0307-y

Bahrami, A., Parast, A., Boncheva, I., & Yazdi, M. (2020). Late Devonian (Famennian) conodonts from Baqer-Abad section, northeast Isfahan province, Central Iran. *Boletín de la Sociedad Geológica Mexicana*, *72*(2), A100619. doi: 10.18268/BSGM2020v72n2a100619

Bahrami, A., Königshof, P., Hartkopf-Fröder, C., & Kaiser, S. I. (2022). Late Devonian–Mississippian conodont biostratigraphy of the Chelcheli section, NE Shahrud (Eastern Alborz, North Iran). *Paläontologische Zeitschrift*, *96*(3), 449–469. doi: 10.1007/s12542-021-00575-6

Barnolas, A., & Pujalte, V. (2004). Cordillera Pirenaica. Definición, límites y división. In J. A. Vera (Ed.), *Geología de España* (pp. 233–240). SGE-IGME.

Becker, R. T., Aboussalam, Z. S., El Hassani, A., Hartenfels, S., & Hüneke, H. (2020). Devonian and basal Carboniferous of the allochthonous nappes at Mrirt (eastern part of Western Meseta)–review and new data. *Frontiers in Science and Engineering*, *10*(1), 87–109.

Boersma, K. T. (1973a). Devonian and Lower Carboniferous conodont biostratigraphy, Spanish Central Pyrenees. *Leidse Geologische Mededelingen*, *49*(2), 303–377.

Boersma, K. T. (1973b). Description of certain Lower Devonian platform conodonts of the Spanish Central Pyrenees. *Leidse Geologische Mededelingen*, *49*(2), 285–291.

Branson, E. B., & Mehl, M. G. (1934). Conodonts from the Grassy Creek shale of Missouri. *Missouri University Studies*, *8*, 171–259.

Branson, E. B., & Mehl, M. G. (1938). The conodont genus *Icriodus* and its stratigraphic distribution. *Journal of Paleontology*, *12*(2), 156–166.

Bultynck, P. (2003). Devonian Icriodontidae: biostratigraphy, classification and remarks on paleoecology and dispersal. *Revista Española de Micropaleontología*, *35*(3), 295–314.

Çapkınoğlu, Ş. (1997). Conodont fauna and biostratigraphy of the Famennian of Büyükada, Istanbul, Northwestern Turkey. *Bollettino della Società Paleontologica Italiana*, *35*(2), 165–186.

Çapkınoğlu, Ş. (2005a). Famennian conodonts from the Ayineburnu Formation of the Istanbul Zone (NW Turkey). *Geologica Carpathica*, *56*(2), 113–122.

Çapkınoğlu, Ş. (2005b). Upper Devonian (Upper Frasnian–Lower Famennian) conodont biostratigraphy of the Ayineburnu Formation (Istanbul Zone, NW Turkey). *Geologica Carpathica*, *56*(3), 223–236.

Çapkınoğlu, Ş., & Gedík, İ. (2000). Late Devonian Conodont Fauna of the Gümüşali Formation, the Eastern Taurides, Turke. *Turkish Journal of Earth Sciences*, *9*(2), 69–89.

Clausen, C. D., Korn, D., & Luppold, F. W. (1991). Litho-und Biofazies des mittel-bis oberdevonischen Karbonatprofiles am Beringhauser Tunnel (Messinghauser Sattel, nordliches Schiefergebirge). *Geologie und Palaontologie in Westfalen*, *18*, 7–65.

Cooper, C. L. (1931). New conodonts from the Woodford Formation of Oklahoma. *Journal of Paleontology*, *5*(3), 230–243.

Corradini, C. (2003). Late Devonian (Famennian) conodonts from the Corona Mizziu Sections near Villasalto (Sardinia, Italy). *Palaeontographia Italica*, *89*, 65–116.

Dreesen, R. (1977). Interspecific morphological relations within the «*quadrantinodosa*-stock» (Branson & Mehl, 1934) (*marginifera*-Zone, Upper Devonian). *Annales de la Société géologique de Belgique*, *99*, 511–529.

Dreesen, R., & Dusar, M. (1974). Refinement of conodont-biozonation in the Famenne area. In J. P. Bouckaert, & M. Street (Eds.), *International Symposium on Belgian Micropaleontological Limits from Emsian to Viséan*, *Geological Survey of Belgium*, *13*, (pp. 1–38.) Namur.

Dreesen, R., & Orchard, M. J. (1974). "Intraspecific" Morphological Variation Within *Polygnathus Semicostatus* Branson & Mehl. In J. Bouckaert, & M. Streel (Eds.), *International Symposium on Belgian Micropaleontological Limits from Emsian to Viséan*, *Geological Survey of Belgium*, *21*, (pp. 1–10). Namur.

Dzik, J. (1976). Remarks on the evolution of Ordovician conodonts. *Acta Palaeontologica Polonica*, *21*(4), 395–459.

Dzik, J. (2002). Emergence and collapse of the Frasnian conodont and ammonoid communities in the Holy Cross Mountains, Poland. *Acta Palaeontologica Polonica*, *47*(4), 565–650.

Dzik, J. (2006). The Famennian "Golden Age" of conodonts and ammonoids in the Polish part of the Variscan Sea. *Palaeontologia Polonica*, *63*, 1–360.

García-López, S., Sanz-López, J., & Pardo, M. V. (1999). Conodontos (bioestratigrafía, biofacies y paleotemperaturas) de los sinclinales de Almadén y Guadalmez (Devónico–Carbonífero Inferior), Zona Centroibérica meridional, España. *Revista Española de Paleontología*, *14*(3), 161–172. doi: 10.7203/sjp.23959

Gholamalian, H. (2007). Conodont biostratigraphy of the Frasnian–Famennian boundary in the Esfahan and

Tabas areas, Central Iran. *Geological Quarterly*, *51*(4), 453–476.

Gholamalian, H., Ghorbani, M., & Sajadi, S. H. (2009). Famennian conodonts from Kal-e-Sardar section, eastern Tabas, central Iran. *Rivista Italiana di Paleontologia e Stratigrafia*, *115*(2), 141–158.

Girard, C., Cornee, J. J., Corradini, C., Fravalo, A., & Feist, R. (2014). Palaeoenvironmental changes at Col des Tribes (Montagne Noire, France), a reference section for the Famennian of north Gondwana-related areas. *Geological Magazine*, *151*(5), 864–884. doi: 10.1017/S0016756813000927

Girard, C., Cornee, J. J., Charruault, A. L., Corradini, C., Weyer, D., Bartzsch, K., Joachimski, M., & Feist, R. (2017). Conodont biostratigraphy and palaeoenvironmental trends during the Famennian (Late Devonian) in the Thuringian Buschteich section (Germany). *Newsletters on Stratigraphy*, *50*(1), 71–89. doi: 10.1127/nos/2016/0318

Gouwy, S., Liao, J.-C., & Valenzuela-Ríos, J. I. (2013). Eifelian (Middle Devonian) to Lower Frasnian (Upper Devonian) conodont biostratigraphy in the Villech section (Spanish Central Pyrenees). *Bulletin of Geosciences*, *88*(2), 315–338. doi: 10.3140/bull.geosci.1341

Gouwy, S., Liao, J. C., & Valenzuela-Rios, J. I. (2016). Graphic correlation of the upper Eifelian to lower Frasnian (Middle-Upper Devonian) conodont sequences in the Spanish Central Pyrenees and comparison with composite standards from other areas. *Palaeontologia Electronica*, *19*(3), 1–18. doi: 10.26879/669

Gouwy, S., Liao, J.-C., & Valenzuela-Ríos, J. I. (2017). Eifelian–Famennian Conodont succession in the Villech sections. *International Conodont Symposium 4. Progress on Conodont investigation* (pp. 82–88). Valencia.

Hartenfels, S. (2011). *Die globalen Annulata-Events und die Dasberg-Krise (Famennium, Oberdevon) in Europa und Nord-Afrika: hochauflösende Conodonten-Stratigraphie, Karbonat-Mikrofazies, Paläoökologie und Paläodiversität*. (PhD Thesis, Universität Münster, Münster).

Hartevelt, J. J. A. (1970). Geology of the upper Segre and Valira valleys, central Pyrenees, Andorra/Spain. *Leidse Geologische Mededelingen*, *45*(1), 167–236.

Hass, W. H. (1959). Conodonts from the Chappel Limestone of Texas. *U.S. Geological Survey Professional Paper*, *294*, 365–399. doi: 10.3133/pp294J

Helms, J. (1959). Conodonten aus dem Saalfelder Oberdevon (Thuringen). *Geologie*, *8*, 634–677.

Helms, J. (1961). Die "nodocostata-Gruppe" der Gattung Polygnathus. *Geologie*, *10*(6), 674–711.

Helms, J. (1963). Zur" phylogenese" und Taxonomie von *Palmatolepis* (Conodontida, Oberdevon). *Geologie*, *12*, 449–485.

Helms, J., & Wolska, Z. (1967). New Upper Devonian conodonts from Poland and Germany. *Acta Palaeontologica Polonica*, *12*(2), 227–238.

Hinde, G. J. (1879). On conodonts from the Chazy and Cincinnati Group of the Cambro–Silurian, and from the Hamilton and Genesee-Shale divisions of the Devonian, in Canada and the United States. *Geological Society of London, Quarterly Journal*, *35*, 351–369. doi: 10.1144/GSL.JGS.1879.035.01-04.23

Huang, C., & Gong, Y. (2016). Timing and patterns of the Frasnian–Famennian event: Evidences from high-resolution conodont biostratigraphy and event stratigraphy at the Yangdi section, Guangxi, South China. *Palaeogeography, Palaeoclimatology, Palaeoecology*, *448*, 317–338. doi: 10.1016/j.palaeo.2015.10.031

Huang, Y. Z., Qi, Y. P., Wang, Q. L., Yao, L., & Chen, J. T. (2023). Latest Devonian–Early Mississippian conodont biostratigraphy in the Naqing section, Guizhou, South China. *Palaeoworld*. doi: 10.1016/j.palwor.2023.02.004

Institut Cartogràfic i Geològic de Catalunya (2023). Mapa Geològic de Catalunya 1:25000. https://betaportal.icgc.cat/visor/client_utfgrid_geo.html [Sep 2023].

Izokh, N. G., Erina, M. V., Obut, O. T., Abdiev, N. K., Kim, A. I., & Rakhmonov, U. D. (2020). Late Devonian conodonts from the Zeravshan-Gissar mountainous area, Uzbekistan. *Paleontological journal*, *54*, 149–156. doi: 10.1134/S0031030120020057

Ji, Q., & Ziegler, W. (1993). The Lali section: an excellent reference section for Late Devonian in south China. *Courier Forschungs-Institut Senckenberg*, *157*, 1–183.

Johnston, D. I., & Chatterton, B. D. (2001). Upper Devonian (Famennian) conodonts of the Palliser Formation and Wabamun Group, Alberta and British Columbia, Canada. *Palaeontographica Canadiana*, *19*, 1–154.

Klapper, G. (2007). Conodont taxonomy and the recognition of the Frasnian/Famennian (Upper Devonian) stage boundary. *Stratigraphy*, *4*(1), 67–76.

Klapper, G., Uyeno, T. T., Armstrong, D. K., & Telford, P. G. (2004). Conodonts of the Williams Island and Long Rapids formations (Upper Devonian, Frasnian–Famennian) of the Onakawana B Drillhole, Moose River Basin, northern Ontario, with a revision of Lower Famennian species. *Journal of Paleontology*, *78*(2), 371–387. doi: 10.1666/0022-3360(2004)078<0371:COTWIA>2.0.CO;2

Kuzmin, A.V. (1990). Asimmetricheskiye pary platformennykh elementov u nekotorykh predstaviteley roda *Polygnathus* (konodonty) [Asymmetric pairs of platform elements in some representatives of the genus *Polygnathus* (conodonts)]. *Paleontologicheskii Zhurnal*, *4*, 66–74.

Liao, J.-C., & Valenzuela-Ríos, J. I. (2008). Givetian and early Frasnian conodonts from the Compte section (Middle–Upper Devonian, Spanish Central Pyrenees). *Geological Quaterly*, *52*(1), 1–18.

Liao, J.-C., & Valenzuela-Ríos, J. I. (2013). The Middle and Upper Devonian conodont sequence from La Guardia D'Àres Sections (Spanish Central Pyrenees). *Bulletin of Geosciences*, *88*(2), 339–368. doi: 10.3140/bull.geosci.1348

Liao, J.-C., & Valenzuela-Ríos, J. I. (2017). Givetian to Famennian conodonts (Middle–Upper Devonian) at CP section. *International Conodont Symposium 4. Progress on Conodont investigation* (pp. 99–105). Valencia.

Lüddecke, F., Hartenfels, S., & Becker, R. T. (2017). Conodont biofacies of a monotonous middle Famennian pelagic carbonate succession (Upper Ballberg Quarry, northern Rhenish Massif). *Palaeobiodiversity and Palaeoenvironments*, *97*, 591–613. doi: 10.1007/s12549-017-0288-x

Martínez-Pérez, C., & Valenzuela-Ríos, J. I. (2012). Polygnathids (Conodonta) around the lower/upper Emsian boundary from the La Guardia d'Àres section (Lower Devonian, Spanish Central Pyrenees). *Bollettino della Società Paleontologica Italiana*, *51*(3), 193–202. doi: 10.4435/BSPI.2012.22

Martínez-Pérez, C., & Valenzuela-Ríos, J. I. (2014). New Lower Devonian Polygnathids (Conodonta) from the Spanish Central Pyrenees, with comments on the early

radiation of the group. *Journal of Iberian Geology*, *40*(1), 141–155. doi: 10.5209/rev_JIGE.2014.v40.n1.44095

Martínez-Pérez, C., Valenzuela-Ríos, J. I., Navas-Parejo, P., Liao, J. C., & Botella, H. (2011). Emsian (Lower Devonian) Polygnathids (Conodont) succession in the Spanish Central Pyrenees. *Journal of Iberian Geology*, *37*(1), 45–64. doi: 10.5209/rev_JIGE.2011.v37.n1.4

Matyja, H. (1993). Upper Devonian of Western Pomerania. *Acta Geologica Polonica*, *43*(1–2), 27–94.

Matyja, H., & Narkiewicz, M. (1995). Conodont stratigraphy of the Upper Devonian in the Janczyce I borehole section, eastern Holy Cross Mts. *Geological Quarterly*, *39*(2), 177–206.

Mawson, R., & Talent, J. A. (1997). Famennian–Tournaisian conodonts and Devonian–Early Carboniferous transgressions and regressions in northeastern Australia. *Special Paper of the Geological Society of America*, *321*, 189–233. doi: 10.1130/0-8137-2321-3.189

Metzger, R. A. (1994). Multielement reconstructions of *Palmatolepis* and *Polygnathus* (Upper Devonian, Famennian) from the Canning Basin, Australia, and Bactrian Mountain, Nevada. *Journal of Paleontology 68(3)*, 617–647. doi: 10.1017/S0022336000025956

Mey, P. H. W. (1967a). The geology of the upper Ribagorzana and Baliera valleys, Central Pyrenees, Spain. *Leidse Geologische Mededelingen*, *41*, 153–220.

Mey, P. H. W. (1967b). Evolution of the Pyrenean Basins during the Late Paleozoic. *International Symposium on the Devonian System* (pp. 1157–1166). Calgary.

Mohamed, T. I. (2015). *Sequence stratigraphy and provenance of the Bakken Formation in southeast Alberta and southwest Saskatchewan* (Ms Thesis, University of Calgary, Calgary).

Mossoni, A. (2015). Selected Famennian (Late Devonian) events (*Condroz*, *Annulata*, *Hangenberg*) in Sardinia and in the Carnic Alps: conodont biostratigraphy, magnetic susceptibility and geochemistry (PhD thesis, Università di Cagliari, Cagliari).

Mossoni, A., Corradini, C., & Pondrelli, M. (2013). Famennian (Late Devonian) conodonts from the Pizzul West section (Carnic Alps, Italy). *GORTANIA, Geologia, Paleontologia, Paletnologia*, *34*, 13–34.

Müller, K. J. (1956). Zur Kenntnis der Conodonten-Fauna des europaischen Devons, 1; Die Gattung *Palmatolepis*. *Abhandlunghen and Senckenbergischen Naturforschenden Gesellschaft*, *494*, 1–70.

Müller, K. J., & Müller, E. M. (1957). Early Upper Devonian (independence) conodonts from Iowa, part I. *Journal of Paleontology*, *31*(6), 1069–1108.

Murphy, M. A., & Valenzuela-Ríos, J. I. (1999). *Lanea* new genus, lineage of Early Devonian conodonts. *Bolletino della Società Paleontologica Italiana*, *37(2/3)*, 321–334.

Narkiewicz, K., & Bultynck, P. (2011). Conodont biostratigraphy of the Upper Devonian in the Lublin area (south-eastern Poland). *Prace Państwowego Instytutu Geologicznego*, *196*, 193–254.

Navas-Parejo, P., Rodríguez-Cañero, R., Somma, R., Martín-Algarra, A., & Perrone, V. (2009). The Frasnian Upper Kellwasser event and a lower Famennian stratigraphic gap in Calabria (southern Italy). *Palaeobiodiversity and Palaeoenvironments*, *89*, 111–118. doi: 10.1007/s12549-009-0006-4

Olivieri, R. (1970). Conodonti e zonatura del Devoniano superiore e riconoscimento di Carbonifero inferiore nei calcari di Corona Mizziu (Gerrei-Sardegna). *Bollettino della Società Paleontologica Italiana*, *8*(2), 63–152.

Over, D. J. (1997). Conodont biostratigraphy of the Java Formation (Upper Devonian) and the Frasnian–Famennian boundary in western New York State. *Special Papers-Geological Society of America*, *321*, 161–178.

Over, D. J. (2007). Conodont biostratigraphy of the Chattanooga Shale, Middle and Upper Devonian, southern Appalachian Basin, eastern United States. *Journal of Paleontology*, *81*(6), 1194–1217. doi: 10.1666/06-056R.1

Over, D. J., Lazar, R., Baird, G. C., Schieber, J., & Ettensohn, F. R. (2009). *Protosalvinia* Dawson and associated conodonts of the upper trachytera zone, Famennian, Upper Devonian, in the eastern United States. *Journal of Paleontology*, *83*(1), 70–79. doi: 10.1666/08-058R.1

Ovnatanova, N. S., Kononova, L. I., Kolesnik, L. S., & Gatovsky, Y. A. (2017). Upper Devonian conodonts of Northeastern European Russia. *Paleontological Journal*, *51*, 973–1165. doi: 10.1134/S003103011710001X

Pander, C. H. (1856). Monographie der fossilen Fische des silurischen Systems des russisch-baltischen Gouvernements. *Buchdruck aus der K. Akademie der Wissenschaften*, *1*, 1–91.

Perri, M. C., & Spalletta, C. (1990). Famennian conodonts from climenid pelagic limestone, Carnic Alps, Italy. *Palaeontographia Italica*, *77*, 55–83.

Perri, M. C., & Spalletta, C. (1991). Famennian conodonts from Cava Cantoniera and Malpasso sections, Carnic Alps, Italy. *Bollettino della Società Paleontologica Italiana*, *30*(1), 47–78.

Perri, M. C., & Spalletta, C. (1998). The Upper *marginifera* Zone (Late Devonian) in the Casera Collinetta di Sotto C section (Carnic Alps, Italy). *Southern Alps Field Trip Guidebook, ECOS VII, Giornale di Geologia*, *60,* 150–157.

Rodríguez-Cañero, R. (1995). El género *Palmatolepis* Ulrich y Bassler (Conodonta) y su aplicación para el reconocimiento de biozonas y biofacies en el Devónico superior del Complejo Maláguide (Cordillera Bética, España). *Revista Española de Paleontología*, *10*(3), 3–23. doi: 10.7203/sjp.24194

Rytina, M. K., Becker, R. T., Aboussalam, Z. S., Hartenfels, S., Helling, S., Stichling, S., & Ward, D. (2013). The allochthonous Silurian–Devonian in olistostromes at "the Southern Variscan front" (Tinerhir region, SE Morocco)-Preliminary data. *International Field Symposium "The Devonian and Carboniferous of Northern Gondwana"–Morocco*, *27* (pp. 11–21). Rabat.

Sánchez de Posada, L. C., Sanz-López, J., & Gozalo, R. (2008). Ostracod and conodont faunal changes across the Frasnian–Famennian (Devonian) boundary at Els Castells, Spanish central Pyrenees. *Revue de Micropaléontologie*, *51*(3), 205–219. doi: 10.1016/j.revmic.2007.06.001

Sandberg, C. A., & Dreesen, R. (1984). Late Devonian icriodontid biofacies models and alternate shallow-water conodont zonation. *Geological Society of America Special Paper*, *196*, 143–178.

Sandberg, C. A., & Ziegler, W. (1973). Refinement of standard Upper Devonian conodont zonation based on sections in Nevada and West Germany. *Geologica et Palaeontologica*, *7*, 97–122.

Sandberg, C. A., & Ziegler, W. (1979). Taxonomy and biofacies of important conodonts of Late Devonian

styriacus-Zone, United States and Germany. *Geologica et Palaeontologica*, *13*, 173–212.
Sannemann, D. (1955a). Beitrag zur untergliederung des Oberdevons nach Conodonten. *Neues Jahrbuch für Geologie und Paläontologie, Abhandlungen*, *100*(3), 324–331.
Sannemann, D. (1955b). Oberdevonische conodonten (to II). *Senckenbergiana lethaea*, *36*, 123–156.
Sanz-López, J. (1995). *Estratigrafía y bioestratigrafía (conodontos) del Silúrico superior–Carbonífero inferior del Pirineo oriental y central* (PhD Thesis, Universitat de Barcelona, Barcelona).
Sanz-López, J. (2002a). Devonian and Carboniferous pre–Stephanian rocks from the Pyrenees. In S. García-López, & F. Bastida (Eds.), Palaeozoic conodonts from northern Spain. *Cuadernos del Museo Geominero*, *1*, 367–389.
Sanz-López, J. (2002b). Devonian and Lower Carboniferous rocks from the Cadí nappe (eastern Pyrenees). In S. García-López, & F. Bastida (Eds.), Palaeozoic conodonts from northern Spain. *Cuadernos del Museo Geominero*, 1, 419–438.
Sanz-López, J., García-López, S., Montesinos, J. R., & Arbizu, M. (1999). Biostratigraphy and sedimentation of the Vidrieros Formation (middle Famennian–lower Tournaisian) in the Gildar-Montó unit (northwest Spain). *Bollettino della Società Paleontologica Italiana*, *37*(2–3), 393–406.
Sattari, E., Bahrami, A., Königshof, P., & Vaziri-Moghaddam, H. (2021). Late Devonian (Famennian) to Carboniferous (Mississippian–Pennsylvanian) conodonts from the Anarak section, Central Iran. *Palaeobiodiversity and Palaeoenvironments*, *101*, 781–802. doi: 10.1007/s12549-020-00462-z
Savage, N. M. (2013). *Late Devonian conodonts from northwestern Thailand*. Bourland Printing, a Trinity Press Company.
Schmidt, G. (1931). Das Paläozoikum der spanischen Pyrenäen. Abhandlungen der Mathematisch-Physikalischen Klasse der Königlich Bayerischen Akademie der Wissenschaften, *3*(5), 980–1065.
Schülke, I. (1995). Evolutive Prozesse bei *Palmatolepis* in der frühen Famenne-Srufe (Conodonta, Ober–Devon). *Göttinger Arbeiten zur Geologie und Paläontologie*, *67*, 1–108.
Schülke, I. (1999). Conodont multielement reconstruction from the Early Famennian (Late Devonian) of the Montagne Noire (Southern France). *Geologica et Palaeontologica*, *3*, 1–123.
Schülke, I., & Popp, A. (2005). Microfacies development, sea-level change, and conodont stratigraphy of Famennian mid-to deep platform deposits of the Beringhauser Tunnel section (Rheinisches Schiefergebirge, Germany). *Facies*, *50*, 647–664. doi: 10.1007/s10347-004-0041-6
Silvério, G. G., Valenzuela-Ríos, J. I., & Liao, J.-C. (2021). Upper Frasnian and Lower Famennian (Upper Devonian) conodonts of the Compte section (Spanish Central Pyrenees). *Spanish Journal of Palaeontology*, *36*(2), 205–220. doi: 10.7203/sjp.36.2.21950
Spalletta, C., Perri, M. C., Over, D. J., & Corradini, C. (2017). Famennian (Upper Devonian) conodont zonation: revised global standard. *Bulletin of Geosciences*, *92*(1), 31–57. doi: 10.3140/bull.geosci.1623
Stichling, S., Becker, R. T., Hartenfels, S., Aboussalam, Z. S., & May, A. (2022). Drowning, extinction, and subsequent facies development of the Devonian Hönne Valley Reef (northern Rhenish Massif, Germany). *Palaeobiodiversity and Palaeoenvironments*, *102*(3), 629–696. doi: 10.1007/s12549-022-00539-x
Strelchenko, T. V., & Kruchek, S. A. (2013). Lower Famennian conodont-based stratigraphy of the Pripyat Trough. *Stratigraphy and Geological Correlation*, *21*, 150–170. doi: 10.1134/S0869593813020081
Suttner, T. J., Kido, E., Ariunchimeg, Y., Sersmaa, G., Waters, J. A., Carmichael, S. K., Batchelor, C. J., Ariuntogos, M., Hušková, A., Slavík, L., Valenzuela-Ríos, J. I., Liao, J.-C., & Gatovsky, Y. A. (2020). Conodonts from Late Devonian Island arc settings (Baruunhuurai Terrane, western Mongolia). *Palaeogeography, Palaeoclimatology, Palaeoecology*, *549*, 109099. doi: 10.1016/j.palaeo.2019.03.001
Szulczewski, M. (1971). Upper Devonian conodonts, stratigraphy and facial development in the Holy Cross Mts. *Acta Geologica Polonica*, *21*(1), 1–130.
Talent, J. A., Gaetani, M., Mawson, R., Molloy, P. D., Conaghan, P. J., Lehnert, O., & Trotter, J. A. (1999). Early Ordovician and Devonian conodonts from the western Karakoram and Hindu Kush, northernmost Pakistan. *Rivista Italiana di Paleontologia e Stratigrafia*, *105*(2), 201–230.
Ulrich, E. O., & Bassler, R. S. (1926). A classification of the tooth-like fossils, conodonts, with descriptions of American Devonian and Mississipian species. *Proceedings of the United States National Museum*, *68*, 1–63. doi: 10.5479/si.00963801.68-2613.1
Valenzuela-Ríos, J. I. (1990). Lochkovian conodonts and stratigraphy at Gerri de la Sal (Pyrenees). *Courier Forschungsinstitut Senckenberg*, *118*, 53–56.
Valenzuela-Ríos, J. I. (1994a). *Conodontos del Lochkoviense y Praguiense (Devónico inferior) del Pirineo central español*. (PhD Thesis, Universidad de Zaragoza, Zaragoza). *Memorias del Museo Paleontológico de la Universidad De Zaragoza*, *5*.
Valenzuela-Ríos, J. I. (1994b). The Lower Devonian conodont *Pedavis pesavis* and the *pesavis* Zone. *Lethaia*, *27*(3), 199–207. doi: 10.1111/j.1502-3931.1994.tb01409
Valenzuela-Ríos, J. I., (2002). Lochkovian and Pragian Conodonts from Segre 1 (Central Spanish Pyrenees). In S. García-López, & F. Bastida (Eds.), Palaeozoic Conodonts from Northern Spain. *Cuadernos del Museo Geominero*, *1*, 403–417.
Valenzuela-Ríos, J. I., & García-López, S. (1998). Using conodonts to correlate abiotic events: an example from the Lochkovian (Early Devonian) of NE Spain. *Paleontologica Polonica*, *58*, 191–199.
Valenzuela-Ríos, J. I., & Liao, J.-C. (2006). Annotations to Devonian Correlation Table, R 357–360 di-ds 06: Spanish Central Pyrenees, southern part. *Senckenbergiana lethaea*, *86*, 105–107. doi: 10.1007/BF03043640
Valenzuela-Ríos, J. I., & Liao, J.-C. (2006b). Pyrenees Middle Devonian Compte. In K. Weddige (Ed.), Devonian Correlation Table. *Senckenbergiana lethaea*, *86*(1), column R360dm06.
Valenzuela-Ríos, J. I., & Liao, J. C. (2012). Color/facies changes and Global Events, a hoax? A case study from the Lochkovian (Lower Devonian) in the Spanish Central Pyrenees. *Palaeogeography, Palaeoclimatology, Palaeoecology*, *367*, 219–230. doi: 10.1016/j.palaeo.2011.09.007
Valenzuela-Ríos, J. I., & Liao, J. C. (2024). Biodiversity and evolutionary phases of Lochkovian (Lower Devonian) conodonts in the Pyrenees: A comparative study.

Marine Micropaleontology, *187*, 102326. doi: 10.1016/j.marmicro.2023.102326

Valenzuela-Ríos, J. I., & Murphy, M. A. (1997). A new zonation of middle Lochkovian (Lower Devonian) conodonts and evolution of *Flajsella* n. gen. (Conodonta). *Geological Society of America Special Paper*, *321*, 131–144.

Valenzuela-Ríos, J. I., Slavík, L., Liao, J. C., Calvo, H., Hušková, A., & Chadimová, L. (2015). The middle and upper Lochkovian (Lower Devonian) conodont successions in key peri-Gondwana localities (Spanish Central Pyrenees and Prague Synform) and their relevance for global correlations. *Terra Nova*, *27*(6), 409–415. doi: 10.1111/ter.12172

Valenzuela-Ríos, J. I., Liao, J.-C., & Martínez-Pérez, C. (2017a). The Devonian in the Compte sections. *International Conodont Symposium 4. Progress on Conodont investigation* (pp. 89–91). Valencia.

Valenzuela-Ríos, J. I., Liao, J.-C., & Martínez-Pérez, C. (2017b). Famennian to Lower Carboniferous? In the Pi section. *International Conodont Symposium 4. Progress on Conodont investigation* (pp. 68–72). Valencia.

Vorontsova, T. N., & Kuzmin, A. V. (1984). The Distribution of New Conodont Species of the Genus *Polygnathus* in the Famennian Deposits of Central Kazakhstan. *Izvestija Akademii Nauk SSSR, Ser. Geol.*, *10,* 58–64.

Weiner, T., & Kalvoda, J. (2016). Biostratigraphic and sedimentary record of the *Annulata* Events in the Moravian Karst (Famennian, Czech Republic). *Facies*, *62*, 1–25. doi: 10.1007/s10347-015-0456-2

Woroncowa-Marcinowska, T. (2006). Upper Devonian goniatites and co-occurring conodonts from the Holy Cross Mountains: studies of the Polish Geological Institute collections. *Annales Societatis Geologorum Poloniae*, *76*, 113–160.

Yazdi, M. (1999). Late Devonian–Carboniferous conodonts from Eastern Iran. *Rivista Italiana di Paleontologia e Stratigrafia*, *105*(2), 167–200.

Yazdi, M., Meysami, A., Mannani, M., Bakhshaei, M. H., & Mawson, R. (2000). Famennian conodonts from the Esteghlal Refractories Mine, Abadeh area, south-central Iran. *Records of the Western Australian Museum, Supplement, 58*, 197–209.

Youngquist, W. L. (1945). Upper Devonian conodonts from the Independence shale (?) of Iowa. *Journal of Paleontology*, *19*(4), 355–367.

Yuan, Z., & Sun, Y. (2023). Upper Devonian conodont fauna from Western Hubei, China and its significance. *Historical Biology, 36*(5), 954–980. doi: 10.1080/08912963.2023.2199763

Zamani, F., Yazdi, M., Bahrami, A., Girard, C., Spalletta, C., & Ameri, H. (2021). Middle Givetian to late Famennian (Middle to Late Devonian) conodonts from the northern margin of Gondwana (Kerman region, Central Iran). *Historical Biology*, *33*(11), 2591–2609. doi: 10.1080/08912963.2020.1819997

Zhang, X. S. (2019). *Late Devonian conodont biostratigraphy, event stratigraphy and chemostratigraphy in South China and western Junggar, NW China*. (PhD Thesis, China University of Geoscience, Beijing).

Zhang, X. S., Over, D. J., Ma, K., & Gong, Y. (2019). Upper Devonian conodont zonation, sea-level changes and bio-events in offshore carbonate facies Lali section, South China. *Palaeogeography, Palaeoclimatology, Palaeoecology*, *531*, 109219. doi: 10.1016/j.palaeo.2019.05.041

Zhang, X. S., Over, D. J., & Gong, Y. M. (2021). Famennian conodonts from the Hongguleleng Formation at the Bulongguoer stratotype section, western Junggar, Northwest China. *Palaeoworld*, *30*(4), 677–688. doi: 10.1016/j.palwor.2020.12.009

Ziegler, W. (1959). Conodonten aus Devon und Karbon Südwesteuropas und Bemerkungen zur bretonischen Faltung (Montagne Noire, Massiv Mounthoumet, Span. Pyrenäen). *Neus Jahrbuch für Geologie und Paläeontologie, Monatshefte*, *7*, 289–309.

Ziegler, W. (1962a). Die Conodonten aus den Geröllen des Zechsteinkonglomerates von Rossenray (südwestlisch Rheinberg/Niederrhein). *Fortschritte in der Geologie von Rheinland und Westfalen 6*, 391–406.

Ziegler, W. (1962b). Taxionomie und Phylogenie Oberdevonischer Conodonten und ihre stratigraphische Bedeutung. *Abhandlunghen des Hessisches Landesamt für Bodenforschung 38*, 1–166.

Ziegler, W. (Ed.) (1977). *Catalogue of conodonts, Volume 3*. Schweizerbart'sche Verlagsbuchhandlung.

Ziegler, W., & Huddle, J. W. (1969). Die *Palmatolepis glabra*-Gruppe (Conodonta) nach der Revision der Typen von Ulrich & Bassler durch JW Huddle. *Fortschritte in der Geologie von Rheinland und Westfalen*, *16*, 377–386.

Ziegler, W., & Sandberg, C. A. (1984). *Palmatolepis*-based revision of upper part of standard Late Devonian conodont zonation. In, D. L. Clark (Ed.), Conodont biofacies and provincialism. *Geological Society of America Special Paper*, *196*, 179–194.

Zwart, H. J. (1979). The geology of the Central Pyrenees. *Leidse Geologische Mededelingen*, *50*(1), 1–74.